FEMALE DOMINANCE HIERARCHIES INFLUENCE RESPONSES TO PSYCHOSOCIAL STRESSORS

AN ABSTRACT

SUBMITTED ON THE 9th DAY OF DECEMBER 2022

TO THE GRADUATE PROGRAM IN BIOMEDICAL SCIENCES

IN PARTIAL FULFILLMENT OF THE REQUIREMENTS

OF THE SCHOOL OF MEDICINE

OF TULANE UNIVERSITY

FOR THE DEGREE OF DOCTOR

OF

PHILOSOPHY BY

Lydia F. Smith-Osborne, D.V.M.

APPROVED:

Jonathan P. Fadok, Ph.D., Director

Jill M. Daniel, Ph.D.

Ricardo Mostany, Ph.D.

Jeffrey G. Tasker, Ph.D.

ABSTRACT

Social buffering and elevated social status confer resilience to the neurobiological consequences of chronic stress in humans. There are well known sex differences in the manifestations and prevalence of stress-linked disorders; depression and anxiety, for example, are some of the most common psychiatric conditions of modernity that disproportionately affect women. Recently, there has been a generational trend of increased prevalence in adults. It has been postulated that this is due to the demands of competitive work environments, socioeconomic stress and social isolation which in turn produce unrelieved chronic, low-grade psychosocial stress. Why some thrive in such environments and others develop stress-related illness is poorly understood. However, animal models of social hierarchies can be studied to investigate the psychosocial factors and neurobiology contributing to this pro-stress social milieu. Social species, including humans and rodents, form dominance hierarchies to ensure survival and promote reproductive success. Traditionally studied in males, rodent hierarchies are considered despotic and dominant social rank is deterministic, i.e. resulting from a history of winning agonistic encounters. In contrast, female hierarchies are thought to be less despotic, and rank is conferred by intrinsic traits. These intrinsic traits have not been specified, but in males deterministic rank is typically associated with differences in corticosterone status and behavior. Unfortunately, depending on the context in which animals are tested, male rank traits are frequently non-reproducible between studies, such that there is no single list of characteristics that can accurately describe male social

identity. Thus, we wanted to investigate whether female social hierarchies and individual traits related to social rank likewise influence stress resilience, specifically to psychosocial stressors representative of those encountered in modern social environments. To that end, using a murine model (*Mus musculus,* strain C57BL/6), we observed the formation of dyadic female hierarchies under varying conditions of ambient light and circadian phase and subjected mice to two forms of chronic psychosocial stress: social isolation and social instability. We found that stable female hierarchies emerged rapidly in dyads and shared some qualities associated with rank in male hierarchies. Using behavioral tests and an enzyme immunoassay designed to detect fecal corticosterone metabolites (FCM), we identified individual traits characteristic of female social rank, some of which were circadian phase or context-dependent. Further, we discovered that female social rank was predicted by behavior and stress status prior to social introduction. The behavioral characteristics suggested that rank is motivation-based, indicating that female rank identity serves an evolutionarily relevant purpose. Rank was further associated with alterations in behavior in response to social instability stress (SIS) and prolonged social isolation, but the different forms of stress produced disparate rank responses in endocrine status. Specifically, socially dominant females appeared to manifest consequences of social isolation stress endocrinologically but were broadly resilient to SIS, with the exception of a rank-general hyperlocomotive phenotype in the open field. In contrast, subordinate animals demonstrated behavioral changes after both forms of psychosocial stress, but FCM changes only occurred in response to SIS. Finally, histological examination of c-Fos protein expression identified brain regions which respond to social novelty or social reunion following chronic isolation in a rank-specific manner. In response to social

isolation, dominant animals expressed c-Fos disproportionately in the paraventricular nucleus of the hypothalamus and in the middle paraventricular thalamus. In contrast, in stress-naïve conditions, social novelty resulted in increased c-Fos expression in subordinates in the prelimbic regions of the medial prefrontal cortex, the lateral septum, and the core of the nucleus accumbens while reducing expression in the anterior paraventricular thalamus. Collectively, these findings demonstrated rank associations in neural activity following social encounters that are sensitive to context, novelty, and prior stress exposure, and which reflect the motivational differences identified in the preceding behavioral experiments. We determined that female social identity is linked to neurobiology, and hierarchies exert context-specific influence upon stress outcomes. These findings can be applied to future studies investigating sex differences in social identity, hierarchies and stress resilience.

FEMALE DOMINANCE HIERARCHIES INFLUENCE RESPONSES TO PSYCHOSOCIAL STRESSORS

A DISSERTATION

SUBMITTED ON THE 9th DAY OF DECEMBER 2022

TO THE GRADUATE PROGRAM IN BIOMEDICAL SCIENCES

IN PARTIAL FULFILLMENT OF THE REQUIREMENTS

OF THE SCHOOL OF MEDICINE

OF TULANE UNIVERSITY

FOR THE DEGREE OF DOCTOR

OF

PHILOSOPHY BY

Lydia Smith-Osborne

Lydia F. Smith-Osborne, D.V.M.

APPROVED:

Jonathan P. Fadok, Ph.D., Director

Jill M. Daniel, Ph.D.

Ricardo Mostany, Ph.D.

Jeffrey G. Tasker, Ph.D.

(page intentionally left blank)

ACKNOWLEDGEMENTS

In a hole in the ground, there lived a postdoc...

Thank you to the Fadok lab; for your ingenuity, hilarity, and camaraderie during my tenure at Tulane. Without the supportive lab environment, fostered by the irreplicable Alexis Resendez, this experience wouldn't have been the same. I found myself at home when I found you all.

Thank you to my fellow T32s, for shared experiences, confusion, and the mutual out-of-placeness. Thank you for the text chains, camping, dinners and writing sessions. Thank you to Dr. Robert Blair for guiding and, when occasion demands, herding us in the right direction. We are so incredibly lucky to have had you in our corner. Tulane chose the right man for the job.

Thank you to Drs. Jill Daniel, Ricardo Mostany, Jeffrey Tasker and Laurie Earls, for taking on a non-traditional candidate and being willing to go with the flow. Thank you for your flexibility, your expertise, and your precious time.

Thank you to Dr. Jonathan Fadok, for your perspective, your enthusiastic interest, and taking the time to "get" me and my project. Thank you for going above and beyond for your team, and for creating a lab community based upon mutual respect and investment. Thank you for taking a chance on me when you didn't have to; I hope it paid off.

Thank you to my close friends for their support, and (timely) wry commentary. Thank you for sharing your lives and your time; it was a rudder to me. Thank you to Mr. Big and Honey, for the small softnesses and the reviving headaches. Thank you, Bruno, my slow and steady companion.

Thank you to my sweet brother Michael and wonderful sister Rachel, for the phone calls that brought me home when I was far away. Big siblings, you kept me on track.

Thank you to Dr. Alexa Smith-Osborne, my mother. Thank you for your example, your unwavering support, your shared experience and commiseration. Your courage has, and always will, inspire me. Thank you for the phone calls, the T-shirts and baking soda, the reviews of Hallmark Christmas movies and the library book club. Thank you for reminding me who I was when I couldn't remember.

Thank you to Alexei Dukov, my partner. Thank you for the priceless gift of perspective; you always remind me what really matters. Thank you for tolerating my forgetfulness, embracing my loopiness, for late night video chats, endless encouragement, and above all, for laughing with me. Thank you for your comfort, and for being Home. Thank you for sharing a hobbit hole with me.

TABLE OF CONTENTS

LIST OF TABLES

LIST OF FIGURES

LIST OF COMMONLY USED ABBREVIATIONS

EIA	Enzyme immunoassay
CORT	Corticosterone
HPA	Hypothalamic-pituitary-adrenal
FCM	Fecal corticosterone metabolites
CE	Competitive exclusion
FCT	Food competition task
OFT	Open field test
EPM	Elevated plus maze
3CSA	Three chamber social approach
NORT	Novel object recognition test
SIS	Social instability stress
mPFC	Medial prefrontal cortex
PL	Prelimbic region of the medial prefrontal cortex
CLA	Claustrum
nAcc	Nucleus accumbens
LS	Lateral septum
PVN	Paraventricular nucleus of the hypothalamus
aPVT	Anterior paraventricular nucleus of the thalamus
mPVT	Middle paraventricular nucleus of the thalamus

1. INTRODUCTION

*Partially adapted from "Dominance hierarchies influence responses to psychosocial stressors" by Smith-Osborne L, Duong A, Resendez A, Palme R, Fadok J. (2022). [Manuscript submitted for publication].

1.1 Stress-linked disorders of modernity

1.1.1 An evolutionary role for psychosocial stress

Psychosocial stress consists of generally low-level stressors arising from social conflict which produce alterations in emotional regulation and goal-oriented behavior (Kogler et al 2015). All social species experience varying degrees of psychosocial stress, which serves important adaptive purposes such as designating social rank during hierarchy formation, facilitating prosocial behavior, and enforcing role and task assignment (Kogler et al 2015, Hüther 1996, Moosa & Ud-Dean 2011, Schweda et al 2019). The benefits of successfully mediated psychosocial stress include membership in a social network and secondary access to its protection, territory, and resources, in addition to less tangible benefits such as emotional support, social capital and a sense of personal identity and fulfillment (Kogler et al 2015, Moosa & Ud-Dean 2011, Heaney & Israel 2008). Additionally, stress responses can be considered a critical component of physiologic homeostasis and general adaptation to existence in a changing and uncontrollable environment (Hüther 1996, Kupriyanov & Zhdanov 2014). Beneficial stress exposure, or eustress, followed by subsequent activation of the hypothalamic-pituitary-adrenal (HPA) axis and engagement of appropriate coping mechanisms, has been linked to enhanced resistance to the detrimental effects of stress later in life (Hüther 1996, Kupriyanov & Zhdanov 2014, Rutter & Sandberg 1992, Crane et al 2019). However, persistent social

conflict and perceived stress (or on the other end of the spectrum, social isolation) may lead to chronic stress maladaptation which can cause significant biological and psychological harm (Siegrist 2008, Backé et al 2012, Kang et al 2020, Greenwood et al 1996, Friedler et al 2015). Importantly, psychosocial stress is considered a risk factor for the development of stress-related mental illness including generalized anxiety disorder (GAD), depression, substance use disorders, and posttraumatic stress disorder (PTSD; Siegrist 2008, Farrer et al 2016, Muntaner et al 1995, Ahmed 2007).

1.1.2 Diseases of modernity

There are inherent facets of modern life that are also risk factors for the development of psychosocial stress-related disorders such as anxiety and depression. These include physical contributors such as consumption of pro-inflammatory and overly refined diets (Jacka et al 2010, Wang et al 2019) as well as disturbed circadian rhythms influenced by nighttime artificial lighting conditions and inadequate daytime exposure to natural light (Blume et al 2019, Osibona et al 2021). In addition, there are socioeconomic contributors including income inequality (Patel et al 2018), perceived loneliness (McQuaid et al 2021, Santini et al 2020) and fractured social networks (Santini et al 2020, Viseu et al 2018, Roohafza et al 2014). Depression, for example, has been termed a "disease of modernity" by Brandon Hidaka (Hidaka 2012), who proposed that a divergence between evolutionary biology and modern-day living is responsible for producing the societal factors conducive to that disorder. There is a large body of literature supporting this theory, and modern domains proposed to be involved in the development and consequences of chronic psychosocial stress include occupational stress, socioeconomic disparity, and

institutionalized discrimination (Hidaka 2012, Bracken 2001, Layte et al 2019, Liu et al 2017, Williams & Neighbors 2001, Noh & Kaspar 2003, Lindström 2022).

1.1.3 Societal implications of chronic psychosocial stress

Mental health disorders related to chronic psychosocial stress, including depression and anxiety, represent some of the greatest burdens on the American health care system. An estimated 21 million American adults experienced a major depressive episode in 2020 (DHHS National Survey on Drug Use and Health 2020), and nearly one in six adults experienced symptoms consistent with generalized anxiety disorder in 2019 (Terlizzi & Villarroel 2020). The COVID-19 pandemic is responsible for a dramatic rise in prevalence, with 41.5% of adults experiencing recent symptoms of anxiety or depression from 2020-2021 (Vahratian et al 2021). Both disorders are frequently comorbid and exhibit a pronounced gender bias, with prevalence being twice as high in women (DHHS National Survey on Drug Use and Health 2020, Terlizzi & Villarroel 2020, Vahratian et al 2021). Psychosocial stress is also a leading cause of morbidity in human cancer patients and has been strongly linked to the development of cardiovascular disease, the two leading causes of death in the United States (Liu et al 2017, Powell et al 2013, Osborne et al 2020, Murphy et al 2020). Collectively, psychosocial stress remains a modifiable risk factor in the development of disorders which pervade modern society and globally affect quality of life. Understanding the neurobiological basis of individual resilience and vulnerability to psychosocial stress therefore represents an important area of research.

1.2 Rodent social hierarchies

1.2.1 Ethological relevance in modeling aspects of human disease

It is difficult to recapitulate this complex modern societal framework within a laboratory environment in a way that is also ethologically relevant. To research the neurobiological underpinnings of stress-related disorders, animal studies have employed various paradigms to produce a stressed behavioral phenotype. The most common of these include chronic unpredictable mild stress, social defeat stress, early maternal separation, and chronic corticosterone administration (Gururajan et al 2019). In modeling depression and generalized anxiety, for example, researchers frequently employ somatic rather than psychological stressors – paradigms incomplete in their ability to reproduce the psychological conditions predisposing an individual to the full spectrum of symptomology (Kogler et al 2015, Gururajan et al 2019, Campos et al 2013). Some outcome measures such as anhedonia have face validity for human illness, but other ethologically meaningful factors pertinent to rodent motivation and mood such as nest building behaviors, expression of different exploratory postures, or changes in patterns of hygiene and grooming behavior, are infrequently considered (Gururajan et al 2019, Weiss et al 1998, Sturman et al 2018, Pollak et al 2010, Gaskill et al 2013, Smolinsky et al 2009, Nollet et al 2013). Furthermore, most animal studies have been performed using male-only subjects despite abundant evidence that many stress-related psychiatric disorders, including anxiety and depression, are nearly twice as common in women (Gururajan et al 2019, Kokras & Dalla 2014). However, it is possible to improve experimental validity by recreating some of the psychosocial stressors experienced in modern life, such as social inequality and loneliness, by harnessing an animal's natural tendencies to form ranked social groups (LeClair & Russo 2021). Exploring inherent differences in individual traits and translating those to ethological characteristics of rodents may also help address some of the inconsistencies in

reproducibility of stress paradigms that are employed to test human therapeutics (Gururajan et al 2019, Pollak et al 2010).

1.2.2 Social living and evolutionary fitness

Social species living in groups form hierarchies for protection, division of labor, to reduce aggression, and to raise young (Moosa & Ud-Dean 2011, Wang et al 2014, Rusu & Krackow 2004, Chase & Seitz 2011). Mutually shared resources and territories promote reproductive success, which is theorized to have promoted the genetic selection of prosocial behavior and allow colonization of otherwise inhospitable environments (Moosa & Ud-Dean 2011, Cornwallis et al 2017). The assumption of specific roles within a social network increases group efficiency through shared learning, and tiered communication reduces predation through avoidance or via 'safety in numbers' (Moosa & Ud-Dean 2011, Ebensperger 2001). Cooperative behavior has been observed in species as diverse as social insects, in which colony stabilization and group homeostasis is contingent upon division of labor and task specialization (Ulrich et al 2018). Further, social support is known to have a buffering effect on the progression of numerous psychiatric conditions including substance abuse, anxiety and major depression (Viseu et al 2018, Roohafza et al 2014, Kleiman & Liu 2013, Birtel et al 2017) and stress-resilient effects of social buffering have likewise been characterized in rodents (Beery & Kaufer 2015). In this respect, social group membership is evolutionarily advantageous.

1.2.3 Traditional characteristics of social rank

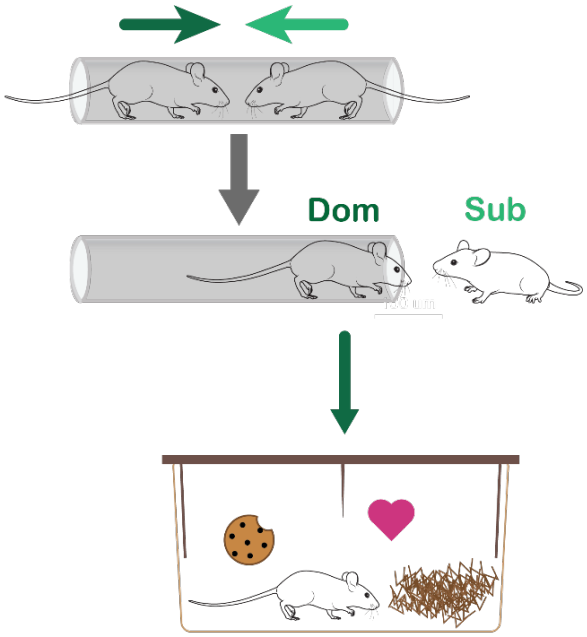

Figure 1. Manifestations of dominance in the laboratory setting

Schematic depicting the dominant advantage in home cage behavior of male rodents. Winning agonistic encounters, such as in the tube test, results in priority access to food rewards, mates, and territory including nesting material and thermoneutral zones. *Dom*, dominant; *Sub*, subordinate.

Individual social status is not equitably rewarding, however (Fig. 1); subordinate rank in male rodents is typically associated with greater expression of social appeasement behaviors, secondary access to limited resources, and lower reproductive success (Wang et al 2014, Chase & Seitz 2011, D'Amato 1988, Wesson 2013). Inconsistently, subordinate status has been also linked to poorer body condition, elevated circulating glucocorticoids, being the recipient of barbering (i.e. excessive allo-grooming stereotypically of the head, whiskers and back), and dispersal from mating harems (Huang et al 2011, Fulenwider et al 2022).

In contrast, dominant male rodents generally have greater access to limited resources such as palatable food rewards, territory, and mates (Fig. 1), express greater social motivation, and emit more courtship vocalizations to receptive females compared to

subordinates (Fulenwider et al 2022, Kunkel & Wang 2018). Dominance in males has been less consistently associated with greater levels of quiescence (contradictorily, also with greater exploration), increased overall consumption of food and water, reduced circulating glucocorticoids, skewed reproductive success, and greater expression of aggressive behaviors such as fighting and chasing (Wang et al 2014, D'Amato 1988, Huang et al 2011, Fulenwider et al 2022, Varholick et al 2018).

Dominance hierarchies are generally thought to emerge from a combination of resource competition and dyadic agonistic and affiliative social interactions (Huang et al 2011, Fulenwider et al 2022). One of the most traditional methods of testing rodent hierarchies is by using the tube test, also called competitive exclusion, wherein two animals are introduced to opposite ends of a clear plastic tube of sufficient width for the passage of only a single animal (Fan et al 2019). This test combines competition over a limited resource – the territory representing safety (i.e. the tube) – with an agonistic encounter – face-to-face contact followed by removal of one individual from the tube. Generally, subordinate animals are more frequently excluded or voluntarily retreat from the tube while the dominant animal maintains access to the protective environment. The results of the tube test strongly agree with other agonistic measures of dominance such as home cage behavioral analysis of fighting behaviors in males, as well as competitive tests of dominance such as urine scent-marking, competition for palatable food rewards, and access to thermoneutral areas in a cold environment (Fulenwider et al 2022, Fan et al 2019).

Similar health and behavioral dominance trends are seen in humans, wherein social rank is often approximated from socioeconomic status and social capital (Wang et al 2014, Beery & Kaufer 2015). Studies of industrialized societies reliably demonstrate an inverse

relationship between socioeconomic status and mortality and morbidity (Patel et al 2018, Wang et al 2014, Schrage et al 2021). In individuals, poor socioeconomic status contributes to the prevalence of stress-related mental illness including anxiety and depression in part through the production of chronic, low-grade psychosocial stress (Patel et al 2018, Viseu et al 2018, Wang et al 2014, Beery & Kaufer 2015). Despite the connection between psychosocial stress and mental illness, there is a lack of consensus on how rank influences – or is influenced by – stress status.

1.2.4 Sex differences

Female dominance hierarchies are comparatively understudied, especially in laboratory rodents (LeClair & Russo 2021, Fulenwider et al 2022). Nevertheless, there is evidence to suggest that manifestation of dominance varies significantly by sex. For example, female rodent hierarchies tend to be less despotic, less linear and more stable compared to their male counterparts (Varholick et al 2018 and 2019, Williamson et al 2019). In mice, it has been shown that female dominance hierarchies form based upon intrinsic individual traits, while male hierarchies form based on a history of winning agonistic encounters (Van Den Berg et al 2015). The intrinsic traits defining female rank have not been elucidated, but there do not appear to be consistent rank differences in body condition, exploration, or glucocorticoid status once female hierarchies become established (Varholick et al 2019). One study demonstrated prolonged estrus in dominant female mice but found no differences in plasma estradiol by rank and no influence of estrous phase on agonistic behavior (Williamson et al 2019). That same study evaluated CD-1 mice living in large communal groups (12 individuals per cohort) and found a significant difference in plasma corticosterone after hierarchical establishment. Since study heterogeneity is likely

a contributor to the variability observed in rank characteristics in male hierarchies (Blanchard et al 1995, Creel 2001, Bartolomucci et al 2001, Williamson et al 2017, Sabanovic et al 2020, Varholick et al 2021), it is possible that female rank traits are also sensitive to context and influenced by social group composition and stress exposure. I am particularly interested in how female social identity can mediate the neurobiological responses to psychosocial stressors relevant to modern living.

1.2.5 Circadian and lighting influence on rodent behavior

Lighting conditions and circadian phase have both been shown to affect rodent behavior in laboratory settings; this has been proposed as one cause of inter-study variability in behavioral research (Kopp 2001). Mice are primarily nocturnal animals; they are more active and engage in spontaneous social behaviors with greater frequency during the dark phase of their circadian cycle (Kopp 2001, Hossain et al 2004, Yang et al 2008). While most behavioral test performance appears to be relatively resilient to circadian phase, there are differences in strain and sex that could reflect individual variability in responsiveness to circadian variation (Hossain et al 2004, Beeler et al 2006, Bains et al 2018). Additionally, ambient lighting exposure can cause dark-housed animals to convert their phase entrainment and can even be aversive at high intensities such as those used in the light-dark box test (Bourin & Hascoet 2003, Zhang et al 2017). Therefore, testing within-strain behaviors in different phases and lighting conditions represents another strategy for exploring the context-sensitivity of rank characteristics within social hierarchies.

1.3 Corticosterone (CORT)

1.3.1 Hypothalamic-pituitary-adrenal (HPA) axis

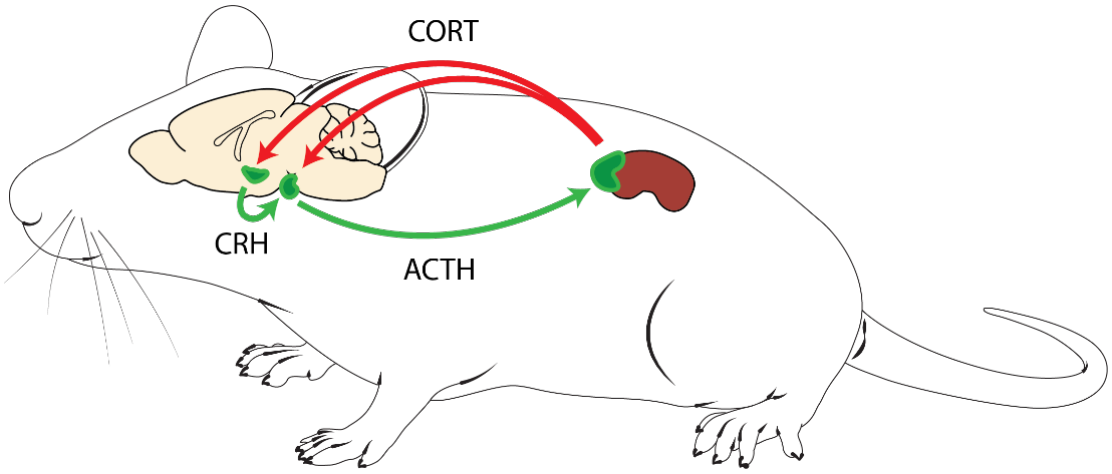

Figure 2. The hypothalamic-pituitary-adrenal axis

Simplified schematic of the major components of the HPA axis with their approximate anatomical location in the rodent (not to scale). Green arrows represent upregulation, and red arrows represent negative feedback by CORT. *CRH*, corticotropin releasing hormone; *ACTH*, adrenocorticotropin hormone; *CORT*, corticosterone.

Corticosterone (CORT), the primary glucocorticoid in rodents and an analogue of human cortisol, is frequently evaluated as an approximate of stress status in the context of social rank (LeClair & Russo 2021, Wang et al 2014, DeVries et al 2003, Zhou et al 2018). CORT is a product of the vertebrate hypothalamic-pituitary-adrenal (HPA) axis, a central regulator of stress responses. The highly conserved neuroendocrine pathway leading to glucocorticoid production is as follows (Fig. 2): in response to a stimulus such as a stressor, parvocellular neurons of the paraventricular nucleus of the hypothalamus (PVN) secrete corticotropin releasing hormone (CRH) which acts on the anterior pituitary gland to release adrenocorticotropin hormone (ACTH) into circulation; this in turn stimulates the zona fasciculata of the adrenal cortex to secrete CORT (or cortisol) (Sheng et al 2021). Negative feedback mechanisms engage in response to rising CORT and binding of lower-affinity glucocorticoid receptors in (among other areas) the PVN, leading to reduced CRH

secretion, suppression of ACTH release from the pituitary, and ultimately normalizing peripheral glucocorticoid levels (Sheng et al 2021). Circulating CORT undergoes extensive hepatic and gastrointestinal metabolism, resulting in excretion of CORT metabolites into the feces (Touma et al 2003).

CORT has several protective factors which regulate physiological homeostasis under stress; it mobilizes energy to meet metabolic demands, reduces inflammatory responses, and suppresses nonessential functions such as reproduction in favor of cardiovascular and autonomic support (Munck et al 1984, Sapolsky et al 2000, Heck & Handa 2019). However, in excess or under conditions of sustained release (e.g., failure of negative feedback mechanisms such as those documented with some pituitary tumors), glucocorticoids can cause significant damage to multiple organ systems. For example, chronically elevated circulating glucocorticoids has been linked to the development of insulin resistance, cardiovascular disease, nonalcoholic fatty liver disease, and a host of stress-related mood disorders including depression (Kang et al 2020, Osborne et al 2020, Sheng et al 2021). However, glucocorticoids are crucial for long-term memory consolidation and learning from emotionally arousing experiences (Dominique et al 2009). Indeed, the balance between physiologic and pathologic stress appears nuanced, as prior stress exposure has been linked to future resilience (Crane et al 2019). Fluctuations in CORT may therefore constitute an adaptive priming effect that is relevant to homeostatic coping.

1.3.2 CORT, social rank, and behavior

Corticosterone has been inconsistently linked to social rank in rodents; while most studies find higher circulating CORT is characteristic of subordinate rank (Williamson et

al 2019, Blanchard et al 1993 and 1995), others show the same trend for dominants (Williamson et al 2017, Haemisch et al 1994, Blanchard et al 1995), and still others find no difference by rank (Kozorovitskiy & Gould 2004, Hunt & Hambly 2006, Pallé et al 2019). There is some evidence that rank related alterations in circulating glucocorticoids are dependent upon context, including resource availability and prior stress exposure (Wang et al 2014, Bartolomucci et al 2001, Blanchard et al 1995, Williamson et al 2017). Additionally, experimental variables including sample source, subject strain and diurnal variations in CORT excretion could account for some variability (Touma et al 2003).

Regardless, the activity of circulating glucocorticoids demonstrably affects rodent behavior and cognition. Acute CORT administration in mice has been shown to produce anti-depressant like effects in behavior (Zhao et al 2009) whereas chronic administration leads to the development of anxiety-like behavior, learned helplessness, and anhedonia (Murray et al 2008, Ali et al 2015). Interestingly, female mice may be more resilient to the pro-depressive and anxiogenic effects of chronic exogenous CORT administration than males (Mekiri et al 2017).

Endogenous CORT has been proposed to modulate the cytokine response to dominance in male mice (Audet et al 2010) as well as being a long-term determinant of rank in rats (Timmer & Sandi 2010, Weger et al 2018) when administered prior to social experience. Since glucocorticoids are involved in memory processing and retrieval, it is possible that glucocorticoid levels are reflective of the consolidation of memories surrounding social rank.

1.3.3 Diurnal and sex differences

Sex differences have been demonstrated in CORT metabolite excretion in mice. Male mice excrete more CORT metabolites into the feces than females, whereas females excrete more in the urine, although diurnal excretion patterns are similar between the sexes (Touma et al 2003). This is of interest because termination of the stress response is sensitive to diurnal variations in glucocorticoid production (Sheng et al 2021, Touma et al 2003). Interestingly, HPA axis responsivity to acute stress is more pronounced in female rodents than males, a difference which is proposed to be under the control of gonadal hormones. Specifically, females demonstrate greater PVN neuronal activation and have a slower return to baseline ACTH and CORT levels following acute stress (Heck & Handa 2019). There is also evidence that females express fewer corticoid receptors in the hypothalamus and pituitary compared to males (Heck & Handa 2019). This divergence translates into relevant endocrinological sex differences in stress responsivity and stress-enhanced learning in the laboratory setting (Solomon et al 2015, Choleris et al 2013), further warranting a specific investigation into female hierarchies within the context of stress resilience.

1.4 Neurobiology of social dominance

1.4.1 Neural correlates of social rank

As is the case with preclinical investigations, most studies into the neural correlates of rank have been performed in male animals. Therefore, findings should be interpreted with the caveat that there are potentially unexplored sex differences in neurobiology that may account for divergent – or even shared – behavioral and endocrinological characteristics observed within female dominance hierarchies. That being said, stable male social hierarchies demonstrate some well-described patterns of neuronal activity consistent with rank. The prefrontal cortex is one region heavily implicated in the manifestation of dominance in male rodents and non-human primates and is associated with superior social status in humans (Wang et al 2014). In male rodents, most evidence points to a role for the medial prefrontal cortex (mPFC) as designating dominant (i.e., alpha) rank through social recognition and regulation of dominance behaviors (Holson 1986, Wang et al 2011, Zhou et al 2017). One pivotal study used viral manipulation of AMPA receptor trafficking to demonstrate that transitive social mobility in male C57/BL6 mice is directly linked to parallel changes in mPFC synaptic efficacy (Wang et al 2011). They additionally found greater neuronal expression of the immediate early gene c-Fos in the prelimbic region of the mPFC of dominant animals following a win in the tube test. Several years later, Fei Zhou of the same lab discovered that spiking activity in putative pyramidal neurons in the anterior cingulate and prelimbic mPFC aligned with effortful winning behavior in the tube test, and that active winning could be inhibited and reproduced through DREADD (designer receptors exclusively activated by designer drugs) and optogenetic manipulation (Zhou et al 2017). They further demonstrated that long term hierarchical status was under

the influence of prefrontal input from the mediodorsal thalamus. As Dr. Van Den Berg previously established, male dominance hierarchies are formed based upon prior history of winning, whereas female hierarchies are based upon intrinsic factors (Van Den Berg et al 2015); repeat winning produced a similar sustained elevation in male hierarchical status in the thalamus-mPFC experiments (Zhou et al 2017). Thus, it is possible that the mPFC plays a different role in female rank and therefore should be investigated along with other areas implicated in mediating social behavior and identity, including the midline thalamus which projects strongly to the prelimbic region of the mPFC (Hoover & Vertes 2007).

1.4.2 Sex differences in social and stress-related neurobiology

To date, while most studies of social neurobiology have not explored sex-specific mechanisms, some sex differences in social (i.e., observational) learning and conditioned responses have been found. Social recognition in rats is mediated by vasopressinergic transmission in males, but not in females (Bluthe & Dantzer 1990). It has also been demonstrated that social learning of food preference is enhanced by acute CORT administration and other mild stressors more in male mice than in females (Choleris et al 2013). Interestingly, there is pharmacologic evidence that contextual anxiety may play an important and sexually dimorphic role in reducing social learning in females (Choleris & Kavaliers 1999).

In addition to social learning, it has been demonstrated that uncontrolled stress exposure impairs classical conditioning and reduces hippocampal dendritic spines in females but has the opposite effect in males and masculinized females (Dalla & Shors 2009). In the absence of stress, intact females outperform males on several classical and operant conditioning tasks, whereas the reverse is true for fear conditioning tasks which

are inherently stressful (Dalla & Shors 2009). For example, during fear conditioning females exhibit less conditioned freezing behavior than males (Maren et al 1994) but demonstrate resistance to extinction after ovariectomy (OVX; Gupta et al 2001). Corroborating and expanding upon these findings, administration of an estrogen receptor beta agonist to OVX females enhanced extinction in rats (Chang et al 2009), supporting the influence of circulating androgens on fear-based learning. Fascinatingly, in a progressive-ratio fear-based avoidance test female rats outperform males in task acquisition but return more frequently to the feared/aversive context and again show impaired extinction of avoidance behavior (Van Haaren et al 1990, Dalla et al 2008). Impaired fear extinction may therefore be reflective of a sexually dimorphic adaptation to traumatic experiences in the form of increased behavioral vigilance.

Collectively, this suggests a role for contextual and applied stress in the attenuation of learning, acquisition and adaptive behaviors in female animals. These studies underscore the importance of evaluating sex differences in social behavior and learning within the context of dominance hierarchies, wherein rank-specific differences in stress status may influence susceptibility to disorders associated with conditioned fear responses, such as generalized anxiety and post-traumatic stress.

2. RESEARCH OBJECTIVE AND STRATEGY

I hypothesized that in mice, female social hierarchies directly influence stress status and therefore also convey relative resilience or vulnerability to behavioral, endocrine, and neurobiological alterations arising from psychosocial stress. I wanted to investigate how protective effects of social partnerships contribute to stress susceptibility in a rank-based manner, reflecting the neurobiological signatures characteristic of rank. To that end, this investigation was performed in two aims – first to determine intrinsic characteristics of female rank and identify neuroanatomical regions involved in rank-skewed social interactions, and second to investigate differences in vulnerability to stress endophenotypes induced by social instability stress or social isolation.

In order to explore dominance within the theoretical framework of inherent differences, it behooves us to evaluate highly linear social groups over time (Chase & Seitz 2011). Thus, pair housed age- and strain-matched adult female mice were analyzed for behavior and fecal corticosterone metabolites using an established enzyme immunoassay (Touma et al 2003 and 2004) before, during, and after hierarchy formation. Since hierarchical stability is inversely related to cage size (Varholick et al 2019, Schuhr 1987), it was hypothesized that initial wins in the tube test would be predictive of future social rank, as has been demonstrated previously (Lindzey et al 1961, Fan et al 2019). Indeed, adult females housed in dyads rapidly formed stable hierarchies, and rank was independent of innate anxiety or locomotor characteristics. Rather, baseline manifestations of rank were discovered wherein subordinate animals are characterized as relatively high-stress until hierarchical stabilization.

Divergent motivation, in addition to baseline endocrine status, defines female social rank. Subordinate females exhibited pro-exploratory motivation akin to the patrolling role observed to be characteristic of rank in male mice (Benton & Brain 1979). In contrast, dominant females expressed a pro-social motivation in the three-chamber social approach task, regardless of contextual novelty. The subordinate behavioral roles were context-specific in that they depended on both the circadian cycle and the anxiogenic nature of the testing environment.

Social rank further affected the behavioral and endocrinological response to social isolation or social instability in distinct ways. Fecal corticosterone metabolites were disproportionately affected by social isolation in dominant animals, while subordinate animals were more affected by unstable social groups. Interestingly, changes in rank-associated behaviors followed an opposite trend; subordinate behavior was more affected by social isolation and dominant behavior was more affected by social instability.

Rank differences also emerged in central c-Fos expression following two scenarios – after exposure to a novel social partner, or after reunion with a familiar social partner following extended social isolation. In response to social stimuli, subordinate animals showed the greatest difference from control in regions related to cognitive processing of social cues and coordination of behavioral responses, whereas dominant animals had a greater difference in regions associated with regions key in modulating homeostasis.

These findings support the hypothesis that rank in females is determined by intrinsic traits rather than through winning as in males. This study of social hierarchies identifies a stress-susceptible phenotype among dominants exposed to social isolation and

subordinates exposed to social instability and contributes new knowledge to understanding the neurobiological correlates of social rank and identity in social groups.

3. EVALUATION AND CHARACTERIZATION OF FEMALE DYADIC SOCIAL HIERARCHIES UNDER STRESS-NAÏVE CONDITIONS

3.1 Materials and Methods

3.1.1 Ethics and biosafety Statement

The Institutional Animal Care and Use Committee at Tulane University reviewed and approved this study (Protocol IDs 652 and 1559, Amendment ID 2774). All experimental animals were housed and cared for by the Tulane Department of Comparative Medicine Uptown. Tissue samples and fecal boli were collected, handled and processed in a Tulane University biomedical laboratory under BSL-1+ conditions.

3.1.2 Study design

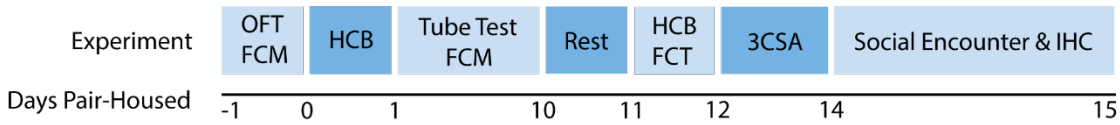

Figure 3: Experimental timeline for hierarchy characterization

OFT, open field test; *FCM*, fecal corticosterone metabolites; *HCB*, home cage behavior; *FCT*, food competition task; *3CSA*, three chamber social approach; *IHC*, immunohistochemistry.

The first investigation was performed over two weeks of co-housing (Fig. 3). Subjects were 28 adult 3–4-month-old female C57BL6/J mice (Jackson Laboratory, Bar Harbor, Maine). Animals were housed on a 12:12 hour reverse light cycle; food and water were provided ad libitum. All testing was performed during the active (dark) phase of the circadian cycle under red LED light.

Prior to pair-housing, animals underwent baseline behavioral testing in the open field test and fecal samples were collected for analysis of corticosterone metabolites. Home cage behaviors were analyzed immediately before pair-housing was initiated. Dominance

hierarchies were tested for seven consecutive days using the tube test, and fecal samples were collected after 24 hours, 72 hours, and 7 days of continuous pair-housing. Body weight was also monitored throughout testing. At 11 total days of pair housing, home cage behaviors were analyzed a second time after a rest period to avoid interference of the tube test with behavioral expression; immediately afterwards an unfasted food competition task was performed in the home cage using a palatable food reward. Three days later, after 14 total days of pair housing, a randomized cohort of paired animals were subjected to the three-chamber social approach task and fecal samples were collected. Afterwards, animals were exposed to a novel social encounter, then transcardially perfused; brains were extracted for analysis of c-Fos expression and adrenal glands were collected and weighed.

3.1.3 Fecal corticosterone metabolite (FCM) EIA

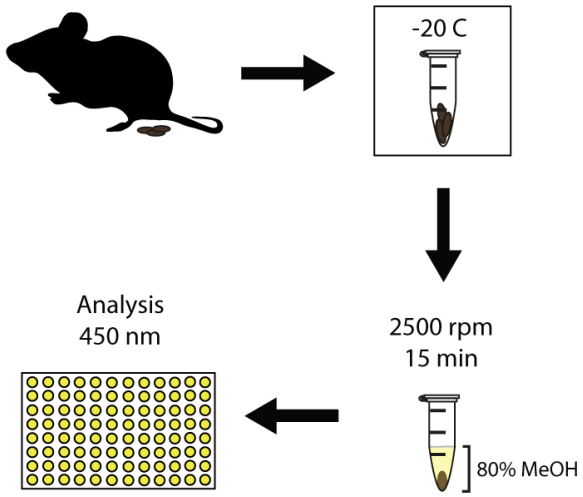

Figure 4. FCM collection, processing and analysis by colorimetric assay

Schematic describing the process of fecal sample collection and extraction prior to indirect assay of metabolite concentration through a colorimetric reaction. Samples are frozen immediately on dry ice and steroid extraction is performed by simple phase-separation of homogenized fecal samples suspended in 80% methanol in deionized water. *C*, Celsius; *MeOH*, methanol; *rpm*, rotations per minute (centrifugation).

Fecal samples were taken at the same time-of-day within experiments, and at least 2 hours into the light cycle of testing. Mice were individually removed from their cage and placed in a plastic beaker on a scale to take body weight measurements (Fig. 4). This process typically resulted in the mouse passing fecal pellets which were immediately collected in microcentrifuge tubes then snap-frozen on dry ice. Mice that did not pass during the weighing were gently handled for several minutes until fecal pellets were produced. Urine contamination was addressed through blotting or lining of the beaker with absorbent tissue (Kimwipe, Kimberly-Clark Professional, GA). Samples were stored at -20°C until analysis using an enzyme immunoassay specific for glucocorticoid metabolites sharing a 5α-3β, 11β-diol structure, as described by Touma et al. (Touma et al 2003 and 2004).

Frozen samples were removed from storage and weighed individually. Large samples were tapered to a maximum of 0.05 g, and samples weighing < 0.02 g were excluded from analysis. Weighed samples were homogenized and underwent simple extraction in 80% methanol (MeOH), followed by centrifugation at 2500 rpm for 15 minutes. A 100 μL sample of supernatant was diluted 1:10 in assay buffer, then stored at -20°C until analysis.

Prior to analysis, samples were thawed and diluted into 1:100 aliquots. Standards, antibodies and biotinylated labels were acquired from Dr. Rupert Palme at the University of Veterinary Medicine in Vienna, Austria. The assay procedure took place over two consecutive days. On the first day, samples (diluted 1:100 in assay buffer) and standards (diluted 1:2.5 in assay buffer) were plated in duplicate in 96-well microtitre plates coated with rabbit IgG, then incubated with primary antibody and biotinylated label overnight at

4°C. The next day, samples were incubated for 45 minutes at 4°C with horseradish peroxidase-conjugated streptavidin (strep-POD), which selectively binds biotin. The strep-POD bound samples were then incubated for 45 minutes at 4°C with tetramethylbenzidine (TMB) solubilized in dimethyl sulfoxide, which reacts with strep-POD to produce a color change (clear to blue) proportionate to the amount of bound conjugate. The TMB reaction is stopped with 2M sulfuric acid producing another color change (blue to yellow), after which plates are read at 450 nm.

All presented data are averages for samples run in duplicate which have intra-assay coefficients of variation (CV) < 10%; values with intra-assay CV > 10% were excluded from analysis or re-run on a new plate. The average inter-assay CV for each experiment is listed below:

Experiment 1 (stress-naïve; n = 6 assays): 5.79%

Experiment 2 (SIS; n = 10 assays): 7.38%

Experiment 3 (isolation; n = 11 assays): 5.84%

3.1.4 Open field test (OFT)

Mice were brought into the testing room in their home cage and allowed to acclimate for at least 30 minutes before all behavioral tests. Activity in the open field test and elevated plus maze was recorded via an overhead camera and behavior tracking was recorded using Cineplex (Plexon, Dallas, TX) software.

The open field test took place in a 45 x 45 x 45 cm square, white PVC arena under either dim red light (< 15 lux) or white light (< 15 lux) conditions, depending on the circadian phase of testing as described for each experiment. Mice were placed in the arena and allowed to explore for 10 minutes. Relevant behaviors were recorded, including

supported and unsupported rears, crosses into and time spent in the inner zone, jumps, grooming time, and fecal boli passed. After each trial the arena was cleaned with 70% ethanol. In the first experiment, the open field test was performed prior to pair housing and hierarchy formation.

3.1.5 Home-cage behavior analysis

Animals were evaluated for social behaviors in the home cage at two time points: initial meeting (pre competitive exclusion) and after 11 days of pair housing (post competitive exclusion). All behavioral evaluation was performed under dim red-light conditions (< 10 lux) during the dark (active) circadian phase. Animals were placed in a clean cage with bedding and without enrichment (i.e., nesting material) and allowed to interact freely. Upon the first social encounter, a 20-minute timer was started, and interactions were recorded by overhead camera and manually scored by two unbiased observers and averaged.

Behaviors with relevance for sociability, dominance, anxiety, and all direct contacts were recorded. Behaviors were treated as counted variables (i.e., +1 added for every occurrence) and categorized as follows:

1) Social affiliative: nose-to-nose sniffing, head sniffing, flank sniffing, anogenital sniffing, allo-grooming, and following.
2) Forepaw touch: one animal places its forepaws on the head, shoulders, or body of another animal followed by vigorous nonsocial environmental sniffing in a sweeping motion above the conspecific. This behavior most closely resembled supported rearing with the conspecific being used in place of a wall or similar

support. Since the behavior was performed frequently but the sniffing was not directed towards the conspecific, this behavior was scored as its own category.

3) Nonsocial: scent marking, scent mark sniffing, auto-grooming, crawling over/under a conspecific towards a nonsocial goal arising from space constraints in the cage.
4) Agonistic: chasing, biting, attack and retreat, boxing, pinning. Agonistic behaviors were not observed during home cage behavior analysis.

3.1.6 Competitive exclusion (CE)

CE took place in 2 phases – training and testing. Prior to training, group-housed animals were habituated to the presence of a 6 x 2.5 cm diameter clear acrylic tube in the home cage for 72 hours to avoid novelty-associated inhibition of training.

1) Training: The testing apparatus consisted of a clear acrylic 30 x 2.5 cm diameter acrylic tube, wide enough for the passage of one mouse at a time. During 10 trials per day, mice were individually trained to run the length of the tube from either direction. Training was performed once daily for two consecutive days.
2) Testing: Dominance testing began after the last day of training. Each animal underwent two reminder trial runs prior to every testing session. After the trial runs, mice were placed on opposite sides of the tube and allowed to meet in the middle. The test was considered complete when one mouse forced the other completely back to its starting side. This was recorded as a win for the mouse that successfully ran the length of the tube, and a loss for the mouse forced out of the tube. A total of 5 dominance trials were performed per day. The dominant status for each testing session was defined as 3 or more wins. Time to complete the test as well as win style was recorded. A win strategy was considered active if the winner employed

agonistic behaviors to force the opponent out (e.g. pushing, push-back, advancing) or passive if non-agonistic methods were employed (i.e. winner refused to retreat but did not actively advance to force out the opponent).

3.1.7 Food competition task (FCT)

The food competition task was performed in unfasted animals to remove the variable of subjective satiety as a primary motivator. 48 hours prior to the experiment, animals were acclimated to receiving a palatable food item (Honey Nut Cheerio; General Mills, Minneapolis, MN) in the home cage to reduce novelty-induced suppression of feeding. Immediately after behavior analysis, a single Cheerio was placed in the center of the home cage. Behavior was recorded by overhead camera for 5 minutes after initial interaction or until the food item was completely consumed. No other food, water, or enrichment was available during this task. Animals were scored for overall time in possession of the food item as a percentage of total time.

3.1.8 Hierarchy characterization

Dyadic encounters in the tube test were evaluated over 7 consecutive days of testing. These encounters were further characterized by win style (active versus passive wins), win proportion, and win latency, as well as by overall hierarchical stability (Fan et al 2019). Additional hierarchical attributes were investigated after testing was completed, including despotism and directional consistency. Dominants in each dyad were evaluated for weighted active wins and win latency, also known as time-to-win (TTW), and a correlation matrix was calculated between hierarchical attributes and dominant win attributes.

Despotism is commonly measured in complex hierarchies as an indicator of how dominance is maintained within a social group (Williamson et al 2016, 2017 and 2019). Despotism describes the proportions of all agonistic encounters that are won by a single individual, the alpha. The more despotic an alpha, the more directionally consistent the hierarchy. In these experiments, despotism was measured in each dyad as the total number of dominant wins after all 7 days of testing (i.e., out of 35 total trials).

Directional consistency describes the linearity of the social group by analyzing how frequently wins occurred with the expected outcome (i.e., in favor of the ultimately dominant individual). Directional consistency is evaluated by calculating the number of wins by the highest-ranking individual weighted against their losses as a proportion of all observed events (Williamson et al 2016, Stevens et al 2007). It is closely related to David's score (see 5.1.3), but since David's score is a measure of individual dominance it is more meaningful when there are multiple potential social partners against which an individual can be tested (Gammell et al 2003). Therefore, David's score analysis was reserved for the social instability experiment, when each animal was tested in a modified round-robin test design against multiple other partners. The directional consistency index (DCI) was calculated from the following equation, where H indicates the outcomes occurring with the highest frequency (i.e., dominant wins) and L indicates the outcomes occurring with the lowest frequency (i.e., dominant losses):

$$\mathrm{DCI} = \frac{(H - L)}{(H + L)}$$

Lastly, to further investigate win style as a possible characteristic of rank and/or hierarchies, the proportion of active wins observed by the dominant individual was weighted against its overall frequency of winning. This index was termed the weighted

active wins (Wtd A) and was calculated as follows, where $Wins_{Dom}$ designates all wins by the dominant individual, $Wins_T$ designates the total number of possible wins (i.e., 35 trials), $Wins_A$ designates active wins by the dominant and $Wins_P$ passive wins by the dominant:

$$\text{Wtd A} = \left(\frac{Wins_{Dom}}{Wins_T}\right) \cdot \left(\frac{(Wins_A - Wins_P)}{Wins_{Dom}}\right)$$

3.1.9 Three chamber social approach (3CSA)

The 3CSA test took place in a 50 x 30 x 30 cm apparatus constructed from white PVC sheets. The device was divided into 3 chambers by walls separated with removable guillotine-style dividers. Each iteration of this test consisted of three distinct groups of mice: experimental (or control) mouse, novel mouse #1 (will become the familiar mouse in the third phase), and novel mouse #2. The test took place in three phases: habituation, sociability test, and social novelty test.

1) Habituation: On the first day, animals are allowed to explore the apparatus with all dividers removed for 10 minutes.
2) Sociability: Sociability and social novelty testing occurred on the same day. Two identical wire mesh cups were placed in either chamber, one to contain the naïve (nonexperimental/control) mouse and the other to remain empty in the opposite chamber (this is the novel object). The central chamber remained empty. The subject mouse was placed in the central chamber for a 5-minute habituation period with the dividers in place, preventing access to the outer chambers. After habituation, novel mouse #1 was placed under the wire mesh cup in one side chamber. The dividers were removed, and the subject mouse was allowed to explore chambers freely for a total of 10 minutes.

3) Social Novelty: The subject mouse was returned to the central chamber while novel mouse #2 was placed under a new mesh cup in the chamber previously containing the novel object. The dividers were removed, and the subject mouse allowed to explore freely for another 10 minutes. Tests were recorded to video via an overhead camera for later analysis by individuals blinded to the experimental parameters. After each animal was tested all chambers were cleaned with 70% ethanol.

3.1.10 Novel social encounter

c-Fos expression was examined in response to two different social contexts to evaluate how social rank alters neural activity in response to social novelty and psychosocial stress. The first context will be described here; the second context occurred after exposure to social isolation stress and is described in Chapter 5. All animals were acclimated to the testing environment for 30 minutes prior to testing. Social contexts occurred under dim (< 10 lux) red light conditions.

Following behavioral testing in the three-chamber social approach, mice were divided into groups based on exposure to a brief social encounter (5 minutes after observation of the first social interaction) with a novel age-, strain-, and sex-matched conspecific in a clean cage. Control animals were placed alone into a clean cage for the same amount of time. Afterwards, all mice were immediately dark housed (i.e., all lights turned off and with covered cages) in their home cage for 90 minutes.

3.1.11 Tissue extraction, fixation and processing

c-Fos expression was assessed in mice that were perfused 90 min following a social context. Animals were deeply anesthetized with 0.5 - 0.7 mL Avertin (12.5 mg/mL 2,2,2-tribromoethanol, Sigma-Aldrich, St. Louis, MO) delivered intraperitoneally. Depth of

anesthesia was evaluated several minutes after injection via responsiveness to tail and toe pinch. Mice were placed in dorsal recumbency, an abdominal incision was made and tissue was dissected through the diaphragm, exposing the thoracic cavity. A window was made in the left atrium using sharp dissection, and a 23G needle connected to tubing and a perfusion pump was inserted into the left ventricle. Mice were transcardially perfused with 40-100 mL cold phosphate-buffered saline (PBS) followed immediately by 40-100 mL cold 4% paraformaldehyde (PFA) in PBS. After whole-body fixation, the brain was extracted from the skull and further fixed in 4% PFA for 24 hours. Then the abdominal incision was extended to the urinary bladder. The left and right kidney were located, the adrenals were identified and then gently removed using Brown-Adson forceps and post-fixed in 4% PFA for 24 hours. After fixation, left and right adrenals were cleansed of peri-adrenal adipose tissue and weighed together.

3.1.12 Immunohistochemistry for c-Fos expression

60 μm coronal slices of PFA-fixed brains were cut on a compresstome vibrating microtome (Precisionary, Greenville, NC) spanning rostral-to-caudal from the mPFC to the middle PVT (approximately Bregma +2.68 to –1.46). Antibody staining was performed on free-floating tissue slices in 12-well plates. Slices were permeabilized with 3 x 15 min washes with 0.5% Tween-20 (Sigma, St. Louis, MO) in PBS (PBST) then blocked in 5% goat serum in PBST for 2 hours at room temperature. Sections were incubated overnight in primary antibodies at 4°C on a shaker. Next the slices were washed in 0.5% PBST (3 X 15 min) and then incubated in secondary antibodies for 2 hours at room temperature. After final washes in PBS (3 x 10 min) slices were mounted onto slides with mounting medium with DAPI (Biotium, Fremont, CA) and cover slipped. The primary antibody was rabbit

anti-cFos (1:2000; 226 003, Synaptic Systems, Germany or 1:1500; 226004, Synaptic Systems, Germany), and the secondary antibody was goat anti-rabbit AlexaFluor 647 (1:500; A-21206, Thermo Fisher Scientific, Waltham, MA).

3.1.13 Fluorescence confocal microscopy of brain slices

Images were obtained using an AxioScan.Z1 slide-scanning microscope (Zeiss, Germany) and a Nikon A1 Confocal microscope (Nikon, Japan). 5x images of whole brain slices were evaluated for gross signal expression using the AxioScan slide-scanner. Regions of intense signal were noted and a literature search was performed to determine which regions had potential applicability for identification of rank differences. Ultimately, seven regions were selected for analysis based upon their relevance to sociability and social identity, stress, and regulation of emotional valence: the prelimbic cortex (PL), claustrum (CLA), nucleus accumbens core (nAccC) and shell (nAccSh), lateral septum (LS), paraventricular thalamus (PVT), and paraventricular nucleus of the hypothalamus (PVN). 10x and 20x images were taken (1024x1024 pixel resolution) using a Nikon A1 confocal microscope with active lasers for far-red (c-Fos labeled nuclei, 640 nm) and blue (4',6-Diamidino-2-phenylindole (DAPI)-labeled nuclei, 405 nm). Regions were identified by slice appearance, location and adjacent landmarks per the third edition Franklin and Paxinos mouse brain atlas (Franklin & Paxinos 2008). For every slice, 20x left and right images were obtained for quantification of each region present (i.e., one image from each hemisphere).

3.1.14 Quantification of c-Fos expression in slices

c-Fos positive nuclei were quantified from 20x .nd2 images using Fiji ImageJ software (NIH, Bethesda, USA) using a protocol adapted from the one described by Petersen et al. (Petersen 2021). First the ImageJ scale was converted to measure in mm according to the image resolution (1024x1024 px). Channels were analyzed separately then merged to confirm overlap of c-Fos immunoreactivity (magenta) and DAPI (blue). Regions of interest (ROI) were drawn using the polygon tool according to the mouse brain atlas (Franklin 2008) and saved to the ROI manager. Background interference was reduced using the rolling ball radius function and a 50-pixel radius. The resulting ROI-only image was converted to a new 8-bit (greyscale) image and blurred prior to thresholding using the ImageJ Moments auto-threshold function. The Analyze Particle plugin was used to identify particles of > 100 px size and > 0.5 circularity (some regions, such as the lateral septum, had different sizing requirements due to relatively larger nuclei). In the case of background signal resulting in erroneous automatically derived particle counts, manual counting was performed using the Cell Counter plugin. Counts were normalized by hemisphere and ROI area by summing the total counts for both hemisphere and dividing by the sum of the areas of the ROIs:

$$\text{Normalized count (per slice)} = \frac{(\Sigma Fos\ cells \cdot 10000)}{(\Sigma ROI\ areas)}$$

Counts are reported as c-Fos positive cells per mm^2. c-Fos expression was quantified in 2-5 slices per structure, per mouse. Final counts were averages of all slices for each animal.

The PVT c-Fos expression was further analyzed for the anteroposterior distribution of slices. The subregions were defined according to the coordinates designated by Gao et al. and Zhu et al. (Gao et al 2020, Zhu et al 2022) as anterior PVT (aPVT; from Bregma: –

0.22mm), middle PVT (mPVT; from Bregma: –0.94mm) and posterior PVT (pPVT; from Bregma: –1.82mm). Slices were grouped by subregion and analyzed across groups by rank and experimental condition. Roughly 55% of the PVT images were obtained from the aPVT (84/152 slices or 55.26%) and 45% from the mPVT (68/152 slices or 44.74%). No images were taken from the pPVT.

3.1.15 Statistical analysis – General

Statistical analysis was performed using Prism version 9.4.1 (GraphPad Software, San Diego, CA). Normality of groups was tested with the Shapiro-Wilk test. Two independent samples were compared using two-tailed unpaired Student's t-test unless data was non-Gaussian in distribution, in which case a Mann-Whitney U-test was used to compare ranks. If the variances of normally distributed data differed significantly in the F test, samples were compared using Welch's test.

When more than two independent samples were compared, two-way ANOVA on factors of Condition (or Stress) and Rank was used for normally distributed data and post-hoc analysis was performed using Sidak's test when significant main effects or interaction effects were found. Tukey's multiple comparisons test was used when more than two groups were compared. In figures, if no significant interaction or main effect was found, only the results of the interaction are shown. If a significant main effect but no interaction was found, both are shown and post hoc analysis was only performed upon the main effect that reached significance. Non-Gaussian data with more than two independent samples were analyzed using Kruskal-Wallis test and post-hoc analysis was performed using Dunn's test when significant main effects were found.

Home cage behavioral interactions were scored manually and reported as tabulated events into 2x2 contingency tables where columns represent social rank and rows represent behavioral categories, then analyzed using the Yate's corrected Chi-square test. Direct contacts in the 3CSA were also scored manually and reported as simple counts in 2x2 contingency tables where columns represent social rank and rows represent independent variables of interest, then analyzed using the Yate's corrected Chi-square test.

Normally distributed correlation data were analyzed using a Pearson correlation, otherwise a Spearman correlation was used. c-Fos percent difference from control mean effect size was calculated with Hedge's g statistic to account for the sample size < 50.

Differences were considered significant if their probability of occurring by chance was less than 5% (i.e., tests returned a p-value of less than 0.05). Significance is designated in figures as follows: *$p < 0.05$, **$p < 0.01$, ***$p < 0.001$, ****$p < 0.0001$.

3.1.16 Statistical analysis – FCM EIA

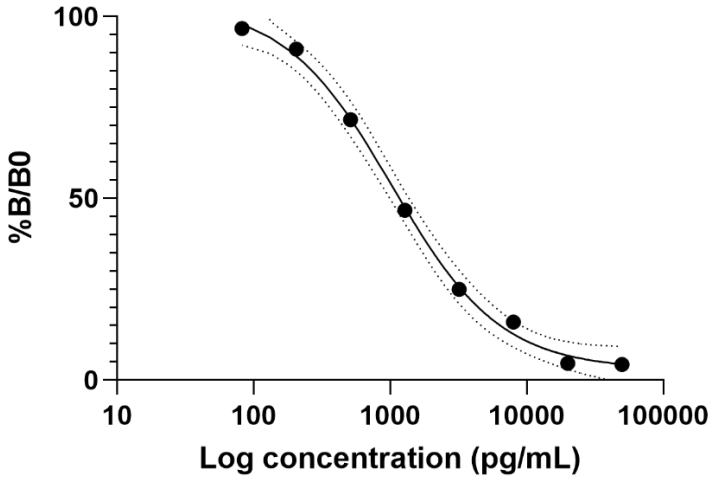

Figure 5. Standard curve used to interpolate well steroid concentrations

An example standard curve derived from a 4-point logistic regression on eight standard values of known concentration. Concentrations presented in log10 format derive a stereotypical sigmoidal standard curve. Dashed lines represent the upper and lower limits of the 95% confidence intervals. *%B/B0*, percent binding over maximum binding.

Optical density (OD) measurements for each well were derived from the plate reader scans. OD values were averaged for the duplicate wells and the coefficient of variation (CV) was calculated for each pair; if CV exceeded 10% the value was excluded from analysis. OD was then converted to percent binding by maximum binding (%B/B0) using the average OD values from the nonspecific binding (NSB) wells and maximum binding (B0) wells put into the following standard formula:

$$\frac{\%B}{B0} = \frac{(Sample\ OD\ -\ NSB)}{(B0\ -\ NSB)} \cdot 100$$

These measurements were input into Prism alongside eight standards (ranging 82 – 50000 pg/mL), the known concentrations of which were used to make a sigmoidal standard curve from which experimental wells were interpolated (Fig. 5). Interpolated sample values were expressed as picograms of steroid per milliliter (pg/mL), which was ultimately converted to nanograms using a dilution factor. The dilution factor accounts for both

sample fecal weight and suspension volume and is derived using the following formula provided in the assay-specific protocol:

$$\text{FCM}\left(\frac{\text{ng}}{\text{g feces}}\right) = \frac{\left(pg\ (\text{interpolated; per well}) \cdot\ extract\ volume\ \cdot dilution\ (\text{e.g. } 100)\right)}{(fecal\ weght\ (\text{in grams}) \cdot sample\ volume \cdot 1000)}$$

Fecal corticosterone metabolites were expressed as nanograms of metabolite per gram of feces. In the above formula, the steroid mass in picograms is derived from the interpolated values, the extract volume is the volume of methanol used in extraction, the dilution factor is 100 (i.e., the 1:100 dilution transferred to each well), the fecal weight is expressed in grams, the sample volume is the volume transferred to the wells, and then dividing by correction factor (1000) expresses the results in nanograms.

FCM values were typically non-normally distributed. Therefore, per guidelines from the assay developer data were tested for normality and if non-Gaussian they were analyzed by a Mann-Whitney U-test or Kruskal-Wallis test (depending on the number of independent variables). Normally distributed data were analyzed by unpaired t-test or two-way ANOVA.

3.2 Results

3.2.1 Dyadic hierarchy formation

We first investigated hierarchy formation, rank characteristics and social behaviors during the dark phase of the murine circadian cycle. Social hierarchies for 14 pair-housed cages were tested daily using competitive exclusion, also known as the tube test, over 7 days total (Fan et al 2019, Fig. 6A). Stability was defined as four consecutive days of identical pair ranking, as was described previously (Fan et al 2019). Adult female dyads rapidly formed stable hierarchies (Fig. 6B, C) with most rank shifts occurring during the first two days of testing (Fig. 6B).

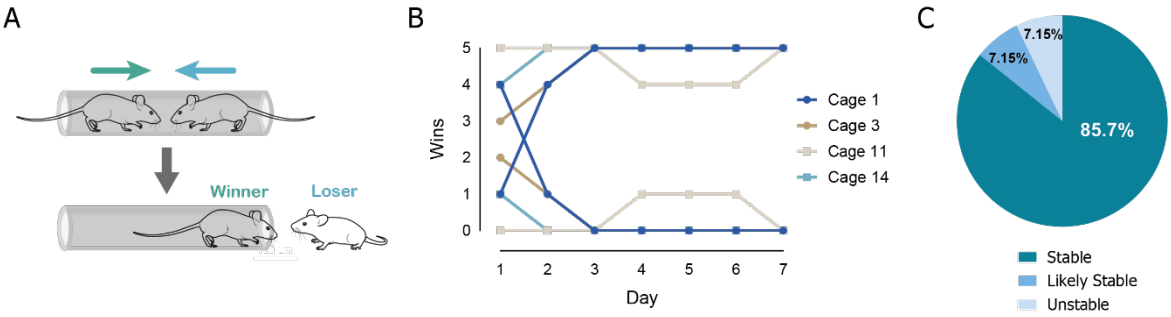

Figure 6. Use of the tube test to evaluate ranks and hierarchy formation

(A) Schematic of a trial of the tube test, or competitive exclusion. Two mice engage in a face-to-face encounter and one mouse wins by forcing the other out of the opposite end of the tube. The mouse to win the majority of 5 trials is the dominant for that day's test.

(B) Sample match data from four different cages (cages #1, #3, #11 and #14) over the 7 consecutive days of competitive exclusion. The dyad of each cage is depicted by two identical lines representing the number of wins (y-axis) per day (x-axis) for each mouse in that pairing. For each day, dominant status is assigned for a mouse that wins 3 or more trials. Likewise, subordinate status is assigned to the mouse that won 2 or fewer trials. Rank shifts between days are therefore represented by lines crossing over one another, as seen with cage #1.

(C) Percentage of pairs that were completely rank-stable by the final day of dominance testing (12 out of 14 total pairs). "Likely stable" describes one hierarchy which on day 7, the final day of testing, had been rank stable for the 3 previous days. "Unstable" describes one hierarchy in which mice switched ranks every day.

By the end of training, the time it took an animal to run the length of the tube did not differ by dominance status, demonstrating that rank did not influence the ability to learn or perform the task (Fig. 7A). As expected, during confrontation dominants won most matches (Fig. 7B), and when subordinates won it took them significantly longer (Fig. 7C) indicating there was increased resistance to losing by dominant animals. During testing there was no difference by rank in win style and most wins were "active", meaning the winner physically forced the other mouse out of the tube through aggressive forward approach and/or pushing (Fig. 7D).

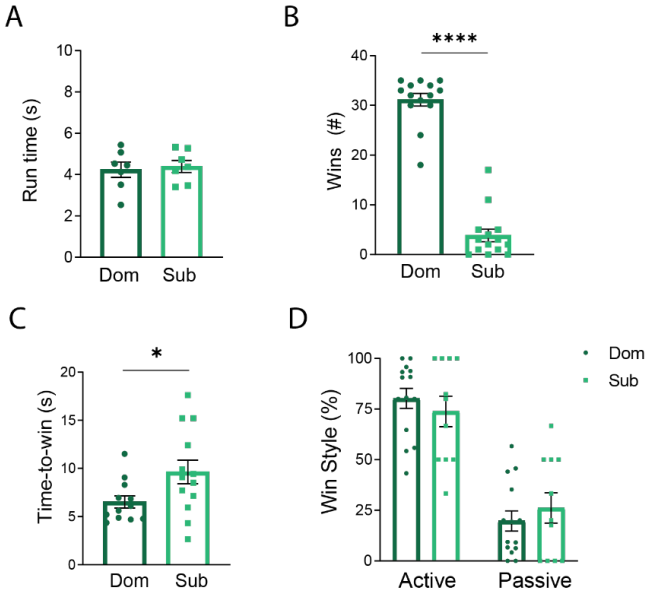

Figure 7. Behavior in the tube test by rank

(A) Average time to run tube on final day of training. N = 14 (7 dom, 7 sub); p = 0.7473 (Unpaired t test, two-tailed).

(B) Total wins at the end of testing. N = 28 (14 dom, 14 sub); ****p < 0.0001 (Mann-Whitney).

(C) Average time-to-win a match. N = 25 (14 dom, 11 sub); *p = 0.0145 (Welch's t test, two-tailed). Three subordinate animals never won a match against their partner and are therefore not included in this analysis.

(D) Percentage of wins of either style at the end of testing. N = 25 (14 dom, 11 sub); significant main effect of Style (F (1, 46) = 77.35, ****p < 0.0001, two-way ANOVA; Sidak multiple comparisons test, Active p = 0.7157, Passive p = 0.7254).

All data expressed as mean ± SEM.

There was a significant positive correlation between a hierarchy's directional consistency and its despotism, as well as a negative correlation between directional consistency and the average time-to-win of that hierarchy's dominant animal (Fig. 8, Table 1). There was a non-significant negative trend relationship between despotism and average dominant time-to-win. The win style of the dominant animal showed no relationship to any other hierarchical attributes.

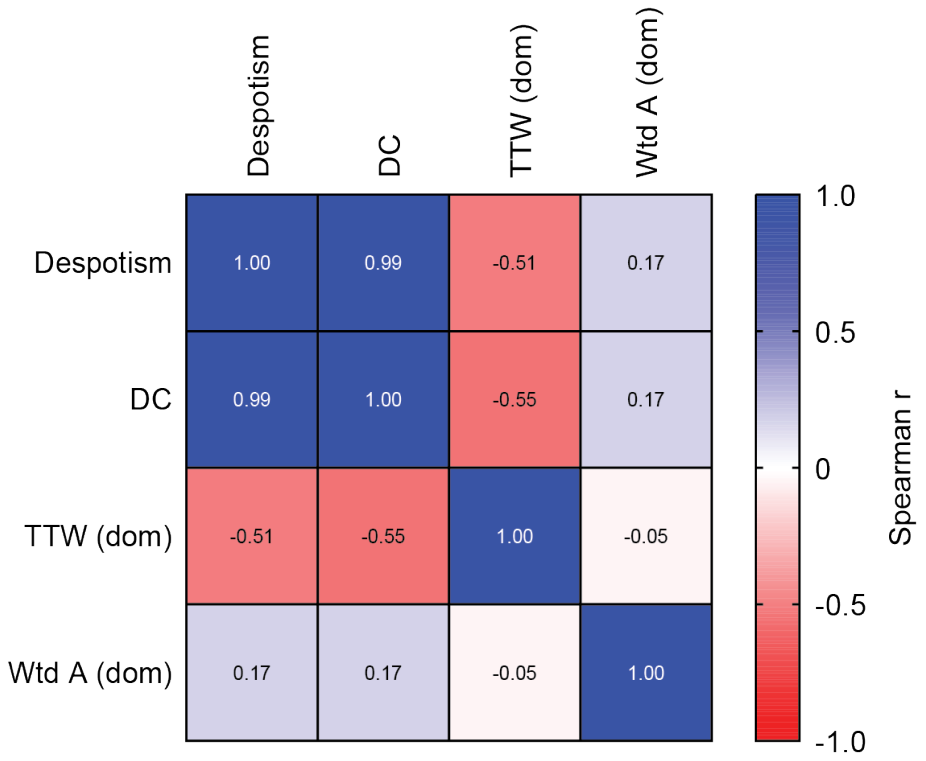

Figure 8. Correlation matrix of hierarchy attributes

Color-coded matrix of r-values for Spearman correlations performed across hierarchical attributes, describing directionality and strength of the relationship. Negative relationships are in shades of red and positive relationships are in shades of blue. *DC*, directional consistency; *TTW (dom)*, average dominant time-to-win; *WtdA (dom)*, weighted dominant active wins.

	Despotism	DC	TTW (dom)	WtdA (dom)
Despotism	1	*0.991 (<0.0001)*	-0.506 (0.067)	0.175 (0.546)
DC	*0.991 (<0.0001)*	1	*-0.546 (0.046)*	0.175 (0.546)
TTW (dom)	-0.506 (0.067)	*-0.546 (0.046)*	1	-0.053 (0.858)
WtdA (dom)	0.175 (0.546)	0.175 (0.546)	-0.053 (0.858)	1

Table 1. Spearman's correlation matrix of hierarchical attributes

Correlation table of values derived from Spearman correlations of hierarchical attributes alongside the significance of the comparison. Numbers are expressed as "r-value (p-value)". Correlations with significant relationships are italicized. *DC*, directional consistency; *TTW (dom)*, average dominant time-to-win; *WtdA (dom)*, weighted dominant active wins.

3.2.2 Home cage behavior

Analysis of home cage behaviors before or after establishing hierarchies did not reveal predictors of rank in social affiliative or nonsocial interactions (Fig. 9A-C). However, one behavior designated as ‘forepaw touch’ was overexpressed by subordinate mice during initial pairing (Fig. 9B, Table 2). Forepaw touch was defined as placement of the forepaws on the head, flank or shoulders of the conspecific accompanied by nonsocial sniffing behavior. It was analyzed separately due to its nonsocial-directed activity following a direct physical interaction. It was closest in presentation to exploratory supported rearing, wherein a mouse uses a wall or other support while engaging in environmental sniffing (Sturman et al 2018). This pattern disappeared when social behavior was reanalyzed after 11 days of continuous pair housing (Fig. 9C, Table 3), indicating the difference was only evident during social introduction. Following 11-day home cage behavior analysis, rank assignment was validated with a food competition task (Fulenwider et al 2022). Results of the food competition task strongly supported the ranks assigned by the tube test (Fig. 9D).

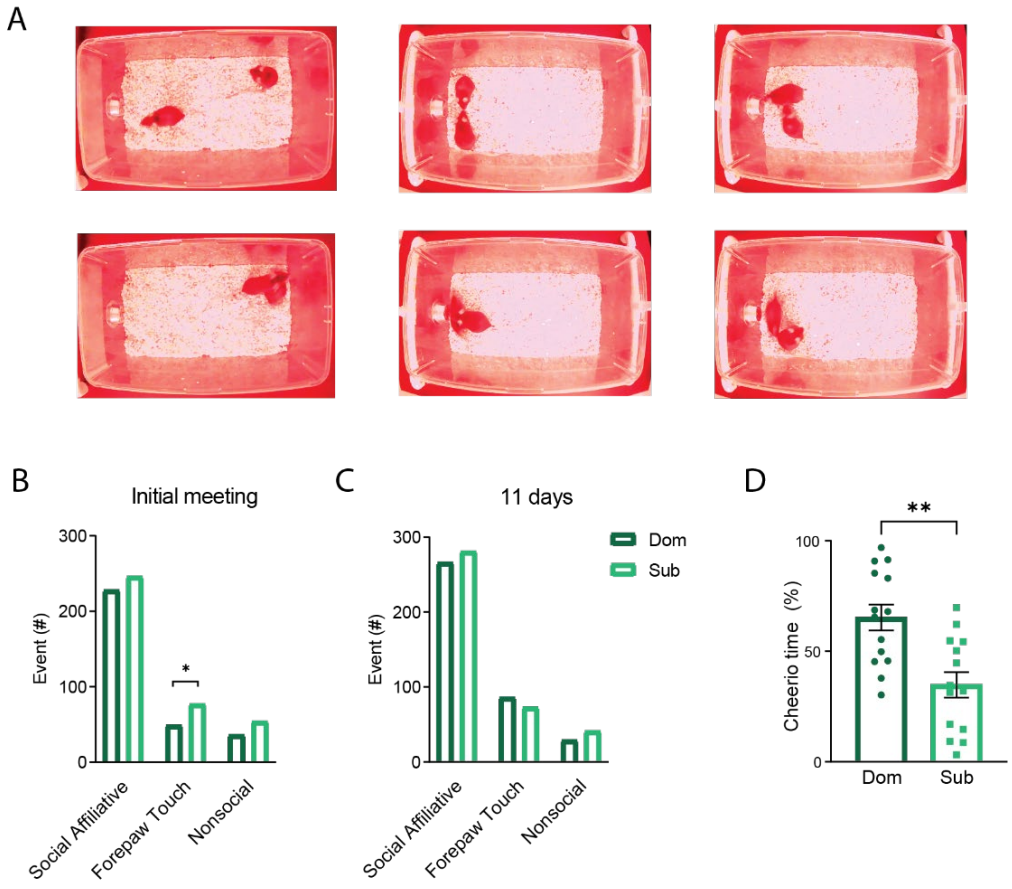

Figure 9. Home cage behavioral analysis and food competition task

(A) Screenshots of example behaviors tabulated during home cage analysis. Top, left-to-right: auto-grooming, nose-to-nose sniffing, flank sniffing. Bottom, left-to-right: forepaw touch, crawl under, anogenital sniffing.

(B) Distribution of behaviors observed during home cage analysis immediately after initial pair introduction. N = 28 (14 dom, 14 sub); no significant relationship between Rank and Social Affiliative (χ2(1, 474) = 0.6081, p = 0.4355); significant relationship between Rank and Forepaw Touch (χ2(1, 126) = 5.782, *p = 0.0162); no significant relationship between Rank and Nonsocial (χ2(1, 90) = 3.209, p = 0.0732, Chi-square test with Yates' correction).

(C) Distribution of behaviors observed during home cage analysis after 11 days of continuous pair housing. N = 28 (14 dom, 14 sub); no significant relationship between Rank and Social Affiliative (χ2(1, 507) = 0.3572, p = 0.5501); no significant relationship between Rank and Forepaw Touch (χ2(1, 159) = 9048, p = 0.3415); no significant relationship between Rank and Nonsocial (χ2(1, 70) = 1.728, p = 0.1887, Chi-square test with Yates' correction).

(D) Percentage of time in direct possession of food reward during food competition task performed after 11 days of pair housing. N = 28 (14 dom, 14 sub); **p = 0.0010 (Unpaired t test, two-tailed).

Data in B and C expressed as simple counts; data in D expressed as mean ± SEM.

	Dom	Sub
Social affiliative	228	246
	100000	100000
	Dom	Sub
Forepaw touch	49	77
	100000	100000
	Dom	Sub
Nonsocial	36	54
	100000	100000

X2, df	Z	P value
0.6081, 1	0.7798	0.4355
X2, df	Z	P value
5.782, 1	2.405	0.0162
X2, df	Z	P value
3.209, 1	1.792	0.0732

Table 2. Contingency tables of home cage behavior counts upon initial introduction

	Dom	Sub
Social affiliative	266	281
	100000	100000
	Dom	Sub
Forepaw touch	86	73
	100000	100000
	Dom	Sub
Nonsocial	29	41
	100000	100000

X^2, df	Z	P value
0.3572, 1	0.5977	0.5501
X^2, df	Z	P value
0.9048, 1	0.9512	0.3415
X^2, df	Z	P value
1.728, 1	1.314	0.1887

Table 3. Contingency tables of home cage behavior counts after 11 days of pairing

3.2.3 Rank performance in OFT prior to pairing

The open field test (OFT) is typically used to observe exploratory, locomotor, and anxiety-like behavioral tendencies. Exploratory behavior can be measured through rearing (Sturman et al 2018), locomotion is tracked through total distance traveled (Sturman et al 2018, Choleris et al 2001), and anxiety is typically characterized by the animal exhibiting thigmotaxis (Simon et al 1994, Cryan & Holmes 2005), which is avoidance of the inner zone of the open arena. In the open field test, future rank was predicted by total and exploratory supported rearing (Fig. 10A, B), but not by stress-sensitive unsupported rearing (Sturman et al 2018), locomotor activity, or anxiety-like behavior (Fig. 10C-F).

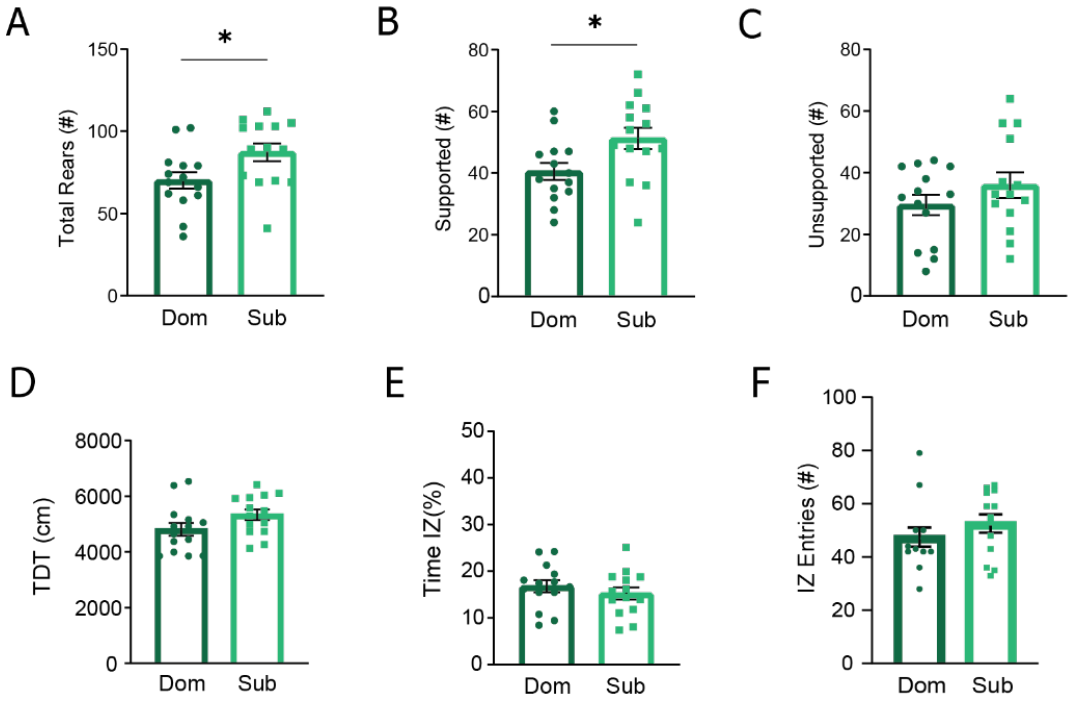

Figure 10. Predictive behavior in the open field test

(A) Total rears in the OFT prior to pair housing. N = 28 (14 dom, 14 sub); *p = 0.0281 (unpaired t-test, two-tailed).

(B) Supported rears in the OFT prior to pair housing. N = 28 (14 dom, 14 sub); *p = 0.0220 (unpaired t-test, two-tailed).

(C) Unsupported rears in the OFT prior to pair housing. N = 28 (14 dom, 14 sub); p = 0.2388 (unpaired t-test, two-tailed).

(D) Total distance traveled in the OFT prior to pair housing. N = 28 (14 dom, 14 sub); p = 0.0912 (Unpaired t test, two-tailed).

(E) Time in the inner zone of the OFT prior to pair housing. N = 28 (14 dom, 14 sub); p = 0.4049 (Unpaired t test, two-tailed).

(F) Entries into the inner zone of the OFT prior to pair housing. N = 28 (14 dom, 14 sub); p = 0.4552 (Unpaired t test, two-tailed).

Data expressed as mean ± SEM. *OFT*, open field test; *TDT*, total distance traveled; *IZ*, inner zone.

3.2.4 Rank performance in 3CSA after stabilization

After 2 weeks of pair housing, a randomly selected cohort of 14 mice were tested in a three-chamber social approach (3CSA) test of sociability and social novelty preference (Fig. 11A). In the first half of the test, the sociability test, the subject mouse has the option to spend time in the chamber containing a novel object or a novel social partner. In the second half, the social novelty preference test, the novel object is replaced with a novel animal, and the subject may explore the novel animal or the familiar one from the first half of the test. Social stimulus animals are contained under a mesh cup, enabling direct sniffing and investigation but no physical contact. Thus, the subject animal has not only the choice of which chamber to spend the test in, but also the choice of whether to approach and investigate the cup. During the sociability test, dominant animals exhibited a social preference in both chamber choice and direct contacts with the social mesh cup, whereas subordinates spent equal time in the social and novel object chambers and made more nonsocial cup contacts as well as more contacts overall (Fig. 11B, C, Table 4). During the social novelty preference test, only subordinate animals displayed a preference for the novel social stimulus in both chamber choice and novel cup contacts, and they again made more contacts overall (Fig. 11D, E, Table 5).

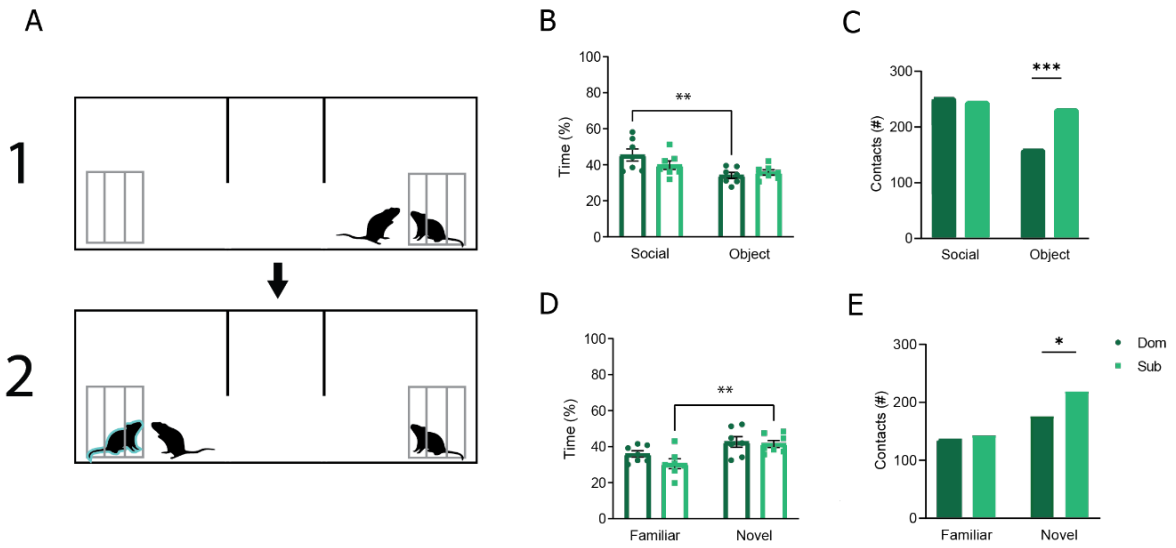

Figure 11. The three-chamber social approach test

(A) Schematic of the three-chamber apparatus and the two test trials performed in succession. 1 represents the sociability test and 2 represents the social novelty preference test.

(B) Percentage of total exploration time in the social or novel object chamber during 3CSA. N = 14 (7 dom, 7 sub); no significant interaction between Chamber x Rank ($F(1, 24) = 2.438$, $p = 0.1315$, two-way ANOVA); significant main effect of Chamber ($F(1, 24) = 10.81$, $^{**}p = 0.0031$, two-way ANOVA; Sidak multiple comparisons test, Dom $^{**}p = 0.0044$, Sub $p = 0.4134$).

(C) Direct contacts with mesh cup in social or novel object chamber during 3CSA. N = 14 (7 dom, 7 sub); significant relationship between Rank and Object contacts ($\chi 2(1, 386) = 13.03$, $^{***}p = 0.0003$); no significant relationship between Rank and Social contacts ($\chi 2(1, 489) = 0.03260$, $p = 0.8567$, Chi-square test with Yates' correction).

(D) Percentage of total exploration time in the familiar social or novel social chamber during 3CSA test. N = 14 (7 dom, 7 sub); no significant interaction between Chamber x Rank ($F(1, 24) = 0.8546$, $p = 0.3645$, two-way ANOVA); significant main effect of Chamber ($F(1, 24) = 13.92$, $^{**}p = 0.0010$, two-way ANOVA; Sidak multiple comparisons test, Dom $p = 0.1140$, Sub $^{**}p = 0.0061$).

(E) Direct contacts with mesh cup in familiar or novel social chamber during 3CSA. N = 14 (7 dom, 7 sub); significant relationship between Rank and Novel contacts ($\chi 2(1, 395) = 4.457$, $^{*}p = 0.0348$); no significant relationship between Rank and Familiar contacts ($\chi 2(1, 276) = 0.2930$, $p = 0.5883$, Chi-square test with Yates' correction).

All data except those in C and E expressed as mean ± SEM.

	Dom	Sub
Object contacts	157	229
	100000	100000

X^2, df	Z	P value
13.03, 1	3.610	0.0003

	Dom	Sub
Social contacts	247	242
	100000	100000

X^2, df	Z	P value
0.0326, 1	0.1806	0.8567

	Dom	Sub
Total contacts	404	471
	100000	100000

X^2, df	Z	P value
4.956, 1	2.226	0.0260

Table 4. Contingency tables of direct contacts counted during sociability test

	Dom	Sub
Novel contacts	176	219
	100000	100000

X^2, df	Z	P value
4.457, 1	2.111	0.0348

	Dom	Sub
Familiar contacts	133	143
	100000	100000

X^2, df	Z	P value
0.2930,1	0.5413	0.5883

	Dom	Sub
Total contacts	309	362
	100000	100000

X^2, df	Z	P value
4.016, 1	2.004	0.0451

Table 5. Contingency tables of direct contacts counted during social novelty test

3.2.5 Biologic and endocrine characteristics of rank

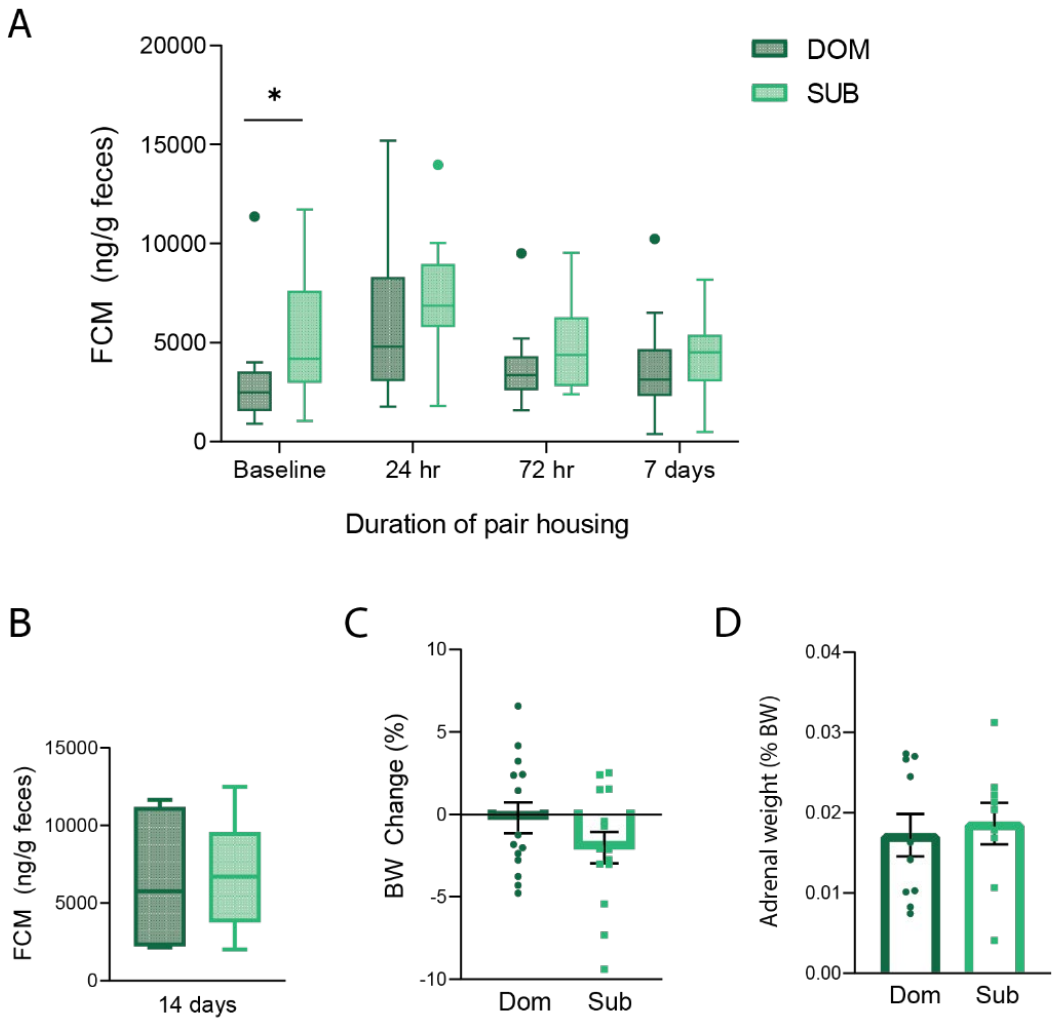

Figure 12. FCM, adrenal weight, and body weight over 2 weeks of pair-housing

(A) FCM excretion over time pair-housed (baseline = prior to pair-housing). N = 28 (14 dom, 14 sub); Baseline *p = 0.0168, 24 hours p = 0.2020, 72 hours p = 0.3164, 7 days p = 0.1852 (Mann-Whitney).

(B) FCM excretion after 2 weeks of pair housing, taken during the 3CSA test. N = 14 (7 dom, 7 sub); 14 days p = 0.8850 (Unpaired t-test, two-tailed).

(C) Percent change in body weight from baseline over two weeks of pair housing. N = 28 (14 dom, 14 sub); p = 0.1876 (Unpaired t test, two-tailed).

(D) Paired adrenal gland weight after two weeks of pair housing expressed as percentage of final body weight. N = 19 (10 dom, 9 sub); p = 0.7197 (Mann-Whitney). One subordinate adrenal gland was damaged during process and these data were excluded from analysis. Data expressed as mean ± SEM. *BW*, body weight.

In addition to exploratory behavior, rank was predicted by fecal corticosterone metabolite (FCM) excretion before pair housing, but not during hierarchy formation or stabilization (Fig. 12A) nor in the cohort tested in the 3CSA after 2 weeks of consecutive pair housing (Fig. 12B). By the end of the tube test sessions, overall FCM was lower compared to the first 24 hours of pair housing (Fig. 12A). Most animals formed stable hierarchies within four days (Fig. 6B, C), meaning that in general an individuals' rank in the first 24 hours of testing predicted their final rank. Therefore, in agreement with home cage behavioral differences (Fig. 9B, C), the rank difference in FCM coincided with the initial period of hierarchical stabilization. At the end of testing, there was no rank difference in body weight change or adrenal weight, suggesting there were no chronic stress effects from maintaining either dominance status (Fig. 12C, D).

3.2.6 c-Fos expression following a novel social encounter

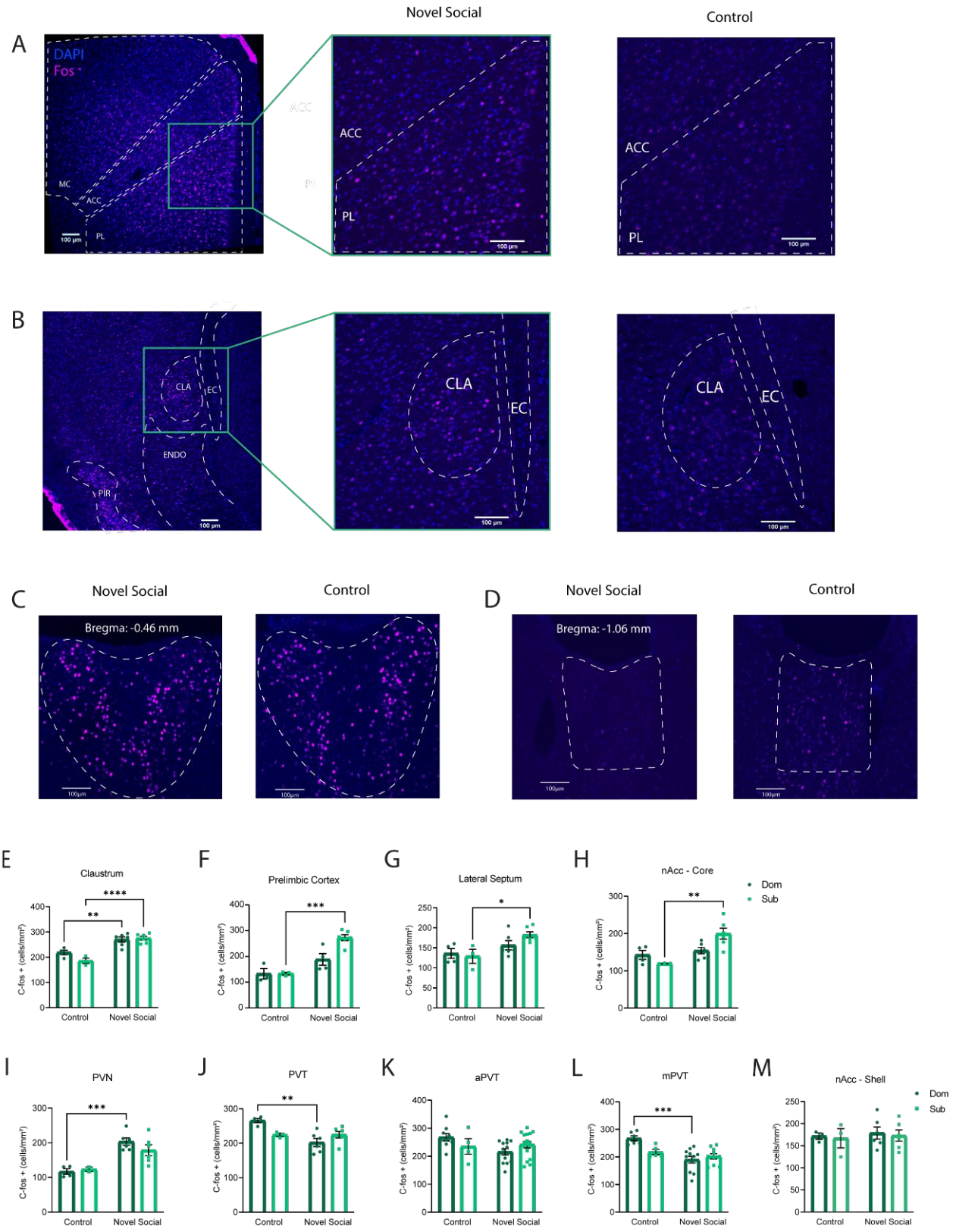

Figure 13. c-Fos expression in stress-naïve mice following a novel social encounter

(A) Representative intensity adjusted images of c-Fos labeling in mPFC. (*Left*) 10x image from an experimental subordinate (Sub); (*Mid*) 20x image containing the PL and ACC of the same animal; (*Right*) 20x image from a control Sub. DAPI counterstain.

(B) Representative intensity adjusted images of c-Fos labeling in CLA. (*Left*) 10x image from an experimental Sub; (*Mid*) 20x image of the same mouse; (*Right*) 20x image from a control Sub.

(C) Representative intensity adjusted images of c-Fos labeling in the aPVT; approximately Bregma: –0.46 mm. (*Left*) 20x image from an experimental dominant (Dom); (*Right*) 20x image from a control Dom.

(D) Representative intensity adjusted images of c-Fos labeling in the mPVT; approximately Bregma: –1.06 mm. (*Left*) 20x image from an experimental Dom; (*Right*) 20x image from a control Dom.

(E) c-Fos expression in CLA; Exp N = 12 (6 dom, 6 sub), Ctrl N = 7 (4 dom, 3 sub); no significant interaction between Condition x Rank ($F(1, 15) = 3.727$, $p = 0.0726$); significant main effect of Condition ($F(1, 15) = 50.48$, ****$p < 0.0001$, two-way ANOVA; Sidak's test, Dom **$p = 0.0032$, Sub ****$p < 0.0001$).

(F) c-Fos expression in PL; Exp N = 10 (4 dom, 6 sub), Ctrl N = 6 (3 dom, 3 sub); significant interaction between Condition x Rank ($F(1, 12) = 6.077$, *$p = 0.0298$); significant main effects of Condition ($F(1, 12) = 32.92$, ****$p < 0.0001$) and Rank ($F(1, 12) = 6.311$, *$p = 0.0273$, two-way ANOVA; Sidak's test, Dom $p = 0.0891$, Sub ***$p = 0.0001$).

(G) c-Fos expression in LS; Exp N = 12 (6 dom, 6 sub), Ctrl N = 7 (4 dom, 3 sub); no significant interaction between Condition x Rank ($F(1, 15) = 1.948$, $p = 0.1831$); significant main effect of Condition ($F(1, 15) = 9.705$, **$p = 0.0071$, two-way ANOVA; Sidak's test, Dom $p = 0.3941$, Sub *$p = 0.0160$).

(H) c-Fos expression in nAcc core; Exp N = 12 (6 dom, 6 sub), Ctrl N = 7 (4 dom, 3 sub); significant interaction between Condition x Rank ($F(1, 15) = 7.533$, *$p = 0.0150$); significant main effect of Condition ($F(1, 15) = 13.27$, **$p = 0.0024$, two-way ANOVA; Sidak's test, Dom $p = 0.7655$, Sub **$p = 0.0012$).

(I) c-Fos expression in PVN; Exp N = 12 (6 dom, 6 sub), Ctrl N = 6 (4 dom, 2 sub); no significant interaction between Condition x Rank ($F(1, 14) = 1.051$, $p = 0.3227$); significant main effect of Condition ($F(1, 14) = 22.03$, ***$p = 0.0003$, two-way ANOVA; Sidak's test, Dom ***$p = 0.0008$, Sub $p = 0.0683$).

(J) c-Fos expression in PVT; Exp N = 12 (6 dom, 6 sub), Ctrl N = 6 (4 dom, 3 sub); significant interaction between Condition x Rank ($F(1, 15) = 8.788$, **$p = 0.0096$); significant main effect of Condition ($F(1, 15) = 8.684$, *$p = 0.0100$, two-way ANOVA; Sidak's test, Dom **$p = 0.0011$, Sub $p > 0.9999$).

(K) c-Fos expression of aPVT slices; Exp N = 27 slices (12 dom, 15 sub), Ctrl N = 13 slices (9 dom, 4 sub); no significant interaction between Condition x Rank ($F(1, 36) = 3.498$, $p = 0.0696$), two-way ANOVA).

(L) c-Fos expression of all mPVT slices; Exp N = 21 slices (11 dom, 10 sub), Ctrl N = 11 slices (6 dom, 5 sub); significant interaction between Condition x Rank ($F(1, 28) = 6.541$, *$p = 0.0162$); significant main effect of Condition ($F(1, 28) = 14.85$, ***$p = 0.0006$, two-way ANOVA; Sidak's test, Dom ***$p = 0.0001$, Sub $p = 0.6212$).

(M) c-Fos expression in nAcc shell; Exp N = 12 (6 dom, 6 sub), Ctrl N = 6 (3 dom, 3 sub); no significant interaction between Condition x Rank ($F(1, 14) = 0.0012$, $p = 0.9732$, two-way ANOVA).

Data expressed as mean ± SEM. *Exp*, experimental group; *Ctrl*, control group; *mPFC*, medial prefrontal cortex; *PL*, prelimbic cortex; *ACC*, anterior cingulate cortex; *MC*, motor cortex; *CLA*, claustrum; *PIR*, piriform cortex; *ENDO*, endopiriform cortex; *EC*, external capsule of the corpus callosum; *nAcc*, nucleus accumbens; *PVN*, paraventricular hypothalamic nucleus; *PVT*, paraventricular thalamic nucleus; *aPVT*, anterior PVT; *mPVT*, middle PVT.

Region	Bregma (range)	Source	SS	F (DFn, DFd)	P value	Post hoc factor	Group	P value
CLA	0.26 – 1.34	Inter. Cond. Rank	1603 21715 847.7	F (1, 15) = 3.727 F (1, 15) = 50.48 F (1, 15) = 1.971	0.0726 <0.0001 0.1807	Cond.	Dom Sub	0.0032 <0.0001
PL	1.54 – 2.68	Inter. Cond. Rank	6485 35135 6734	F (1, 12) = 6.077 F (1, 12) = 32.92 F (1, 12) = 6.311	0.0298 <0.0001 0.0273	Cond.	Dom Sub	0.0891 0.0001
LS	0.14 – 1.18	Inter. Cond. Rank	1206 6007 394.4	F (1, 15) = 1.948 F (1, 15) = 9.705 F (1, 15) = 0.6372	0.1831 0.0071 0.4372	Cond.	Dom Sub	0.3941 0.0160
nAcc - Core	0.74 – 1.78	Inter. Cond. Rank	5148 9065 539.3	F (1, 15) = 7.533 F (1, 15) = 13.27 F (1, 15) = 0.7892	0.0150 0.0024 0.3884	Cond.	Dom Sub	0.7655 0.0012
nAcc - Shell	0.74 – 1.78	Inter. Cond. Rank	1.135 167.0 115.8	F (1, 14) = 0.0012 F (1, 14) = 0.1724 F (1, 14) = 0.1195	0.9732 0.6843 0.7347			
PVN	-0.22 – -1.22	Inter. Cond. Rank	878.8 18424 323.9	F (1, 14) = 1.051 F (1, 14) = 22.03 F (1, 14) = 0.3872	0.3227 0.0003 0.5438	Cond.	Dom Sub	0.0008 0.0683
PVT	-0.22 – -1.34	Inter. Cond. Rank	4424 4372 370.9	F (1, 15) = 8.788 F (1, 15) = 8.684 F (1, 15) = 0.7367	0.0096 0.0100 0.4042	Cond.	Dom Sub	0.0011 >0.9999
aPVT by slice	-0.22 – -0.82	Inter. Cond. Rank	6719 4096 91.05	F (1, 36) = 3.498 F (1, 36) = 2.132 F (1, 36) = 0.0474	0.0696 0.1529 0.8289			
mPVT by slice	-0.94 – -1.34	Inter. Cond. Rank	6826 15497 2507	F (1, 28) = 6.541 F (1, 28) = 14.85 F (1, 28) = 2.402	0.0162 0.0006 0.1324	Cond.	Dom Sub	0.0001 0.6212

Table 6. 2-way ANOVA table: c-Fos expression after social novelty

Inter., interaction; *Cond.*, condition; *SS*, sum-of-squares; *PL*, prelimbic cortex; *CLA*, claustrum; *LS*, lateral septum; *nAcc*, nucleus accumbens; *PVN*, paraventricular hypothalamic nucleus; *PVT*, paraventricular thalamic nucleus; *aPVT*, anterior PVT; *mPVT*, middle PVT; *Dom*, dominant; *Sub*, subordinate.

This IHC experiment was designed to determine whether rank is associated with changes in neural activity in response to social stimuli in both the presence and absence of

psychosocial stress. Therefore, I examined the expression of the immediate early gene c-Fos after exposure to a novel social encounter (Fig 13A-D), or after social reunion with a familiar social partner following chronic social isolation (contexts described in Chapter 3 and Chapter 6, respectively).

Social novelty increased c-Fos expression across ranks in the claustrum (CLA; Fig. 13E), although interestingly subordinates had insignificantly lower claustral expression than dominants under the control condition (solitary exposure to a novel cage). Specifically in subordinates, social novelty increased c-Fos in the prelimbic cortex (PL), the lateral septum (LS), and the core of the nucleus accumbens (nAccC) (Fig. 13F-H). In contrast, in dominants social novelty increased c-Fos expression in the paraventricular nucleus of the hypothalamus (PVN) and reduced it in the paraventricular thalamus (PVT) (Fig. 13I, J). Upon examining slice coordinates, it was found that this decrease in c-Fos expression was specific for the middle PVT (mPVT) and not the anterior PVT (aPVT) (Fig. 13K, L). No differences were observed in c-Fos expression in the nAcc shell (nAccSh) by rank or experimental condition (Fig. 13M).

3.3 Discussion

3.3.1 Dyadic hierarchy formation

In this study I paired adult female mice and studied the formation and maintenance of dyadic female social hierarchies under different conditions. Females rapidly formed stable rank pairings that remained consistent during behavioral testing and over several weeks of co-housing (Fig. 6C, B; Fig. 9D). Dominant status was characterized in the tube test by winning the majority of matches and by greater resistance to losing, but not by a difference in overall win style (Fig. 7B-D). Additionally, the win style of the dominant animal showed no relationship to despotism or directional consistency, indicating win style is less cohesively related to dominance and hierarchy characteristics than is average time-to-win (Figure 8, Table 1). Collectively this suggests that both ranks use similar strategies to win, but that subordinates retreat from the tube more readily. It also shows that average time-to-win is a measure sensitive to both social identity and hierarchical constitution in female mice, which has not been demonstrated previously. I argue that the tendency of the subordinates to retreat is furthermore reflective of one of the intrinsic traits of that rank revealed by the OFT and other behavioral tests; a pro-exploratory motivation.

3.3.2 Home cage behavior

Rank characteristics identified in home cage behaviors were also dependent upon hierarchical constitution and potentially, novelty. None of these behaviors were elicited by actions of the investigator, except those observed in the food competition task (FCT; Fig. 9D).

Animals that became subordinate in future pairings engaged more frequently in the pseudo-social “forepaw touch” behavior in the home cage upon initial meeting, but not

once hierarchies became established (Fig. 9A-C, Table 2, Table 3). Unlike the other behaviors tabulated during this analysis, forepaw touch has not been explicitly described in the literature to-date but presented most similarly to supported rearing behavior in the open field (Sturman et al 2018). Initially it was categorized as a push behavior akin to "boxing" and "wrestling" behaviors characteristic of intermale aggression (Scott 1966, Nordman et al 2020), but this was disregarded due to the absence of reciprocal aggression or escape behaviors on the part of the conspecific.

Indeed, aggressive agonistic behaviors were not observed outside of pushing in the tube test, and not even during the food competition task although animals did "steal" the food reward from one another's paws and mouths quite readily. Fascinatingly, a subset of female pairs exhibited a behavior that resembled "sharing", wherein one animal indicated interest in a food item possessed by the social partner via sniffing, and the possessor responded by either dropping or passing the food item to its partner. Importantly, this behavior was always reciprocal; when the original possessor of the food item expressed renewed interest, the other social partner relinquished it to them and engaged in another passive or exploratory behavior. This was distinct from the "stealing" behavior, which was met with resistance to giving up the food reward either by pulling away, running away, or snatching the food back immediately upon losing it. This "sharing" behavior was only present in a minority of pairs and was difficult to characterize under red light conditions, therefore it was not analyzed statistically. It is included in this discussion because food sharing is documented in rodents (Mogil 2012), and therefore could be studied in the context of characterizing female hierarchies in the future.

Of note, tail rattling was only observed anecdotally during the tube test after completion of a match, and typically by the expelled animal, but was infrequent and not measured. Additionally, once cages were covered and prepared for return to the vivarium after the tube test, sounds indicating fighting were occasionally noted. Therefore, a further investigation into interfemale aggression could include a period of unobserved home cage behavior monitoring immediately following the tube test. Since fear conditioning is known to elicit tail rattling behavior, this could also be used in the future to expand this contextual study to non-agonistic fear-based responses.

Interestingly, neither social affiliative nor non-social interactions differed by rank, although in general subordinates engaged in more behaviors of any type. This suggests that subordinates express more investigative behaviors in social contexts, and forepaw touch specifically in novel social environments. Given the evidence for social novelty in established subordinates and exploratory preferences in future subordinates (see 3.3.3 and 3.3.4), forepaw touch may be novelty-sensitive and ethologically both a social and exploratory behavior.

3.3.3 Rank performance in OFT prior to pairing

In the open field, future subordinates engaged in more rearing behavior than dominants independent of locomotor activity and anxiety-like behavior (Fig. 10A-F). Rearing is considered an exploratory behavior and has two general manifestations: supported and unsupported (Sturman et al 2018, Wesson 2013). Supported rearing is a relatively stable characteristic of exploration and general activity, whereas unsupported rearing is considered a stress-sensitive behavior in that acute stress and aversive environments reduce its occurrence in the open field (Sturman et al 2018). Therefore, along

with home cage behavioral differences, the expression of specifically more supported rears in the open field was considered evidence of more exploratory behavior in future subordinates.

These behavioral characteristics may underlie a broader difference in motivation that influences, or is influenced by, an animals' social status. For example, in male mice subordinate animals have been observed to assume exploratory behaviors upon first exposure to the open field (Benton & Brain 1979, Varholick et al 2018). Despite this, a recent meta-analysis (Varholick et al 2021) found that study heterogeneity has resulted in lack of a clear relationship between behavior in the open field and rank in male mice. It is also important to note that all behavioral tests in that analysis were listed as outcome measures, implying none were used in a predictive capacity prior to dominance testing. The behavioral differences observed in this study may therefore represent some of the intrinsic traits defining female social status (Van Den Berg et al 2015), since they were independent of a history of winning agonistic encounters. Further studies will be necessary to determine the importance of context novelty in reproducing these baseline differences during different phases.

3.3.4 Rank performance in 3CSA after hierarchy stabilization

After hierarchies stabilized, dominants exhibited greater sociability in the 3CSA whereas subordinates demonstrated a greater preference for social novelty and made more direct cup contacts overall in either context (Fig. 11 A-E, Table 4, Table 5). Given that in the first half of the test both exploratory offerings were novel, these findings suggest a greater motivation for exploration in novel contexts for subordinate females and a pro-social motivation for dominant females. Notably, when home cage behavior was measured

after stabilization (i.e., when the pairing was no longer novel), the rank difference in forepaw touch had disappeared (Fig. 9C, Table 3). Considering the results from baseline OFT and home cage behavior, these findings collectively support a greater general exploratory drive in subordinates.

3.3.5 Biologic and endocrine characteristics of rank

Several sex differences in behavioral and biological attributes associated with rank in male mice were observed; female subordinates excreted more fecal corticosterone metabolites (FCM) at baseline but not throughout testing in the absence of applied stressors (Fig. 12A, B), and female subordinates lost an insignificantly greater amount of weight at the end of 14 days of continuous pair housing (Fig. 12C). At the experimental endpoint, adrenal weights demonstrated that hierarchy maintenance did not cause disproportionate chronic stress in either rank (Fig. 12D), which agreed with 14-day fecal corticosterone metabolite measurements (Fig. 12B).

The predictive subordinate elevation in corticosterone metabolite excretion prior to hierarchical stabilization coincided with predictive behavioral attributes characteristic of exploratory motivation. Circulating glucocorticoids, beyond indicating subjective responses to stressors, exert well-established influence over behavior (Zhao et al 2009, Murray et al 2008, Ali et al 2015). Therefore, while higher baseline fecal corticosterone metabolite excretion is characteristic of subordinate females it does not necessarily signify that subordinate status is inherently more stressful, but rather may serve a secondary purpose that influences the behavioral manifestations of subordinate rank.

3.3.6 c-Fos expression following a novel social encounter

In rodents, it has been shown that in the medial prefrontal cortex (mPFC) the anterior cingulate cortex receives mostly sensorimotor information whereas the prelimbic cortex (PL) receives limbic information including through the claustrum (CLA) and midline thalamus (Hoover & Vertes 2007). The prelimbic cortex is furthermore involved in social decision making and response coordination to valenced social encounters; the prelimbic cortex becomes activated in socially isolated male mice exposed to a novel male conspecific (Wang et al 2014), and prelimbic GABAergic ensembles elicit differential responses to novel versus familiar social encounters (Zhao et al 2022). Importantly, increased excitability in the dorsal mPFC, including the prelimbic region, is associated with dominance in male mice (Wang et al 2011 and 2014). Interestingly, social novelty disproportionately increased prelimbic c-Fos expression in subordinates (Fig. 13F), supporting its role in novelty salience while also suggesting a sex-difference in the prelimbic manifestation of dominance that has not been described previously. The rank difference also further supports a generally heightened responsiveness to novelty in subordinate females.

The claustrum (CLA) is a lateralized region that also coordinates salience detection, vigilance, and attention, but it is primarily associated with the integration and relay of cortical and limbic information (Goll et al 2015, Jackson et al 2020). The elevation of claustral c-Fos expression in both ranks is likely indicative of a general increase in arousal and information processing (Fig. 13E). However, the patterns of c-Fos expression in other areas examined may lend insight into how animals of different rank recruit the claustrum in response to social novelty.

Whereas the claustrum is a cortical-adjacent integratory hub, the centrally located lateral septum (LS) is in an anatomically favorable position to receive and transmit information throughout the brain. It follows that the lateral septum has well-established roles in mediating social behavioral responses including social aggression, recognition, and preference (Gabor et al 2012, Zoicas et al 2014, Menon et al 2018 and 2021). One potential role for the lateral septum is valence modulation of social stimuli (Menon et al 2021). For instance, increased c-Fos expression in the lateral septum has been demonstrated in socially avoidant female mice (Menon et al 2018), but oxytocin (OXT) signaling in the lateral septum is involved in social fear extinction and prosocial behavior (Menon et al 2018, Zoicas et al 2014). Perhaps one of the most well-researched functions of the lateral septum involves the regulation of aggression, which in rodents is modulated by both OXT and arginine vasopressin (AVP) in a sex-specific manner (Gabor et al 2012, Menon et al 2021). In this study, c-Fos expression in the lateral septum increased in subordinate animals following social novelty (Fig. 13G). Since in the three-chamber social approach task (3CSA) subordinates did not demonstrate avoidance behavior (Fig. 11 D, E) it is possible that the subordinate lateral septum actively recruits OXT signaling mechanisms to promote social fear extinction and facilitate approach in socially novel contexts. Future functional and cell-type studies are necessary to test this hypothesis.

The nucleus accumbens (nAcc) is part of the mesocorticolimbic system, which is involved in coordinating reward motivated behavior in response to stimuli such as social interactions and addictive substances (Salgado & Kaplitt 2015, Dolen et al 2013, Rogers-Carter et al 2019, Saddoris et al 2013). The nucleus accumbens is divided into two functionally distinct regions – the core and the shell. The nucleus accumbens core is

associated with social reward and social decision making and has been shown to be crucial for value assignment during Pavlovian conditioning (Dolen et al 2013, Rogers-Carter et al 2019, Saddoris et al 2013). Importantly, the core is heavily involved in motor outputs related to reward approach and acquisition (Saddoris et al 2013). In contrast, the nucleus accumbens shell is associated with greater dopaminergic signaling to un-cued reward delivery and aversive stimuli such as foot shock, as well as with the assignment of hedonic value to stimuli (Saddoris et al 2013). In this study, neither intervention produced a significant change in the nucleus accumbens shell (Fig. 13M and 31K), suggesting that neither rank nor social isolation stress influences the hedonic value of social interaction in females. Of course, further studies investigating expression in response to social novelty following social isolation could produce different results. Social novelty produced an increase in c-Fos expression in the core, but this change was specific to subordinates (Fig. 13H). This is consistent with the proposed narrative of neural changes facilitating social approach in the context of social novelty and may reflect the higher exploratory drive that is characteristic of subordinates behaviorally.

The paraventricular nucleus of the hypothalamus (PVN), a component of the eponymous hypothalamic-pituitary-adrenal (HPA) axis, has been implicated in several functions regulating social behavior including emotional state perception (Froemke & Young 2021, Wu & Hong 2022), and social transmission of stress (Sterley et al 2018). The PVN is also a key region in the maintenance of social homeostasis; PVN CRH neurons are capable of rapid feedback in coordinating behavior responses to acute stress, and OXT and AVP signaling in the PVN regulate social affiliation (Matthews & Tye 2019). Importantly,

both aversive and appetitive stimuli can acutely stimulate PVN activity and result in corticosterone production (Buwalda et al 2012).

In dominant animals, social novelty increased c-Fos expression in the PVN (Fig. 13I). On its own, this could be interpreted as social novelty inducing a stress response in dominants or instigating prosocial behavior (or both). Since social avoidance was not a characteristic of dominants in the three-chamber social approach (Fig. 11 B, C), but dominants instead divided time equally between familiar and novel social partners (Fig. 11 D, E), this could indicate that the investigation by dominant females primarily served the purpose of reinforcing their own dominance status. If that is the case, increased activity in the PVN could reflect an adaptation to a social context requiring exertion of dominance to signify rank. In other words, the pro-social motivation of dominant females may not be affiliative in nature, but rather territorial. However, it is equally important to note that subordinate animals did experience an increase in expression that did not reach significance. Therefore, the selective difference in dominant animals in the novel social encounter may simply be a result of low subordinate population size. Of course, this trend in subordinates could also be interpreted as an effect of condition; novel social encounters are certainly more stimulating, and likely more stressful, than placement in a novel cage and the PVN is sensitive to arousing stimuli (Buwalda et al 2012). Nevertheless, the results of the social isolation experiment lend greater insight into this rank-specific change (see Chapter 6, Fig. 31 and Fig. 32).

The paraventricular thalamus (PVT) is a also key homeostatic regulator that has important roles in modulating arousal, valence and motivation (Gao et al 2020, Zhu et al 2022, Penzo & Gao 2021). Like the PVN, the PVT has been shown to influence prosocial

behavior in rodents (Wu & Hong 2022, Penzo & Gao 2021, Yamamuro et al 2020). The paraventricular thalamus furthermore is essential for the appropriate execution of context-dependent approach or avoidance behavior (Choi & McNally 2017, Choi et al 2019). Importantly, it has been recently demonstrated that the murine paraventricular thalamus has spatially and genetically distinct neuronal subpopulations with divergent associations in processing rewarding and aversive stimuli (Gao et al 2020, Zhu et al 2022). Both the anterior and posterior regions of the paraventricular thalamus exhibit reduced GCaMP6s activity during social interactions (Gao et al 2020). However, activity in the anterior PVT (aPVT) is further involved in conveying high- and low-arousal information to the cortex and fear state information to the brainstem, whereas the posterior PVT (pPVT) increases activity in response to somatic aversive stimuli such as foot shock or tail suspension (Gao et al 2020, Zhu et al 2022). Within the aPVT, different functional connectivity has also been found in neurons between Bregma –0.22 to –0.94 and a subpopulation called the middle PVT (mPVT) which starts at Bregma –0.94. Specifically, the mPVT and pPVT maintain higher brainstem connectivity via the parabrachial nucleus and may be more sensitive to aversion than the aPVT (Zhu et al 2022). Therefore, we also examined the anteroposterior distribution of paraventricular thalamus c-Fos expression across groups.

A novel social encounter reduced dominant c-Fos expression in the paraventricular thalamus (Fig. 13J), and upon analyzing slice coordinates we found that the decrease reached significance in the mPVT slices but not in the aPVT slices (Fig. 13K, L). The decreased c-Fos expression in mPVT suggests that the paraventricular thalamus of dominant animals exposed to social novelty suppresses aversive signaling pathways and facilitates social investigation through PVN and claustral activation. The PVN and PVT

possibly coregulate social homeostasis in dominants by detecting the change in social environment and regulating effector responses eliciting prosocial investigatory behavior. Functional studies will be required to test this hypothesis, but the c-Fos pattern indicates animals of different ranks employ distinct neural strategies for responding to social novelty; namely, downregulation of the mPVT and upregulation of the PVN is unique to dominants whereas upregulation of the prelimbic cortex, lateral septum, and nucleus accumbens core is unique to subordinates.

To summarize, in agreement with behavior, the subordinate-specific pattern of enhanced c-Fos expression in the prelimbic cortex, lateral septum, and nucleus accumbens core is consistent with a pro-exploratory motivation engaging salience evaluation, attention and social approach in the context of social novelty. Collectively this suggests a disproportionate effect of social novelty on decision making, information relay, and potentially social reward in subordinates, which is consistent with the rank difference in social novelty preference identified in the three-chamber social approach task. Conversely, dominant animals engage a contrasting pattern of activity through the PVN and PVT, suggesting dominants interpret novel social scenarios as a derivation from baseline requiring homeostatic correction. Indeed, the lack of prelimbic recruitment in dominants is consistent with a study in mPFC-lesioned rats which demonstrated elevated PVN c-Fos mRNA expression in response to acute stressors (Figueiredo et al 2003). Interestingly, in that same study mPFC lesions did not result in elevated claustral c-Fos expression after restraint stress, suggesting the recruitment of the claustrum in our study is involved in the salience processing of the stressor. This is supported by the fact that the elevation in claustrum c-Fos expression was ubiquitous across ranks.

4. CIRCADIAN INFLUENCE ON RANK CHARACTERISTICS

4.1 Materials and Methods

4.1.1 Study design

Since the original experiment was conducted during the dark phase, and circadian rhythms and lighting conditions can affect behavior and CORT excretion (Yang et al 2008, Zhang et al 2017, Touma et al 2003, Pobbe et al 2010), baseline open field behavior and fecal corticosterone metabolites were compared across phases to evaluate the influence of time-of-day on predictive rank characteristics. The mice that would be used in the social instability stress (SIS) experiment had identical treatment to the original dark phase experiment until the tube test was employed, and their baseline data were analyzed as a comparative cohort tested during the light phase. Rank was retrospectively incorporated into the analysis based upon final David's score assigned after the social instability experiment or based upon dyadic results of the tube test for the control animals.

4.1.2 Housing, lighting conditions and circadian phase

Dark circadian phase subjects were 28 adult 3–4-month-old female C57BL6/J mice (Jackson Laboratory, Bar Harbor, Maine). Animals were housed on a 12:12 hour reverse light cycle; food and water were provided ad libitum. All testing was performed during the active (dark) phase of the circadian cycle under red LED light.

Social instability subjects were 40 adult 3–4-month-old female C57BL6/J mice (Jackson Laboratory, Bar Harbor, Maine). Animals were housed on a 12:12 hour light cycle; food and water were provided ad libitum. All testing was performed during the inactive (light) phase of the circadian cycle under ambient white light.

All fecal samples were obtained during the same time-of-day within experiments, and at least 2 hours into the phase of behavioral testing (i.e., 2 hours after lights “on” for light circadian phase experiment or “off” for dark circadian phase experiment).

4.1.3 Open field test

Light intensity in the open field test was matched to that used during the dark phase experiment (<15 lux). The dark circadian phase experiment used red LED overhead lighting and the light circadian phase experiment used white fluorescent overhead lighting. Other than the use of white light, administration of the OFT was no different than the previous experiment (see 3.1.4 for methods). A luxometer compatible with detection of LED light and red wavelengths was used to monitor intensity of light in the center of the open field arena prior to each experiment.

4.2 Results

4.2.1 Phase differences in the open field

In the open field test, phase significantly affected rearing behavior (Fig.14 A-C). Total rearing (Fig. 14A) and supported rears (Fig. 14B) were significantly higher during the dark phase in subordinates only. Unsupported rearing, which is sensitive to acute stress (Sturman et al 2018), was lower during the light phase (Fig. 14C), indicating that light phase testing was more stressful, or alternatively that it produced greater vigilance. Crossings into the inner zone (IZ) of the open field were more frequent during the dark phase (Fig. 14D), but overall time spent in the inner zone was not affected by phase (Fig. 14E), suggesting increased exploratory activity but not anxiolysis during the dark phase (Simon et al 1994, Choleris et al 2001, Cryan & Holmes 2005). There was no effect of phase on total distance traveled (TDT) for animals of either rank (Fig. 14F).

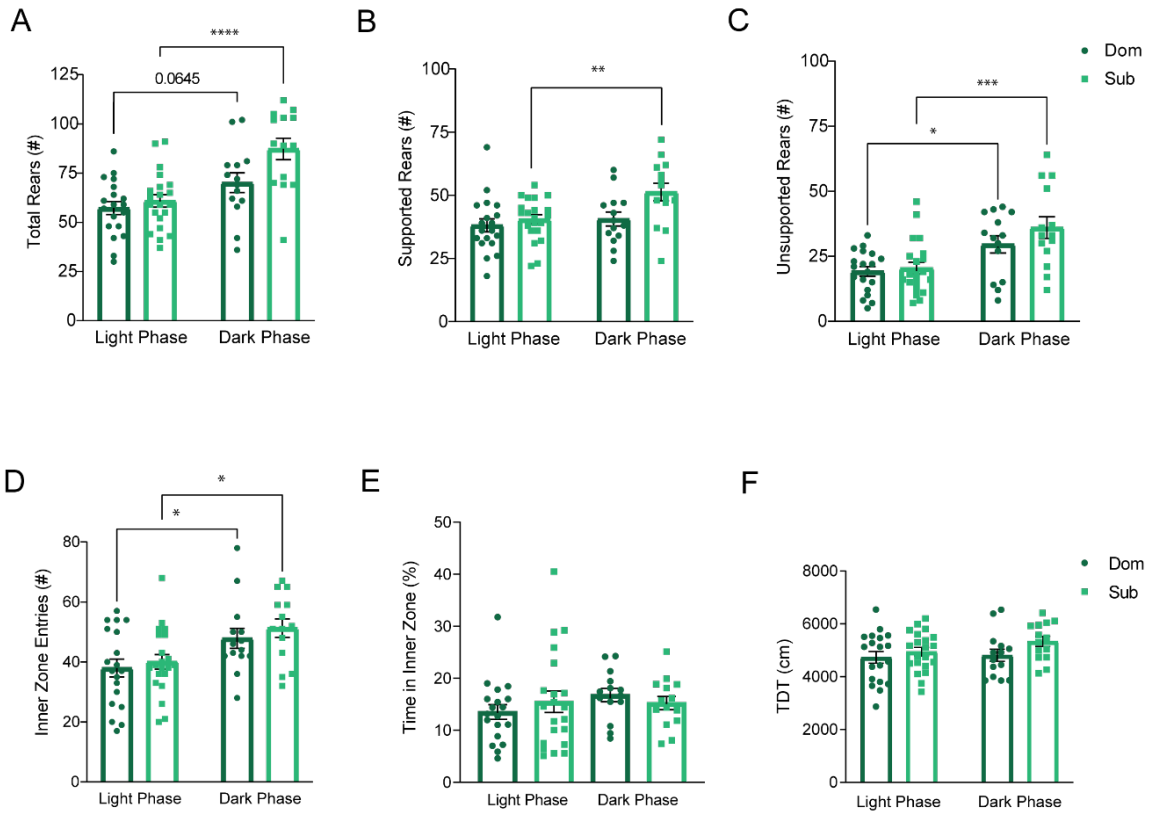

Figure 14. Circadian influence on behavior in the OFT

(A) Total rears in the OFT. Light Phase N = 40 (19 dom, 21 sub), Dark Phase N = 28 (14 dom, 14 sub); no significant interaction between Phase x Rank ($F(1, 64) = 2.670$, $p = 0.1072$); significant main effects of Phase ($F(1, 64) = 22.58$, ****$p < 0.0001$) and Rank ($F(1, 64) = 6.328$, *$p = 0.0144$, two-way ANOVA; Sidak's multiple comparisons test, Dom $p = 0.0645$, Sub ****$p < 0.0001$).

(B) Supported rears in the OFT. Light Phase N = 40 (19 dom, 21 sub), Dark Phase N = 28 (14 dom, 14 sub); no significant interaction between Phase x Rank ($F(1, 64) = 2.535$, $p = 0.1163$); significant main effects of Phase ($F(1, 64) = 6.418$, *$p = 0.0138$) and Rank ($F(1, 64) = 6.235$, *$p = 0.0151$, two-way ANOVA; Sidak's multiple comparisons test, Dom $p = 0.7622$, Sub **$p = 0.0089$).

(C) Unsupported rears in the OFT. Light Phase N = 40 (19 dom, 21 sub), Dark Phase N = 28 (14 dom, 14 sub); no significant interaction between Phase x Rank ($F(1, 64) = 0.8231$, $p = 0.3677$); significant main effect of Phase ($F(1, 64) = 20.89$, ****$p < 0.0001$, two-way ANOVA; Sidak's multiple comparisons test, Dom *$p = 0.0252$, Sub ***$p = 0.0004$).

(D) Inner zone entries in the OFT. Light Phase N = 40 (19 dom, 21 sub), Dark Phase N = 28 (14 dom, 14 sub); no significant interaction between Phase x Rank ($F(1, 64) = 0.05040$, $p = 0.8231$); significant main effect of Phase ($F(1, 64) = 12.77$, ***$p = 0.0007$, two-way ANOVA; Sidak's multiple comparisons test, Dom *$p = 0.0438$, Sub *$p = 0.0170$).

(E) Time spent in IZ in the OFT prior to pair housing. Light Phase N = 40 (19 dom, 21 sub), Dark Phase N = 28 (14 dom, 14 sub); no significant difference across groups (H (3) = 4.008, p = 0.2606, Kruskal-Wallis). (F) Distance traveled in the OFT. Light Phase N = 40 (19 dom, 21 sub), Dark Phase N = 28 (14 dom, 14 sub); no significant interaction between Phase x Rank (F (1, 64) = 0.5697, p = 0.4531, two-way ANOVA).
Data expressed as mean ± SEM. *OFT*, open field test; TDT, total distance traveled; *IZ*, inner zone.

4.2.2 Phase effect on FCM excretion

Baseline FCM data was non-normally distributed and was therefore analyzed across phase and rank with the Kruskal-Wallis test (Fig. 15). While there was a significant difference between groups in baseline FCM, rank was the primary source of this variation as evidenced by a lack of any statistically significant effect of phase on within-rank values.

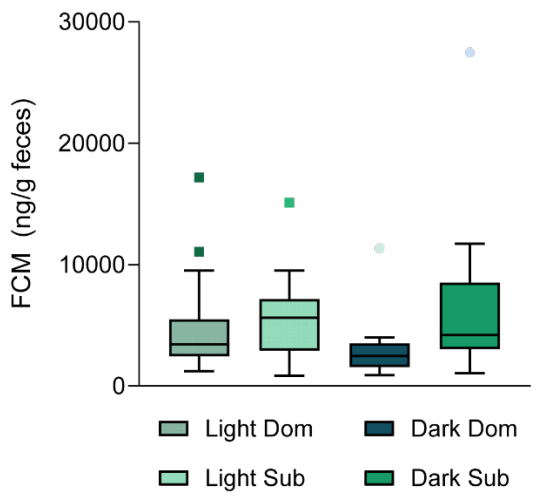

Figure 15. Circadian influence on FCM excretion

Baseline fecal corticosterone metabolites (FCM) across circadian phases. Light Phase N = 40 (19 dom, 21 sub), Dark Phase N = 28 (14 dom, 14 sub); significant difference between groups (H (3) = 9.521, *p = 0.0231, Kruskal-Wallis; Dunn's multiple comparisons test, Dom Light v. Dark, p = 0.1403; Sub Light v. Dark, p > 0.9999).
Box-and-whisker plots are displayed according to the Tukey method; boxes extend from Q1 to Q3, inner fences extend +/- 1.5 IQR, dots convey outliers, and horizontal lines designate the median.

4.3 Discussion

4.3.1 Phase differences in the open field

Mice are nocturnal by nature and in a laboratory setting they have been observed to exhibit spontaneous social behaviors more frequently during the dark phase of their circadian cycle (Yang et al 2008, Pobbe et al 2010, Bartolomucci et al 2004, Richetto et al 2019). To optimize the conditions for social interactions during the time-limited home cage behavior analysis, in the first experiment mice were housed on a reverse light cycle. In subsequent experiments mice were tested during the light phase to facilitate behavioral tests which are performed under lighting conditions that would disturb the circadian rhythm of dark-housed animals (Zhang et al 2017).

Circadian phase during testing affected exploratory behaviors independent of locomotion and anxiety (Fig. 14A-F). The effect on the stress-sensitive (i.e., unsupported) rearing behavior affected both ranks (Fig. 14C), whereas the exploratory effect disproportionately affected subordinate animals (Fig. 14B), eliminating the rank differences observed during the active phase. This indicates that there is likely a stress component associated with testing in the light versus the dark phase (Sturman et al 2018), and that subordinate characteristics are disproportionately affected by phase, respectively. Interestingly, while animals made more entries into the anxiogenic inner zone (IZ) during the dark phase, there was no phase effect on total time spent in the inner zone of the open field (Fig. 14 D, E). It is possible that the travel produced by increased inner zone entries was effectively replaced by thigmotaxis in the light phase, resulting in no overall difference in locomotion (Fig. 14F). Since phase differences were observed for exploratory rearing but not for total distance traveled (TDT), this suggests that rearing is ethologically distinct from locomotor activity.

The absence of a phase difference in distance traveled is interesting because dark phase testing has traditionally been associated with increased locomotor activity in the open field when subjects were male C57BL/6 mice (Hostetter 1966, Valentinuzzi et al 2000), but reduced total distance traveled when subjects were male or female C57BL/6N mice (Richetto et al 2019). One recent study using C57BL/6J of either sex in a circular and brightly lit open field found no difference by phase or sex in distance traveled (Tsao et al 2022). Since our data agree, this could represent a strain-difference in circadian influence on behavior that is independent of sex. Of course, many environmental factors including slight changes in temperature, lighting or ambient ultrasounds can affect behavior in the open field (Valentinuzzi et al 2000), so the effect observed here requires further investigation wherein these external variables are strictly controlled to ensure it is reproducibly the result of circadian influence.

4.3.2 Phase effect on FCM excretion

Absolute fecal corticosterone metabolite recovery was not influenced by phase as demonstrated previously (Touma et al 2003), but the baseline rank differences were only statistically significant during the dark phase (Fig. 15). While the overall relationship between rank and baseline FCM was unaltered, it is likely that the conditions producing the significant differences between dominant and subordinate fecal corticosterone metabolites were not met during the light phase, possibly due to differences in diurnal excretion patterns (Touma et al 2003). As such, the relationship between fecal corticosterone metabolites and rank should be interpreted with careful attention to the context in which it is acquired. Indeed, the literature remains conflicted regarding the relationship between social identity, sex and stress status (Varholick et al 2018 and 2021,

Williamson et al 2017). It is therefore prudent to consider variables influencing steroid recovery, including species- and sex-specific excretion patterns, sample source (e.g., feces, urine, hair, or blood), and the temporal proximity to any stressors. For example, a cage cleaning 8 hours prior may be insignificant for a direct murine CORT sample from the tail vein, but certainly becomes a factor to consider when collecting daytime fecal samples for metabolite analysis.

5. EFFECT OF SOCIAL INSTABILITY STRESS ON RANK-CHARACTERISTIC BEHAVIOR AND ENDOCRINE STATUS

5.1 Materials and Methods

5.1.1 Study design

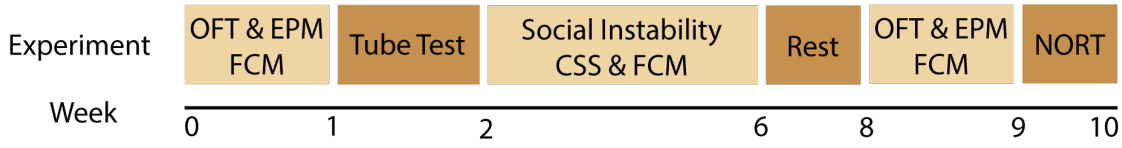

Figure 16. Experimental timeline for social instability experiment

OFT, open field test; *EPM*, elevated plus maze; *FCM*, fecal corticosterone metabolites; *CSS*, coat state score; *NORT*, novel object recognition test.

In this experiment, after two days of training the tube test was performed once prior to starting the social instability paradigm, then repeated during every stress session to test the current dominance status of the prior pairing. Coat state score, body weight, and fecal samples were taken at that time. Behavioral testing was performed prior to the tube test and evaluated for phase differences (see Chapter 4), and then repeated after the completion of 4 weeks of social instability stress (SIS). In this experiment I further explored the behaviors expressed in the anxiogenic context of the elevated plus maze (EPM). Additionally, at the end of the 4-week social instability paradigm a novel object recognition test (NORT) was performed to identify underlying and SIS-responsive rank differences in recognition which could be responsible for the differences observed in the three-chamber social approach task.

5.1.2 Social instability stress (SIS) paradigm

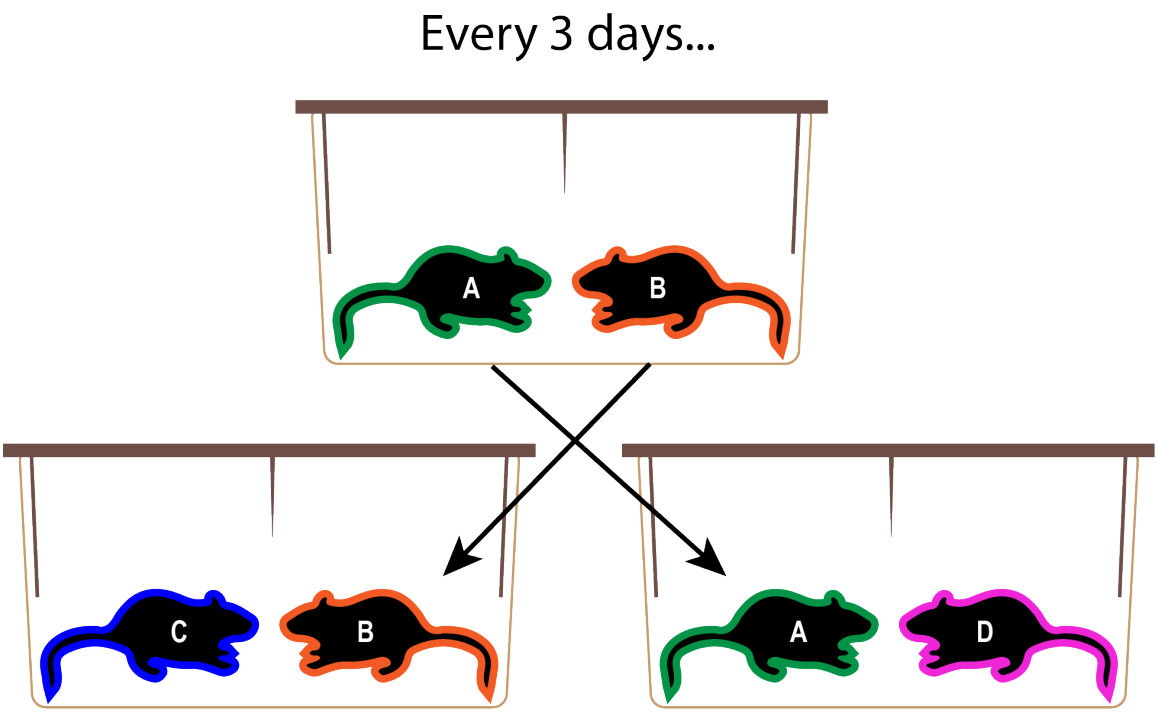

Figure 17. Social instability stress schematic

The social instability model of chronic psychosocial stress was first proposed by M.V. Schmidt et al. as a translatable and ethologically valid way to model depression in mice (Schmidt et al 2007). The original model used social groups of four male CD1 mice subjected twice weekly to novel social group composition and lasted for 7 consecutive weeks. This is an attempt to mimic both loss of social support and social instability, which are implicated in the onset of depression in humans (Sterlemann et al 2008). They established it as a valid model of chronic stress when they found that endocrinological, neurological and behavioral stress effects arising from the paradigm persisted following a one-week rest period. It has since been amended several times, first by the same group who validated the paradigm in female CD1 mice (Schmidt et al 2010), and most recently by Yohn et al., who demonstrated that the paradigm was effective in male and female

C57BL/6J social groups ranging in size from 3-5 mice and that behavioral effects were independent of estrous phase in females (Yohn et al 2019).

The social instability stress paradigm used in this experiment was adapted from the protocol described by Yohn et al. (Yohn et al 2019, Fig. 17); every 3rd day pair-housed mice (n = 24) were introduced to a novel age- and strain-matched conspecific and these pairs lived continuously together until the next social group rearrangement. Pairs that had cohabitated for the previous 3 days were subjected to competitive exclusion prior to introduction to the next social partner to determine the social rank achieved in the previous pairing. Pairs that had shared a cage for a social instability session were not re-paired for at least four sessions to avoid confounders from prior social experience. This paradigm was repeated for a total of four weeks, which was then followed by a 2-week rest period which tested the chronicity of effects in the absence of regular social stress. Control animals were continuously pair-housed, and these pairs were tested in the tube test during each instability session to control for handling stress associated with repeated competitive exclusion.

5.1.3 Win/loss sociomatrices and David's score

A

ID	2225	2067	2083	2093	2045	2085	2016	2200	2276	2180	2092	2095	2251	2098	2153	2054	2071	2053	2058	2073	2059	2174	2199	2177	w	w2
2225	*	NA	NA	0 (0.0)			4 (0.8)						0 (0.0)			3 (0.6)			3 (0.6)			4 (0.8)		0 (0.0)	2.8	4.8
2067	NA	*	NA			5 (1.0)			3 (0.6)			5 (1.0)			5 (1.0)			5 (1.0)		1 (0.2)			8 (0.8)	5.6	20.12
2083	NA	NA	*						2 (0.4)		2 (0.4)				8 (0.8)		5 (1.0)				0 (0.0)		0 (0.0)	0 (0.0)	2.6	7.84
2093	10 (1.0)			*	NA	NA		5 (1.0)					5 (1.0)			5 (1.0)			5 (1.0)		3 (0.6)	3 (0.6)	3 (0.6)		6.2	19.26
2045				NA	*	NA	3 (0.6)	1 (0.2)		3 (0.6)				2 (0.2)			2 (0.4)				0 (0.0)	1 (0.2)			2.2	4.7
2085		0 (0.0)		NA	NA	*	10 (1.0)		0 (0.0)					4 (0.8)		4 (0.8)			4 (0.8)				3 (0.6)		4	9.36
2016	1 (0.2)				2 (0.4)	0 (0.0)	*	NA	NA			0 (0.0)						0 (0.0)		0 (0.0)					0 (0.0)	0.6	1.44
2200				0 (0.0)	4 (0.8)		NA	*	NA	10 (1.0)	2 (0.4)		1 (0.2)	0 (0.0)	5 (1.0)										3.4	5.96
2276		2 (0.4)	3 (0.6)			5 (1.0)	NA	NA	*									5 (1.0)	5 (1.0)	5 (1.0)		9 (0.9)			5.9	17.81
2180					2 (0.4)			0 (0.0)		*	NA	NA				2 (0.4)	1 (0.2)				0 (0.0)		0 (0.0)	0 (0.0)	1	2.12
2092			3 (0.6)					3 (0.6)		NA	*	NA					10 (1.0)		5 (1.0)	3 (0.6)			0 (0.0)	1 (0.2)	4	10.14
2095		0 (0.0)					5 (1.0)			NA	NA	*	1 (0.2)					1 (0.2)		9 (0.9)	0 (0.0)	1 (0.2)			2.5	5.17
2251	5 (1.0)			0 (0.0)				4 (0.8)				4 (0.8)	*	NA	NA			8 (0.8)		5 (1.0)			3 (0.6)		5	16.18
2098					8 (0.8)	1 (0.2)		5 (1.0)					NA	*	NA	5 (1.0)	1 (0.2)		5 (1.0)			2 (0.4)			4.6	9.92
2153		0 (0.0)	2 (0.2)					0 (0.0)					NA	NA	*		0 (0.0)	2 (0.4)				0 (0.0)	0 (0.0)		0.6	1.96
2054	2 (0.4)			0 (0.0)		1 (0.2)				3 (0.6)				0 (0.0)		*	NA	NA			0 (0.0)			1 (0.2)	1.4	3.68
2071			0 (0.0)		3 (0.6)					4 (0.8)	0 (0.0)			4 (0.8)	5 (1.0)	NA	*	NA		1 (0.2)					3.4	6.86
2053		0 (0.0)					5 (1.0)		0 (0.0)			4 (0.8)	2 (0.2)		3 (0.6)	NA	NA	*		5 (1.0)					3.6	6.26
2058	2 (0.4)			0 (0.0)		1 (0.2)			0 (0.0)		0 (0.0)			0 (0.0)					*	NA	NA		0 (0.0)		0.6	1.92
2073							5 (1.0)		0 (0.0)		2 (0.4)	1 (0.1)	0 (0.0)				4 (0.8)	0 (0.0)	NA	*	NA				2.3	5.17
2059		4 (0.8)	5 (1.0)	2 (0.4)	5 (1.0)					5 (1.0)		5 (1.0)				10 (1.0)			NA	NA	*				6.2	16.66
2174	1 (0.2)			2 (0.4)	4 (0.8)				1 (0.1)			4 (0.8)		3 (0.6)	5 (1.0)							*	NA	NA	3.9	10.75
2199			5 (1.0)			2 (0.4)				5 (1.0)	5 (1.0)		2 (0.4)		5 (1.0)				10 (1.0)			NA	*	NA	5.8	12.4
2177	5 (1.0)	2 (0.2)	5 (1.0)				5 (1.0)			5 (1.0)	4 (0.8)					4 (0.8)						NA	NA	*	5.8	12.44
l	4.2	1.4	4.4	0.8	4.8	3	6.4	3.6	1.1	6	3	4.5	2	2.4	6.4	5.6	3.6	3.4	6.4	4.7	0.8	3.1	1.2	1.2		
l2	10.7	1.32	6.94	1.56	15.2	5.86	23.04	7.56	2.91	15.92	7.24	9.47	3.58	8.1	18.46	12.28	14.76	7.56	13.42	13.07	0.76	7.65	3	2.84		

B

ID	2089	2075	2070	2061	2074	2080	2094	2088	2097	2056	2072	2062	2081	2064	2086	2175
2089	*	40 (1.0)														
2075	0 (0.0)	*														
2070			*	40 (1.0)												
2061			0 (0.0)	*												
2074					*	29 (0.725)										
2080					11 (0.27	*										
2094							*	0 (0.0)								
2088							40 (1.0)	*								
2097									*	39 (0.97)						
2056									1 (0.03)	*						
2072											*	4 (0.09)				
2062											36 (0.91	*				
2081													*	0 (0.0)		
2064													40 (1.0)	*		
2086															*	0 (0.0)
2175															40 (1.0)	*

Figure 18. Win/loss sociomatrices of SIS and control animals

Sociomatrices representing the total number and proportion (in parentheses) of wins for any given pair of animals as determined by 5 tube test trials per social instability stress (SIS) session. Row animal IDs correspond to all wins for that animal and column IDs correspond to their losses. See David's score equation below for details on variables and calculations.

(A) Sociomatrix of the results of all win/loss encounters in social instability stress (SIS) experimental animals. Since different animals were encountered upon each successive pairing, a David's score could be calculated from the relative and weighted wins (w, w2) and losses (l, l2) of every individual.

(B) Sociomatrix of the results of all win/loss encounters in control animals.

Mice arrived at the facility in groups of five and were allowed to acclimate for one week prior to testing. Animals that arrived at the facility together were never co-housed during the social instability stress experiment to avoid confounders from prior social experience. These animal pairings are represented in the sociomatrix as "NA" (Fig. 18A). Animals are also color-coded in the sociomatrix to indicate with which group they were acclimated upon arrival. At least two animals from each arrival group were used as controls (and were also never co-housed) to avoid confounders from over-representation of any acclimation-established hierarchies in either the experimental or control cohort.

David's score (DS) is a widely used measure of individual dominance that weighs an animal's wins against the relative dominance of its opponents (Gammell et al 2003). David's score is calculated from a sociomatrix of the win/loss results of pairwise agonistic encounters wherein each cell represents the trial outcome and dominance proportion, P_{ij}, of wins and P_{ji}, losses of individual i versus any given opponent j. In this experiment David's score is calculated from the results of each tube test session according to the following standard formula:

$$DS = w + w_2 - l - l_2$$

Where, for individual i...

$$w = \Sigma P_{ij}$$

$$w_2 = \Sigma\left(P_{ij} \cdot w\right) \text{ of all of i's opponents}$$

$$l = \Sigma P_{ji}$$

$$l_2 = \Sigma\left(P_{ji} \cdot l\right) \text{ of all of i's opponents}$$

Interaction frequency was identical between dyads, for both experimental and control groups. Control animals were never paired with more than one other individual and

therefore their rank was assigned from overall wins in the tube test (Fig. 18B). Control animal ranks remained stable throughout all four weeks of the stress paradigm.

5.1.4 Housing, lighting conditions and circadian phase

Subjects were 40 adult 3–4-month-old female C57BL6/J mice (Jackson Laboratory, Bar Harbor, Maine). Animals were housed on a 12:12 hour light cycle; food and water were provided ad libitum. All testing was performed during the inactive (light) phase of the circadian cycle under ambient white light. The open field test (OFT) and novel object recognition test (NORT) took place under dim lighting conditions (<15 lux). The elevated plus maze (EPM) took place under bright lighting conditions (180 ± 5 lux). Fecal samples were taken during the same time period each day within experiments, and at least 2 hours into the light cycle of testing.

5.1.5 Elevated plus maze (EPM)

Mice were placed on an elevated (60 cm), cross-shaped opaque PVC maze consisting of two 5 x 28 cm open arms and two 5 x 28 cm arms enclosed by 38 cm walls. Animals were allowed to freely explore the apparatus for 5 minutes. After each trial the maze was cleaned with 70% ethanol.

5.1.6 Coat state score (CSS)

Animals were assessed for changes in coat state associated with poor well-being and self-care (Nollet et al 2013). Eight body regions (head, neck, back, forepaws, hind paws, tail, abdomen, and anogenital region) were assessed and assigned a score based on appearance as follows: 0 = well-kempt, clean and shiny, 0.5 = moderately unkempt or dull, 1.0 = poorly kept, very dull and dirty or patchy. The points for all regions were summed to

assign a single coat state score for each animal. Higher scores therefore indicate a worse coat state.

5.1.7 Novel object recognition test (NORT)

The open field apparatus was used to conduct this test, which was performed over two trials. During trial 1, two identical Rubik's cubes (Rubik's Ltd, Hungary) were placed in opposing corners of the open field, 5 cm away from the walls. The subject was placed in the apparatus and allowed to explore freely for 10 minutes. 24 hours later the second trial was performed, in which one of the identical objects was replaced with a novel object, a Rubik's pyramid (Rubik's Ltd, Hungary), and an identical cube used in the first trial. The subject was again allowed to explore for 10 minutes. Behavior was recorded via an overhead camera for later analysis.

Time exploring each object and number of entries into a 3cm x 3cm zone surrounding the object were scored. Exploration was counted as sniffing, touching, and all forms of interacting with the object other than climbing. Novelty object preference index (PI) was calculated as the proportion of time spent interacting with a novel object over total exploration time.

5.1.8 Nest building test (NBT)

Figure 19. Examples of nest shapes

Photographs of nests assigned a flat (*left*), cup (*middle*), and bowl (*right*) shape. Nests were scored 24 hours after exposure to a novel cage with new nesting material. Animals were housed individually during the test.

The nest building test (NBT) is performed under individual housing conditions, which may constitute a stressor. Therefore, nest building was measured following the novel object recognition test to avoid confounds of temporary isolation stress. 8-10 grams of brown crinkle nesting material was placed in the center of a clean cage with normal bedding. The subject mouse was introduced into the new cage with nesting material and left undisturbed with ad libitum food and water for 24 hours. At the end of 24 hours the cage lid was gently lifted, and a score of the nesting material was recorded. Every attempt was made to ensure the mouse remained undisturbed in the nest when photographs were taken. This is because when the mouse attempts to rapidly escape the nest, it can damage the nesting material and skew the analysis of the nest shape or wall height. The photographs shown above were deliberately obtained after the mouse had been moved for photographic quality purposes. The nesting material shown here was preserved as closely as possible to its state when the mouse was still present. Nest quality was graded on a 0-5 scale according to the rubric proposed by Hess et al. (Hess et al 2008, Gaskill et al 2013),

wherein a base score was assigned from the nest shape and partial scores were added for the presence and height of the walls as follows:

0 – nesting material untouched (not observed in this experiment)

1 – nesting material disturbed but no obvious nest formed

2 – flat nest

+ 0.25 for every raised shallow wall (max 4 walls)

3 – cup-shaped nest

+ 0.25 for every raised wall (max 4 walls)

4 – bowl-shaped nest

+ 0.25 for every raised, curved wall (max 4 walls)

5 – dome-shaped nest providing complete coverage for a mouse, +/- an exit hole

5.2 Results

5.2.1 David's score and distribution of rank

In the social instability stress (SIS) paradigm social hierarchies were disrupted every three days by the replacement of one social partner with a novel sex-, age- and strain-matched conspecific. This model requires mice to re-form social groups and disables social support structure, a model of social stress that is thought to be more ethologically relevant to the development of major depression in humans (Bartolomucci et al 2004, Schmidt et al 2010, Yohn et al 2019).

Since new pairings occurred during each session, match data were used to assign a David's score (DS; see 5.1.3) to every experimental subject (Gammell et al 2003). The David's score allows investigation into whether the degree of dominance correlates with rank characteristics, because it weights an individual's winning status against the winning status of its' opponents. In this experiment David's scores ranged from -27.4 (most subordinate animal) to 23.1 (most dominant animal), with 11 dominant animals and 13 subordinate animals emerging at the experimental endpoint. The mean of the David's scores (-0.01) was used to divide the experimental animals into ranked groups (i.e., Sub = DS < -0.01, Dom = DS > -0.01).

Control pairings were subjected to the tube test at every social instability stress session alongside the experimental animals, but they never changed social partners. Therefore, they were exposed to all of the same stressors except social instability. All 8 pairs of control animals were rank stable by the end of testing, and in agreement with the original dark phase experiment, most pairs' final rankings reflected their original social status.

5.2.2 Rank behavior in the OFT before and after SIS

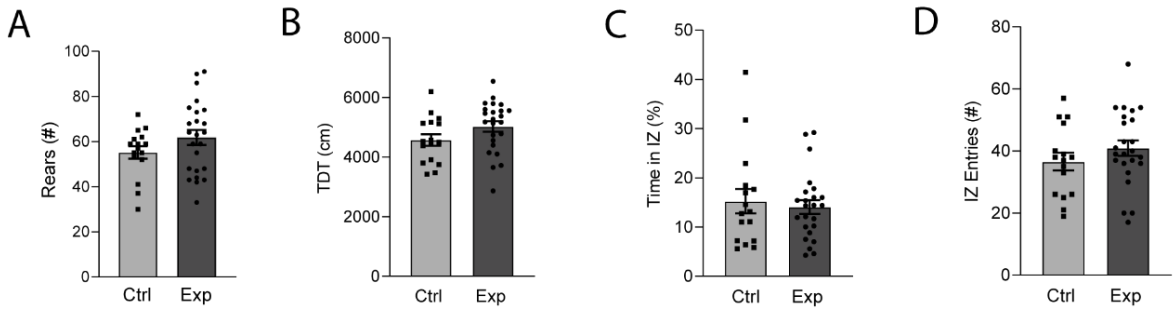

Figure 20. Behavior in the OFT before SIS

(A) Total rears in the OFT prior to SIS. N = 40 (24 Exp, 16 Ctrl); p = 0.1587 (Unpaired t test, two-tailed).

(B) Total distance traveled in the OFT prior to SIS. N = 40 (24 Exp, 16 Ctrl); p = 0.0989 (Unpaired t test, two-tailed).

(C) Time in inner zone of the OFT prior to SIS. N = 40 (24 Exp, 16 Ctrl); p = 0.9674 (Mann-Whitney).

(D) Entries into the inner zone of the OFT prior to SIS. N = 40 (24 Exp, 16 Ctrl); p = 0.2609 (Unpaired t test, two-tailed).

Data expressed as mean ± SEM. *SIS*, social instability stress; *OFT*, open field test; *TDT*, total distance traveled; *IZ*, inner zone; *Exp*, experimental; *Ctrl*, control.

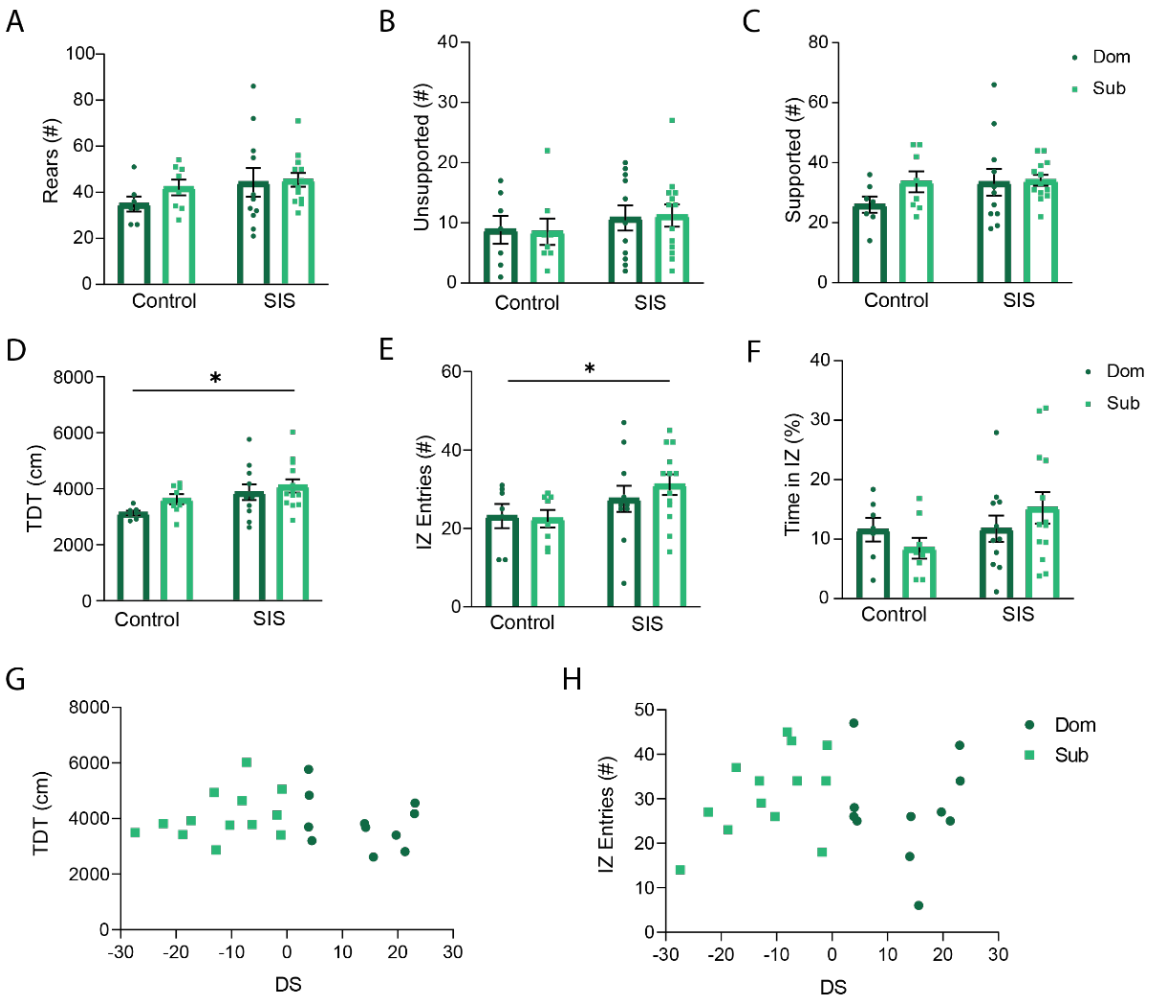

Figure 21. Behavior in the OFT after SIS

(A) Post-SIS total rears in the OFT. Stress N = 24 (11 dom, 13 sub), Ctrl N = 15 (7 dom, 8 sub); no significant interaction between Stress x Rank (F (1, 35) = 0.4467, p = 0.5083, two-way ANOVA).

(B) Post-SIS unsupported rears in the OFT. Stress N = 24 (11 dom, 13 sub), Ctrl N = 15 (7 dom, 8 sub); no significant interaction between Stress x Rank (F (1, 35) = 0.03134, p = 0.8605, two-way ANOVA).

(C) Post-SIS supported rears in the OFT. Stress N = 24 (11 dom, 13 sub), Ctrl N = 15 (7 dom, 8 sub); no significant interaction between Stress x Rank (F (1, 35) = 1.029, p = 0.3175, two-way ANOVA).

(D) Post-SIS total distance traveled in the OFT. Stress N = 24 (11 dom, 13 sub), Ctrl N = 15 (7 dom, 8 sub); no significant interaction between Stress x Rank (F (1, 35) = 0.284, p = 0.5974); significant main effect of Stress (F (1, 35) = 6.074, *p = 0.0188, two-way ANOVA; Sidak's multiple comparisons test, Dom p = 0.0943, Sub p = 0.3025).

(E) Post-SIS inner zone entries in the OFT. Stress N = 24 (11 dom, 13 sub), Ctrl N = 15 (7 dom, 8 sub); no significant interaction between Stress x Rank (F (1, 35) = 0.4906, p = 0.4883); significant main effect of

Stress (F (1, 35) = 4.628, *p=0.0384, two-way ANOVA; Sidak's multiple comparisons test, Dom p = 0.5495, Sub p = 0.0852).

(F) Post-SIS time in OFT inner zone expressed as a percentage of total exploration time. Stress N = 24 (11 dom, 13 sub), Ctrl N = 16 (7 dom, 8 sub); no significant interaction between Stress x Rank (F (1, 35) = 1.793, p = 0.1891, two-way ANOVA)

(G) Correlation between DS and TDT in SIS subjects. N = 24 (11 dom, 13 sub); Dom R = -0.3276, p = 0.3254, Sub R = 0.3498, p = 0.2414 (Pearson's correlation).

(H) Correlation between DS and IZ entries in SIS subjects. N = 24 (11 dom, 13 sub); Dom R = -0.0326, p = 0.9242, Sub R = 0.4867, p = 0.0917 (Pearson's correlation).

Data expressed as mean ± SEM except for G and H. One outlier was identified for post-SIS OFT TDT data; this animal was excluded from behavior analysis (Grubb's, alpha = 0.05). *SIS*, social instability stress; *OFT*, open field test; *TDT*, total distance traveled; *IZ*, inner zone.

Animals were randomly assigned to either experimental or control group status. Prior to social instability stress (SIS), there were no pre-existing differences in rearing, locomotor, or anxiety-like behaviors in the open field test between groups (Fig. 20A–D). Therefore, animals were retrospectively combined by rank to look for predictive differences, which were analyzed according to circadian phase in Chapter 4 (Fig. 14).

Social instability stress did not alter rearing in the open field (Fig. 21A–C). However, it did induce changes consistent with a hyperlocomotion phenotype; animals exposed to 4 weeks of social instability stress had an elevated total distance traveled (TDT) and made more frequent crossings into the inner zone (IZ) (Fig. 21D, E). As discussed previously, increased time in the inner zone is associated with behavioral anxiolysis and is responsive to antidepressant drugs (Simon et al 1994, Choleris et al 2001, Cryan & Holmes 2005). Here, the increase in inner zone entries was attributed to greater locomotor activity because SIS-exposed mice did not spend more time in the inner zone overall (Fig. 21F). Therefore, this and the increased total distance traveled were collectively interpreted as an elevation in general activity rather than representing the development of an anxiolytic

phenotype. There was no correlation between David's score and either distance traveled or inner zone entries following social instability stress (Fig. 21G, H).

5.2.3 Rank behavior in the EPM before and after SIS

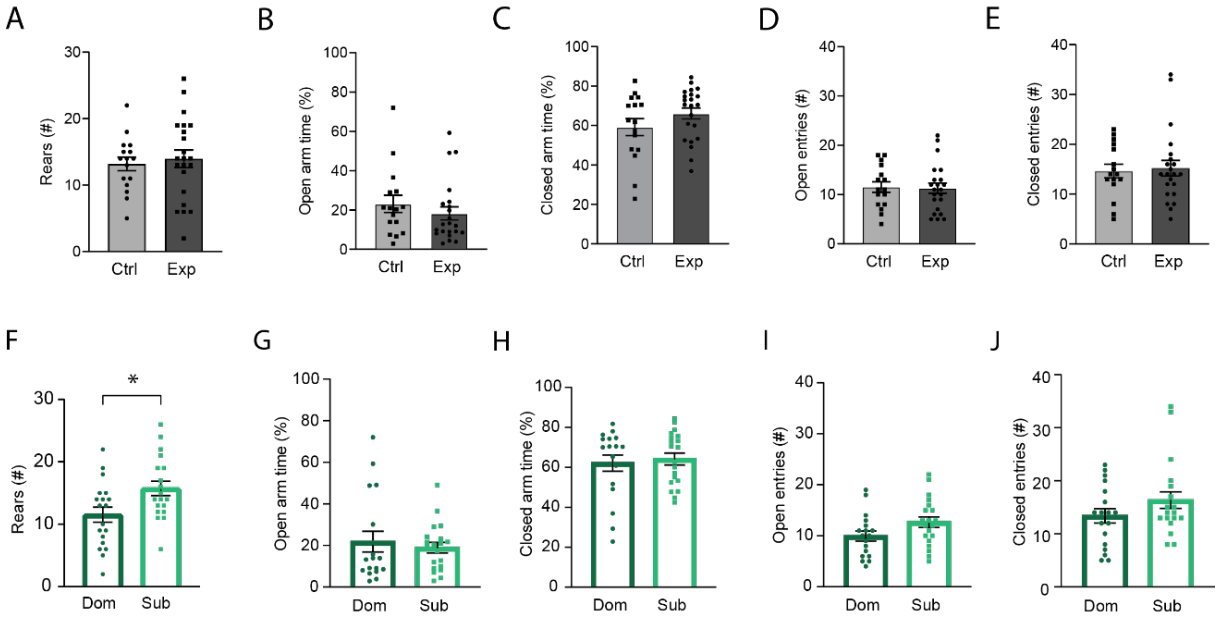

Figure 22. Behavior in the EPM before SIS

(A) Pre-SIS rearing behavior in the EPM. $N = 38$ (22 Exp, 16 Ctrl); $p = 0.6707$ (Unpaired t test, two-tailed).

(B) Pre-SIS time in the EPM open arms. $N = 38$ (22 Exp, 16 Ctrl); $p = 0.5686$ (Mann-Whitney).

(C) Pre-SIS time in the EPM closed arms. $N = 38$ (22 Exp, 16 Ctrl); $p = 0.1711$ (Unpaired t test, two-tailed).

(D) Pre-SIS EPM open arm entries. $N = 38$ (22 Exp, 16 Ctrl); $p = 0.8836$ (Unpaired t test, two-tailed).

(E) Pre-SIS EPM closed arm entries. $N = 38$ (22 Exp, 16 Ctrl); $p = 0.8893$ (Mann-Whitney).

(F) Pre-SIS rearing in the EPM by rank. $N = 38$ (18 dom, 20 sub); $*p = 0.0304$ (Unpaired t test, two-tailed).

(G) Pre-SIS open arm time in the EPM by rank. $N = 38$ (18 dom, 20 sub); $p = 0.6389$ (Mann-Whitney).

(H) Pre-SIS closed arm time in the EPM by rank. $N = 38$ (18 dom, 20 sub); $p = 0.8285$ (Mann-Whitney).

(I) Pre-SIS EPM open arm entries by rank. $N = 38$ (18 dom, 20 sub); $p = 0.0714$ (Unpaired t test, two-tailed).

(J) Pre-SIS EPM closed arm entries by rank. $N = 38$ (18 dom, 20 sub); $p = 0.2717$ (Mann-Whitney).

Data expressed as mean ± SEM. Two animals fell during the pre-SIS EPM; these were excluded from analysis.

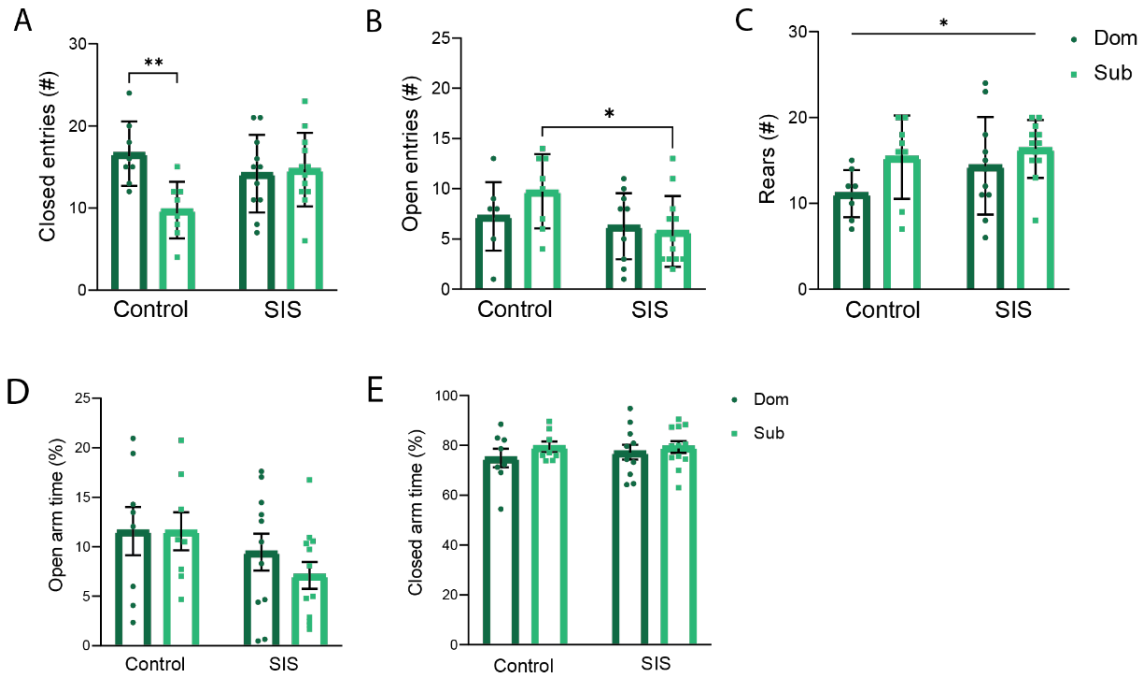

Figure 23. Behavior in the EPM after SIS

(A) Post-SIS closed arm entries in the EPM. Stress N = 23 (11 dom, 12 sub), Ctrl N = 16 (8 dom, 8 sub); significant interaction between Rank x Stress ($F(1, 35) = 7.030$, *$p = 0.0120$); significant main effect of Stress ($F(1, 35) = 5.300$, *$p = 0.0274$, two-way ANOVA; Sidak's multiple comparisons test, SIS $p = 0.9545$, Control **$p = 0.0054$).

(B) Post-SIS open arm entries in the EPM. Stress N = 23 (11 dom, 12 sub), Ctrl N = 16 (8 dom, 8 sub); no significant interaction between Stress x Rank ($F(1, 35) = 1.789$, $p = 0.1897$); significant main effect of Stress ($F(1, 35) = 4.850$, *$p = 0.0343$, two-way ANOVA; Sidak's multiple comparisons test, Dom $p = 0.7960$, Sub *$p = 0.0322$).

(C) Post-SIS rearing in the EPM. Stress N = 23 (11 dom, 12 sub), Ctrl N = 16 (8 dom, 8 sub); no significant interaction between Stress x Rank ($F(1, 35) = 0.6461$, $p = 0.4269$); significant main effect of Rank ($F(1, 35) = 4.807$ *$p = 0.0351$, two-way ANOVA; Sidak's multiple comparisons test, SIS $p = 0.4903$, Control $p = 0.1146$).

(D) Post-SIS time exploring open arms of the EPM. Stress N = 23 (11 dom, 12 sub), Ctrl N = 16 (8 dom, 8 sub); no significant interaction between Stress x Rank ($F(1, 35) = 0.3831$, $p = 0.5400$, two-way ANOVA).

(E) Post-SIS time exploring closed arms of the EPM. Stress N = 23 (11 dom, 12 sub), Ctrl N = 16 (8 dom, 8 sub); no significant interaction between Stress x Rank ($F(1, 35) = 0.1837$, $p = 0.6708$, two-way ANOVA).

Data expressed as mean ± SEM. One animal fell during the post-SIS EPM and was excluded from analysis.

In addition to the open field test, animals were evaluated for behavioral changes in the elevated plus maze (EPM) before and after 4 weeks of social instability. Prior to social instability stress, there were no differences between experimental animals and controls in rearing behavior and time spent in, or entries into, the open or closed arms (Fig. 22A-E). Since no pre-existing differences were found, groups were combined to look for baseline rank differences. Supported rearing in the elevated plus maze differed by rank in a pattern identical to that observed in the open field test performed during the dark circadian phase (Fig. 22F). There were no rank differences in time spent in either open or closed arms or in total arm entries (Fig. 22G-J).

In the post-social instability elevated plus maze test, which occurred following a 2-week rest period (Fig. 16), control animals demonstrated a rank difference in closed arm entries that was absent in SIS-exposed animals (Fig. 23A) and stressed subordinates made significantly fewer open arm entries than controls (Fig. 23B). Also, social instability stress increased exploratory rearing behavior in the elevated plus maze compared to controls (Fig. 23C). These exploratory changes occurred independently of anxiety-like characteristics because overall time in the open and closed arms was unaffected by social instability stress exposure (Fig. 23D, E).

5.2.4 Effect of SIS on behavior in the NORT

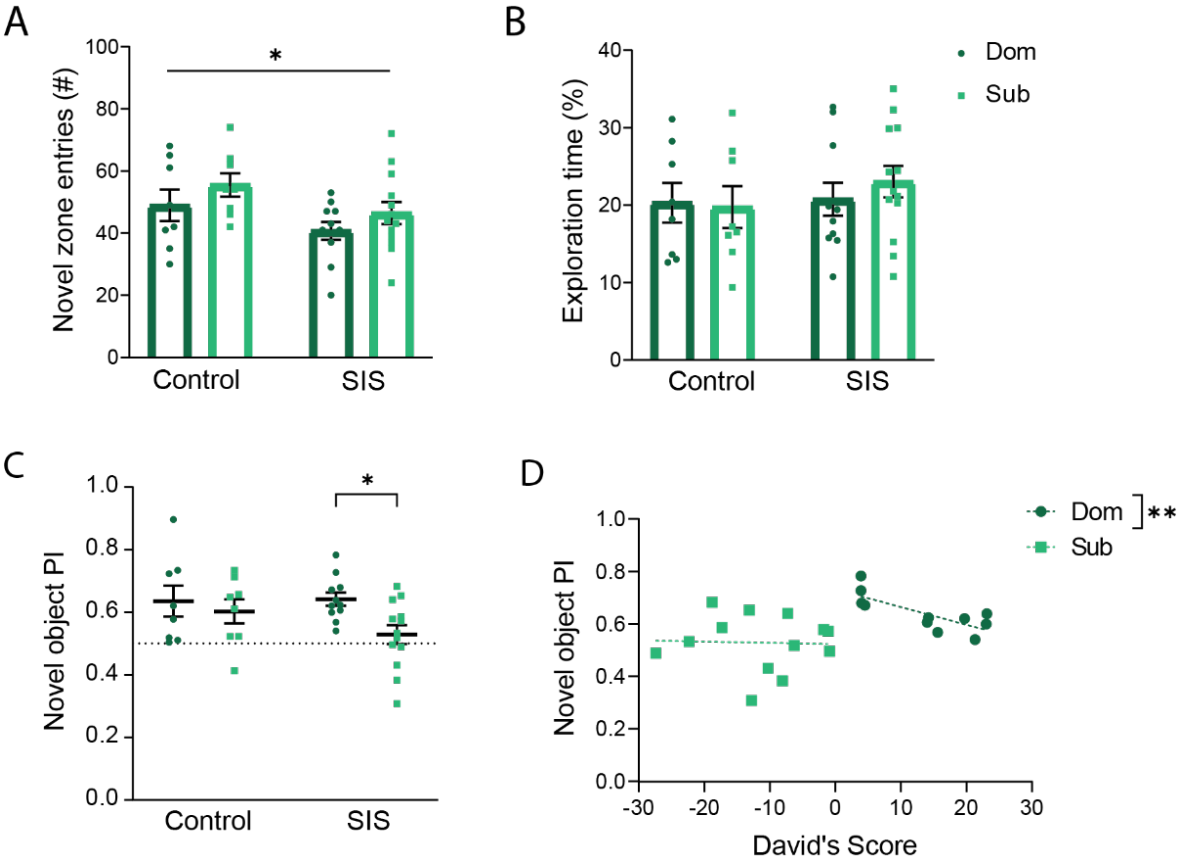

Figure 24. Effects of SIS on performance in the NORT

(A) Entries into the novel object zone during NORT. Stress N = 24 (11 dom, 13 sub), Ctrl N = 16 (8 dom, 8 sub); no significant interaction between Rank x Stress ($F (1, 36) = 0.0135$, $p = 0.9082$); significant main effect of Stress ($F (1, 36) = 5.017$, *$p = 0.0314$, two-way ANOVA; Sidak's multiple comparisons test, Dom $p = 0.2746$, Sub $p = 0.1878$).

(B) Post-SIS total exploration time in NORT. Stress N = 24 (11 dom, 13 sub), Ctrl N = 16 (8 dom, 8 sub); no significant interaction between Stress x Rank ($F (1, 36) = 0.3597$, $p = 0.5524$, two-way ANOVA).

(C) Preference index for the novel object during NORT. Stress N = 24 (11 dom, 13 sub), Ctrl N = 16 (8 dom, 8 sub); no significant interaction between Rank x Stress ($F (1, 36) = 1.351$, $p = 0.2527$); significant main effect of Rank ($F (1, 36) = 4.482$, *$p = 0.0412$, two-way ANOVA; Sidak's multiple comparisons test, SIS *$p = 0.0275$, Control $p = 0.7894$).

(D) Correlation between DS and novel object PI in SIS subjects. N = 24 (11 dom, 13 sub); Dom $R = -0.7728$, **$p = 0.0053$, Sub $R = -0.03603$, $p = 0.9070$ (Pearson's correlation); Dom $F (1, 9) = 13.34$, $R^2 = 0.5972$, Sub $F (1, 11) = 0.01430$, $R^2 = 0.001298$, (simple linear regression).

Data expressed as mean ± SEM, except for D. *SIS*, social instability stress; *NORT*, novel object recognition test; *PI*, preference index.

A novel object recognition test (NORT) was performed to identify rank differences in recognition memory which could be responsible for the three-chamber social approach (3CSA) behavioral patterns (Fig. 11). Social instability stress reduced the entries into the novel object zone (Fig. 24A) without affecting overall object exploration time (Fig. 24B). Notably, social instability selectively reduced subordinate novelty preference (Fig. 24C). Following social instability stress, dominants possessed a significant negative correlation between David's score (DS) and novelty preference that was not present in subordinates (Fig. 24D).

5.2.5 Changes in FCM, CSS, body weight and NBT

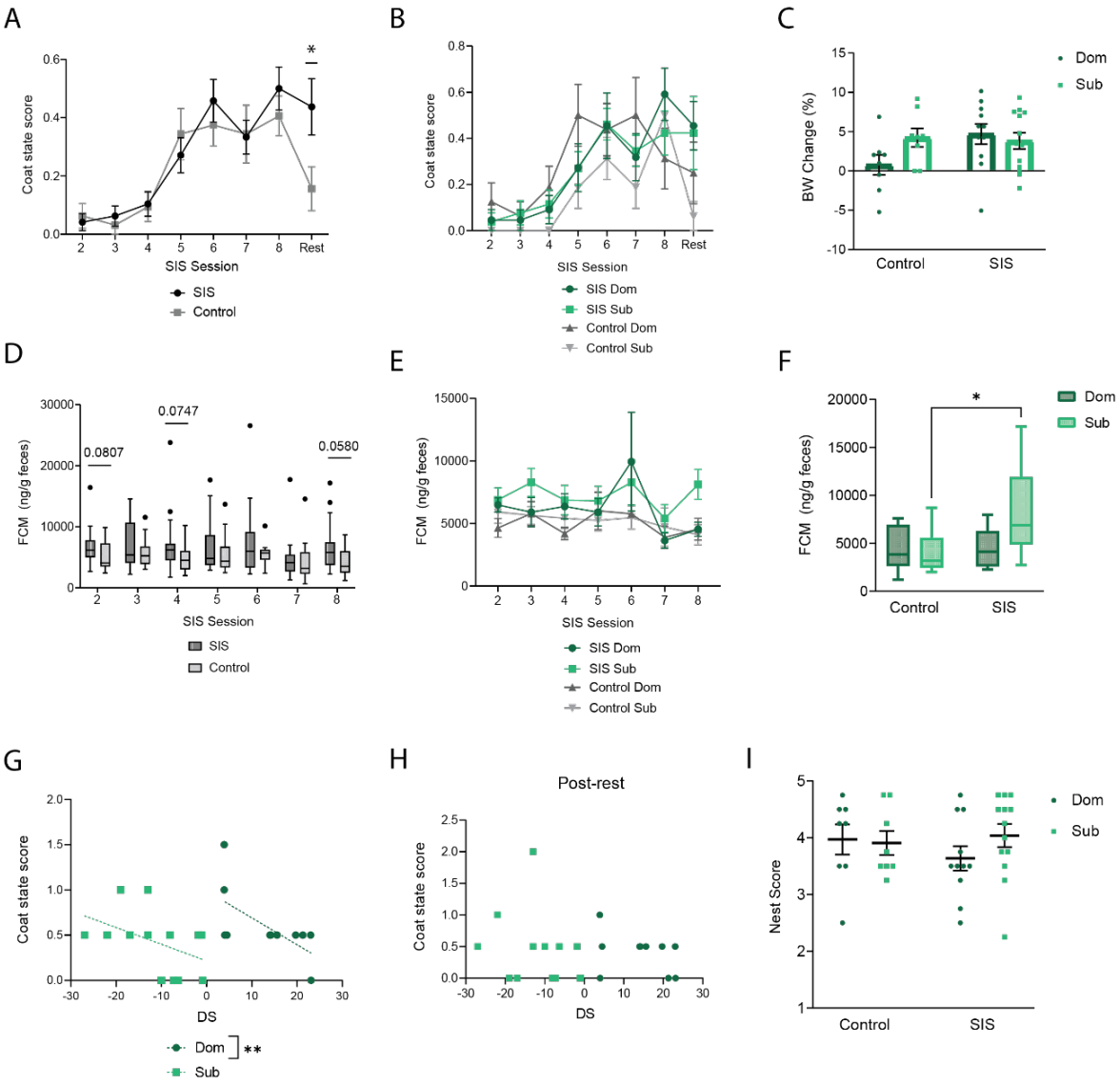

Figure 25. Changes in FCM, CSS, body weight and NBT

(A) Stress vs. Control CSS taken during every SIS session and after the rest period. Stress N = 24, Ctrl N = 16; Rest *p = 0.0267 (Mann-Whitney).

(B) Ranked CSS takena during every SIS session and after the rest period. Stress N = 24 (11 dom, 13 sub), Ctrl N = 16 (8 dom, 8 sub); no significant differences between ranks were identified during testing (Post-rest; H (3) = 6.701, p = 0.0821, Kruskal-Wallis test).

(C) Change in body weight from baseline to the final SIS session, by rank and condition. Stress N = 24 (11 dom, 13 sub), Ctrl N = 16 (8 dom, 8 sub); no significant interaction between Rank x Stress (F (1, 36) = 3.115, p = 0.0860, two-way ANOVA).

(D) Stress vs. Control FCM during SIS. Stress N = 24, Ctrl N = 16; Session 2, p = 0.0807; Session 4, p = 0.0747; Session 8, p = 0.0580 (Mann-Whitney).
(E) Ranked FCM during SIS. Stress N = 24 (11 dom, 13 sub), Ctrl N = 16 (8 dom, 8 sub); significant difference was only identified at session 8; see Fig. 25E
(F) FCM taken at the final SIS session, by rank and condition. Stress N = 24 (11 dom, 13 sub), Ctrl N = 16 (8 dom, 8 sub); significant interaction between Rank x Stress ($F(1, 36) = 4.163$, *p = 0.0487); significant main effect of Stress ($F(1, 36) = 4.354$, *p = 0.0441, two-way ANOVA; Sidak's multiple comparisons test, Dom p = 0.9993, Sub *p = 0.0106).
(G) Correlation between DS and CSS in SIS subjects at the final session. N = 24 (11 dom, 13 sub); Dom R = -0.7822, **p = 0.0020, Sub R = -0.5193, p = 0.0711 (Spearman's correlation); Dom $F(1, 9) = 6.067$, $R^2 = 0.4027$, Sub $F(1, 11) = 2.660$, $R^2 = 0.1948$, (simple linear regression).
(H) Correlation between DS and CSS in SIS subjects following the rest period. N = 24 (11 dom, 13 sub); Dom R = -0.5893, p = 0.0576, Sub R = -0.3553, p = 0.2305 (Spearman's correlation).
(I) Nest building scores after the post-SIS rest period, by rank and condition. Stress N = 24 (11 dom, 13 sub), Ctrl N = 16 (8 dom, 8 sub); no significant interaction between Rank x Stress ($F(1, 36) = 1.036$, p = 0.3155, two-way ANOVA).
Data expressed as mean ± SEM except for correlations and FCM, where box-and-whisker plots are displayed according to the Tukey method; boxes extend from Q1 to Q3, inner fences extend +/- 1.5 IQR, dots convey outliers, and horizontal lines designate the median. FCM values with intra-assay CV > 10% or missing samples were excluded from analysis. No outliers were removed. FCM data from SIS sessions 2 – 7 were non-normally distributed and analyzed with Kruskal-Wallis tests. Session 8 data was normally distributed and therefore analyzed with a 2-way ANOVA.

Coat state score (CSS) was also evaluated as a pharmacologically validated measure of well-being (Nollet et al 2013). Of note, all animals experienced a deterioration of coat state throughout the experiment (Fig. 25A). This is likely attributable to the handling stress of repeated use of the tube test to monitor changes in experimental and control hierarchies. This is further supported by the finding that after a 14-day rest period the control group coat state score improved while that of the SIS-exposed group remained elevated (Fig. 25A). These data suggest a lasting effect of social instability stress on self-maintenance behavior. There was no obvious influence of rank on coat state during social instability stress or in the rest period (Fig. 25B). However, changes in coat state were not

solely due to group differences in weight gain as there were no significant differences in weight change from baseline at the end of social instability stress (Fig. 25C). Further, during the final social instability session there was a significant negative correlation between dominant David's score and coat state that became a non-significant trend following the two-week rest period (Fig. 25G, H).

Fecal samples were collected at the end of each tube test session for analysis of fecal corticosterone metabolites (FCM). Overall, FCM did not differ significantly between experimental and control animals, though there was a trend for higher FCM excretion in the social instability group during the second, fourth, and eighth session of the stress paradigm (Fig. 25D). Prior to the final social instability session there were no clear rank differences in fecal corticosterone metabolites (Fig. 25E); however, at the experimental endpoint, social instability exposure had produced a disproportionate effect on subordinate animal FCM excretion (Fig. 25F). Following social instbaility and the 2-week rest period, there were no differences by rank or condition nest building scores (Fig. 25G).

5.3 Discussion

5.3.1 David's score and distribution of rank

Following the analysis of social hierarchy formation, I next wanted to explore the intersectionality of rank, environmental context, and social stress. Therefore, mice were subjected to a chronic form of psychosocial stressor – social instability stress (SIS) – to determine how rank influences behavior and corticosterone status in the face of hierarchical uncertainty (Fig. 16). Ranks were monitored with the tube test and behavioral testing was performed prior to initiating the social instability stress paradigm, and then repeated afterwards following a 2-week rest period. The distribution of David's scores revealed that the population was slightly skewed towards subordinate status (11 dominant and 13 subordinate animals total). In a future experiment it would be interesting to determine whether David's score dictated the same behavioral responses in stress-naïve animals existing in larger social groups.

Here, we apply the SIS paradigm to social groups consisting of as few as two animals, and further extend the chronicity of certain stress effects to after 2 weeks of rest even when the paradigm is only employed for four consecutive weeks. Overall, we have simplified the stress paradigm for greater usability in laboratory settings and expanded upon its versatility for applications to smaller social groups.

5.3.2 Rank behavior in the OFT before and after SIS

Prior to social instability stress, groups did not differ by experimental condition or by rank in any behaviors measured in the open field test (Fig. 14 and Fig. 20). It was discovered in the circadian phase comparative analysis that baseline behavioral associations of rank were context-dependent; while in the dark circadian phase the rearing

behavior in the open field predicted rank, this was not the case during the light circadian phase. In fact, light phase testing reduced rearing behavior overall, which suggests that rank behavioral associations may be more readily elicited when activity and exploratory drive is greater, such as during the dark phase of the circadian cycle (Fig. 14 A-C). This supports the concept that exploratory drive serves a role-based purpose in female mice that is recruited when environmental and contextual demands encourage exploration. This could also help explain the elevated dark phase fecal corticosterone metabolite excretion observed in subordinate animals prior to hierarchy formation (Fig. 12A); elevated circulating glucocorticoids could promote the exploratory behaviors during the dark phase in novel environments and social contexts. When the context changes, such as when the environment or social group is no longer novel or when the circadian phase promotes rest versus activity, the motivation becomes altered, and behavior is representative of that change. Notably, subordinates generally maintained the pattern of elevated FCM compared to dominants in other scenarios even when the difference did not reach significance (Fig. 12A, B and Fig.15), which could represent a form of biological priming that prepares subordinates for experiencing and responding behaviorally to contextual changes. Whether changes in glucocorticoids precede and therefore dictate those behavioral changes, or whether the reverse is true, requires further investigation. One potential experiment could explore the utility of glucocorticoid priming in responding to novel and familiar environmental, social, and hedonic contexts. Consequently, given the contradicting results of many studies evaluating activity in the open field under different phases (Hostetter 1966, Valentinuzzi et al 2000, Richetto et al 2019), it would be

worthwhile to consider the social makeup of the home cage environment as well as glucocorticoid status when interpreting behavioral results.

Following social instability stress, experimental animals demonstrated elevated total distance traveled (TDT) and inner zone entries in the open field, but no changes in rearing behavior or overall time spent in the inner zone (Fig. 21A-F). There was no significant correlation between David's score and total distance traveled or inner zone entries, indicating the changes in locomotor activity were also independent of relative individual dominance (Fig. G, H). Collectively, this was interpreted as social instability inducing a hyperlocomotive phenotype in the open field regardless of rank. It also further supports the finding in the original dark circadian phase experiment that rearing is likely ethologically distinct from general locomotion as measured by total distance traveled (Fig. 10).

5.3.3 Rank behavior in the EPM before and after SIS

Prior to social instability stress, there were no differences by experimental condition in behavior in the elevated plus maze (EPM; Fig. 22A-E). Interestingly, the novel environment of the EPM was able to reproduce the baseline rank-difference in exploratory (supported) rearing behavior even during the light phase of the circadian cycle (Fig. 22F), indicating that testing environment, as well as circadian phase, can influence rank-associated behavioral phenotypes. Since the elevated plus maze is widely used to evoke an unconditioned approach-avoidance conflict (Walf & Frye 2007), this suggests an additive effect of environmental context and stress on behavior. This furthermore supports the findings in the comparative circadian analysis, in which changes in context were prerequisite to eliciting rank-based behaviors (Fig. 14). In an anxiogenic environment, for

example, the group needs for exploration may outweigh the individual desire to remain in a protected enclosed space. An alternative interpretation is that subordinate animals were more inclined to engage in rearing behavior because they were more anxious and therefore spent more time exploring the closed arms. However, this is disputed by the finding that ranks spent equal time in the open and closed arms and made similar numbers of entries into each space (Fig. 22G-J). Further experimentation will be required to fully document the ability of different testing environments, such as in the light-dark box test (Bourin & Hascoet 2003), the O-maze (Kulkarni et al 2007), and the open field under bright lighting conditions, to elicit the exploratory behavioral phenotype in subordinate animals.

Following social instability stress and a 2-week rest period, control animals demonstrated a rank-based difference in arm exploration that was absent in animals previously exposed to social instability. Specifically, dominant control animals made more entries into the closed arms and fewer entries into the open arms, which could constitute an avoidance phenotype (Fig. 23A, B). SIS-exposed subordinates, but not control subordinates, adopted a similar phenotype, indicating that in the elevated plus maze, stress-naïve subordinate animals possess a pro-exploratory motivation that is abolished by social instability. Interestingly, social instability increased rearing in the elevated plus maze overall, although the effect was greater in dominant animals and eliminated the over-representation by subordinates observed at baseline (Fig. 23C). These changes in activity and exploration appear to be largely independent of anxiety, although SIS-exposed animals spent an insignificantly lower amount of time in the open arms (Fig. 23D). Since a pro-exploration motivation was established as characterizing subordinate animals under non-stressed conditions in the original dark circadian phase experiment, these findings were

collectively considered evidence for a loss of trait behavior which persisted even two weeks after the cessation of stress. In a future study, it would be interesting to see whether reducing the rest period to one week would be sufficient to reveal a short-term anxiogenic phenotype in arm time, since the trend two weeks out appears to show that subordinates exposed to social instability prefer to avoid the open arms of the elevated plus maze.

5.3.4 Effect of SIS on behavior in the NORT

In the novel object recognition test (NORT) social instability stress reduced entries into the novel object zone for both ranks without affecting total exploration time but reduced overall novelty preference only in subordinates (Fig 24 A-C). This indicates that while both ranks exhibit a degree of neophobia post-SIS, novelty recognition is unimpaired in dominants. This is further evidence, along with the elevated plus maze data, that social instability stress disproportionately affected the behavior of subordinate animals. Further testing could discriminate between novelty preference and novelty memory deficits by using a shorter timeframe, such as a 1-hour interval between habituation to the identical objects and novelty testing.

There was also a significant negative correlation between the David's score and the novelty preference index in dominant animals exposed to social instability stress, meaning that as an animal's dominance increased its novelty preference became reduced (Fig. 24D). Therefore, individual dominance introduces some degree of discrimination in novelty approach behavior following chronic social instability. No correlation between subordinance and preference was observed, which is interesting considering the subordinate novelty preference established in the three-chamber social approach task (3CSA; Fig. 11D, E).

It is possible that the subordinate novelty preference is specific to social contexts, or that relative subordinance is less important in designating approach behavior compared to dominance. For instance, it could be that dominance in females exists on a larger spectrum than subordinance, which is more binary and reflects a singular state. One theory to explain this phenomenon is that since dominance is at risk of being lost, and therefore requires greater effort to maintain, it can elicit a greater variety of individual differences in behavior than subordinate status. This 'challenge hypothesis' is supported by the dominant pattern of approach behavior in the 3CSA and by the pattern of c-Fos expression in the PVN and mPVT after exposure to social novelty (Fig. 11 and Fig. 13). Since David's score were not calculated for control pairs as they maintained the same social partner throughout testing, further experiments are required to determine whether increased dominance is associated with lowered novelty preference or recognition in stress-naïve females. However, the results of the three-chamber social approach task indicate that dominant mice do not have a deficit in social novelty recognition.

To summarize the behavioral findings, social instability produced a generalized hyperlocomotive behavioral phenotype in the open field, but increased avoidance behavior in the elevated plus maze and reduced novelty preference in the novel object recognition test selectively in subordinate animals.

5.3.5 Changes in FCM, CSS, body weight and NBT

Although at various timepoints there was a trend of increasing fecal corticosterone metabolite excretion in the SIS-exposed group, the relationship only reached near-significance (Fig. 25D). Considering rank, social instability stress did not increase final fecal corticosterone metabolite measurements in dominant animals compared to control,

which likely contributed to the lack of a clear stress effect at the experimental endpoint (Fig. 25E, F). Given the lack of a clear rank trend prior to the eighth social instability session, it would be worthwhile to perform a future study extending the social instability paradigm out another several sessions to ensure that the rank difference is reproducible. Nonetheless, the results support an emergent chronic effect of social instability stress on subordinates.

Coat state score (CSS) is a stress-sensitive measure of what is considered depression-like behavior in rodents (Nollet et al 2013). Higher coat state score is associated with a worsening coat state and indicates a deficit of normal self-care behaviors. Coat state score increased over time for both SIS-exposed and control animals, indicating the repeated administration of the competitive exclusion (tube test) task may have resulted in deterioration of coat maintenance via either auto (self) of allo (mutual) grooming (Fig. 25A). After a two-week rest period, however, the control group coat state improved while the SIS-exposed group did not, indicating a failure to return to normal maintenance hygiene behaviors in the absence of repeated testing and handling. While overall there were no rank effects on coat state score (Fig. 25B), there was a significant correlation between improved coat state and David's score for dominant animals during the final social instability session that became nonsignificant following the 2-week rest period (Fig. 25G, H). This suggests that social instability stress, acting as a reinforcer of status for the most dominant animals, may result in improved self-maintenance. It also correlates with the fecal corticosterone metabolite data taken at the final social instability session, which demonstrated a lack of a stress effect of SIS on dominant animals (Fig. 25F). However, since allo-grooming may also contribute to coat score it is possible that more dominant individuals are groomed

more as an appeasement signal by subordinate pairs (Spruijt et al 1992). After establishing stable ranks during the rest period, during which SIS-exposed animals were continuously pair housed with the same social partner, this dominant advantage was no longer present (except as a trend), indicating a challenging social environment was prerequisite to create a significant effect on coat state. Future studies including home cage analysis of auto- and allo-grooming behavior in nascent and established hierarchies would be useful in determining the cause of the improved coat state score.

Social instability stress did not produce changes in nest building scores after the rest period (Fig. 25I), indicating coat state score may be a more sensitive measure of the effects of chronic stress on habitual behavior than nest building in female C57BL/6J mice. However, an analysis of rank behavior in stress-naïve mice exposed to novel nesting material of various types could further support or refute the effect of rank on task assignment in social groups.

Overall, social instability produced a disproportionate effect on the stress status and motivated behaviors of subordinate animals compared to dominants. Future experiments could evaluate the role of David's score-derived rank on eliciting different neurologic patterns of activity in response to social challenge (i.e., novelty) or reunion (i.e., familiarity, such as derived from social exposure to a former social partner introduced during the SIS paradigm).

6. EFFECT OF CHRONIC SOCIAL ISOLATION ON RANK-CHARACTERISTIC BEHAVIOR AND ENDOCRINE STATUS

6.1 Materials and Methods

6.1.1 Study design

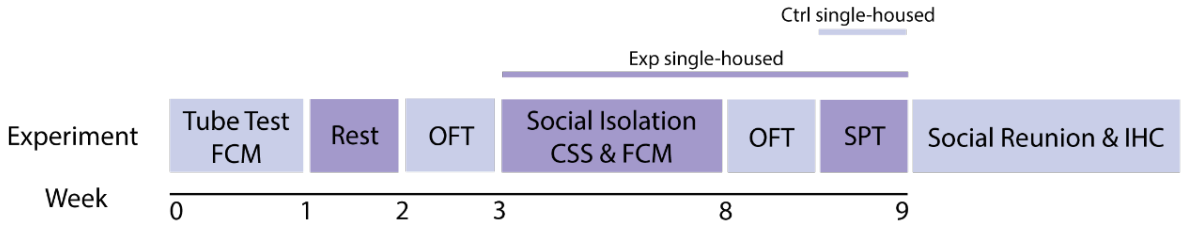

Figure 26. Experimental timeline for social isolation experiment

FCM, fecal corticosterone metabolites; *OFT*, open field test; *CSS*, coat state score; *SPT*, sucrose preference test; *IHC*, immunohistochemistry.

Pair-housed mice underwent competitive exclusion to determine rank over a period of four days; ranks were considered stable if consistent for all four days (Fan et al 2019). Mice were then continuously pair housed for 10 days, after which they underwent a baseline (pre-stress) open field test. Pairs were randomly assigned to the experimental (n = 14) or control (n = 8) group. Experimental mice were transitioned to isolation housing with standard enrichment for a total of 7 weeks, the first 5 of which were undisturbed other than periodic assessment of fecal samples, coat state score, and body weight. Control mice remained in continuous pair-housing for the same period. Post-stress behavioral testing began during week 6, when the final fecal sample was taken, and subsequently control mice were isolated for the sucrose preference test in week 7. At the end of the isolation period, experimental mice were re-introduced to their original social partner then euthanized via trans-cardial perfusion via the method described in 3.1.11.

6.1.2 Housing, lighting conditions and circadian phase

Subjects were 22 adult 3–6-month-old female C57BL6/J mice (Jackson Laboratory, Bar Harbor, Maine). Animals used in this experiment consisted of control animals from the SIS experiment that were continuously co-housed after testing for at least one month (n = 16), in addition to a new cohort of mice (n = 8) which were similarly tested for hierarchies and then allowed to remain co-housed until testing in the social isolation experiment. Therefore, hierarchies were established and stable prior to social isolation. Animals were housed on a 12:12 hour light cycle; food and water were provided ad libitum. All testing was performed during the inactive (light) phase of the circadian cycle under ambient white light. The open field test took place under dim lighting conditions (<15 lux). Fecal samples were taken during the same time period each day within experiments, and at least 2 hours into the light cycle of testing.

6.1.3 Sucrose preference test (SPT)

The sucrose preference test is performed to detect the development of anhedonia in rodents, who under non-stressed conditions generally prefer to consume a mildly sweet solution when offered the choice between that and plain water (Liu et al 2018). This test was performed in the home cage with unfasted animals, and mice were individually housed during testing. Mice were acclimated to the presence of two sipper tubes filled with water in the cage for 72 hours prior to testing to reduce neophobia and identify preexisting side bias. Afterwards, the two tubes were replaced with one containing water and the other containing a 1% sucrose solution. Over the next four days, each tube was weighed once daily to determine the amount of water or sucrose solution consumed over the previous 24 hours. The tube position alternated each day to account for and reduce potential side bias

(Liu et al 2018). Sucrose preference was calculated as the percentage of the volume of sucrose consumed divided by the total fluid intake over the test period. Anhedonia was defined as less than a 65% preference for consuming sucrose, which has been shown to correlate with other measures consistent with a depressive phenotype including behavioral despair, increased intracranial self-stimulation threshold, and reduced exploration (Strekalova et al 2004 and 2006, Strekalova & Steinbusch 2010).

$$\text{Sucrose PI } = Volume\frac{(Sucrose)}{(Sucrose\ +\ H_2O)} \cdot 100$$

6.1.4 Social reunion following chronic isolation

After chronic social isolation, experimental animals were reunited with their former co-housing partner in a new cage and allowed to interact for 15 minutes. In order to explore the effect of social isolation alone (i.e., in the absence of social stimuli) and control for the effect of a novel environment, a subset of isolated animals underwent continued isolation in a clean empty cage for the same amount of time. Control animal pairs were placed together into a novel empty cage. Afterwards, all mice were immediately dark housed (i.e., overhead lights turned off, covered cages) for 90 minutes prior to transcardial perfusion. Adrenal glands and brains were extracted, fixed in 4% PFA, and brain slices were processed for immunohistochemical detection of c-Fos expression in a manner identical to that described in 3.1.12. Adrenal glands were weighed as pairs after dissection of periadrenal adipose tissue, and weights were expressed as a percentage of the individual's final total body weight.

6.1.5 Percent difference in c-Fos expression from control mean

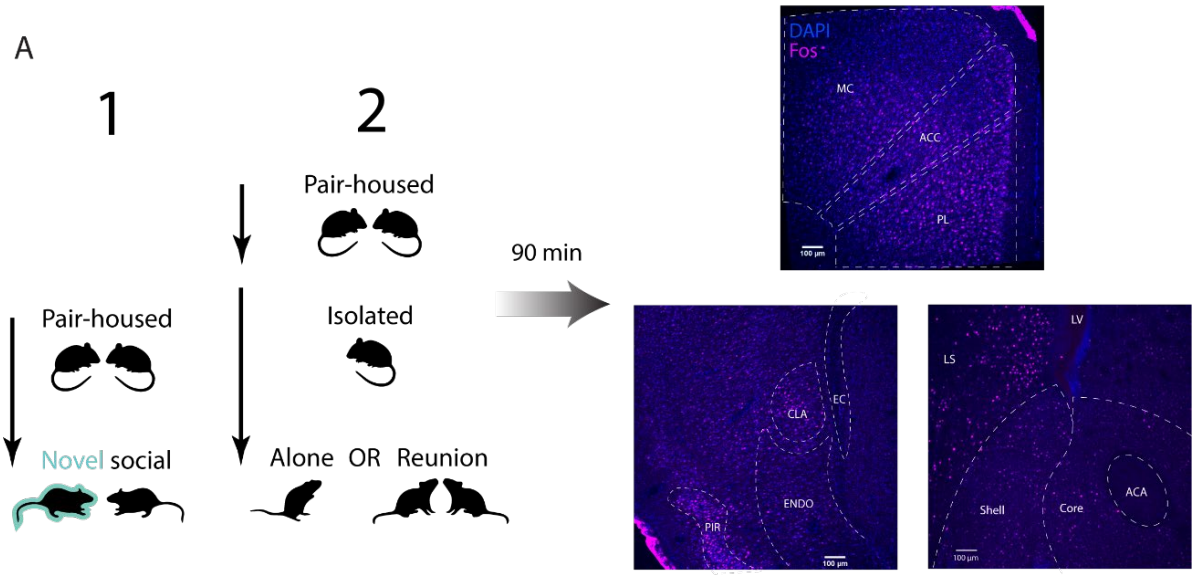

Figure 27. Social contexts used for c-Fos analysis

Schematic depiction of the c-Fos experiments. In context 1, following 3CSA, 20 mice from the original dark phase experiment were divided into groups based on exposure to a brief social encounter with a novel age-, strain-, and sex-matched conspecific in a clean cage. Control animals were placed alone into a clean cage. In context 2, following chronic social isolation, animals were either reunited with their former co-housing partner or remained alone in a new cage. Control animals were continuously pair housed in a clean cage. *PL*, prelimbic cortex; *ACC*, anterior cingulate cortex; *MC*, motor cortex; *CLA*, claustrum; *PIR*, piriform cortex; *ENDO*, endopiriform cortex; *EC*, external capsule of the corpus callosum; *Shell*, nucleus accumbens shell; *Core*, nucleus accumbens core; *LS*, lateral septum; *LV*, lateral ventricle; *ACA*, anterior part of the anterior commissure.

Images were obtained under the same conditions and using the same equipment described in 3.1.13, and subsequently quantified in ImageJ and normalized according to the protocol described in 3.1.14.

In addition to obtaining absolute counts, I characterized the magnitude and directionality of c-Fos expression arising from stress-naïve animals exposed to social novelty and socially isolated animals reunited with their familiar social partner (Fig. 27, Fig. 32). To accomplish this, rank effects were compared between paradigms by calculating

the percent difference of every animal from the control mean of their corresponding rank in that experiment. Effect sizes for the differences between the means were then calculated for each rank and within each region using Hedge's g statistic, an adjustment of Cohen's d statistic that corrects for a small population size such as n < 50 (Becker 2000, Hentschke & Stuttgen 2011, Heckert 2018). Hedge's g statistic is calculated as follows, where m_1 is the mean of one population, m_2 is the mean of the comparison population, and sd_P is the sample-size weighted pooled standard deviation:

$$g = \frac{(m_1 - m_2)}{sd_P}$$

The weighted standard deviation (SD) index is calculated as follows, where n_1 and s_1 refer to the population size and SD of m_1, and n_2 and s_2 refer to the population size and SD of m_2, respectively:

$$sd_P = \sqrt{\left(\frac{\left((n_1 - 1)s_1^2 + (n_2 - 1)s_2^2\right)}{\left((n_1 - 1) + (n_2 - 1)\right)}\right)}$$

In general, effect sizes are considered small if g = 0.2, medium if g = 0.5, and large if g = 0.8 (Becker 2000, Heckert 2018). Hedge's g statistic values for all groups are listed in Table 9.

6.2 Results

6.2.1 Rank behavior in the OFT before and after isolation

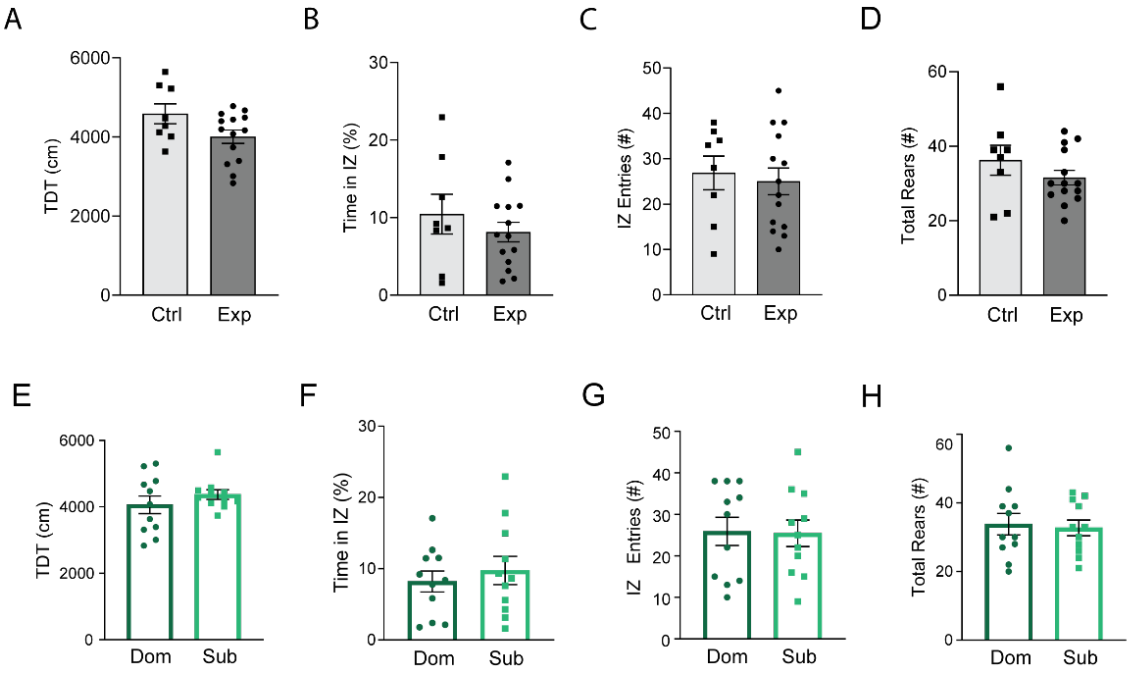

Figure 28. Behavior in the OFT before social isolation

(A) Pre-isolation total distance traveled in the OFT. N = 22 (14 Exp, 8 Ctrl); p = 0.0647 (Unpaired t test, two-tailed).

(B) Pre-isolation time in the inner zone of the OFT. N = 22 (14 Exp, 8 Ctrl); p = 0.4349 (Welch's test).

(C) Pre-isolation entries into the inner zone of the OFT. N = 22 (14 Exp, 8 Ctrl); p = 0.6990 (Welch's test).

(D) Pre-isolation total rears in the OFT. N = 22 (14 Exp, 8 Ctrl); p = 0.3728 (Mann-Whitney).

(E) Total distance traveled in the OFT prior to social isolation by rank. N = 22 (11 dom, 11 sub); p = 0.5190 (Mann-Whitney).

(F) Time in the inner zone of the OFT prior to social isolation by rank. N = 22 (11 dom, 11 sub); p = 0.5393 (Unpaired t test, two-tailed).

(G) Entries into the inner zone of the OFT prior to social isolation by rank. N = 22 (11 dom, 11 sub); p = 0.8850 (Mann-Whitney).

(H) Total rears in the OFT prior to social isolation by rank. N = 22 (11 dom, 11 sub); p = 0.7835 (Unpaired t test, two-tailed).

Data expressed as mean ± SEM. *OFT*, open field test; *TDT*, total distance traveled; *IZ*, inner zone.

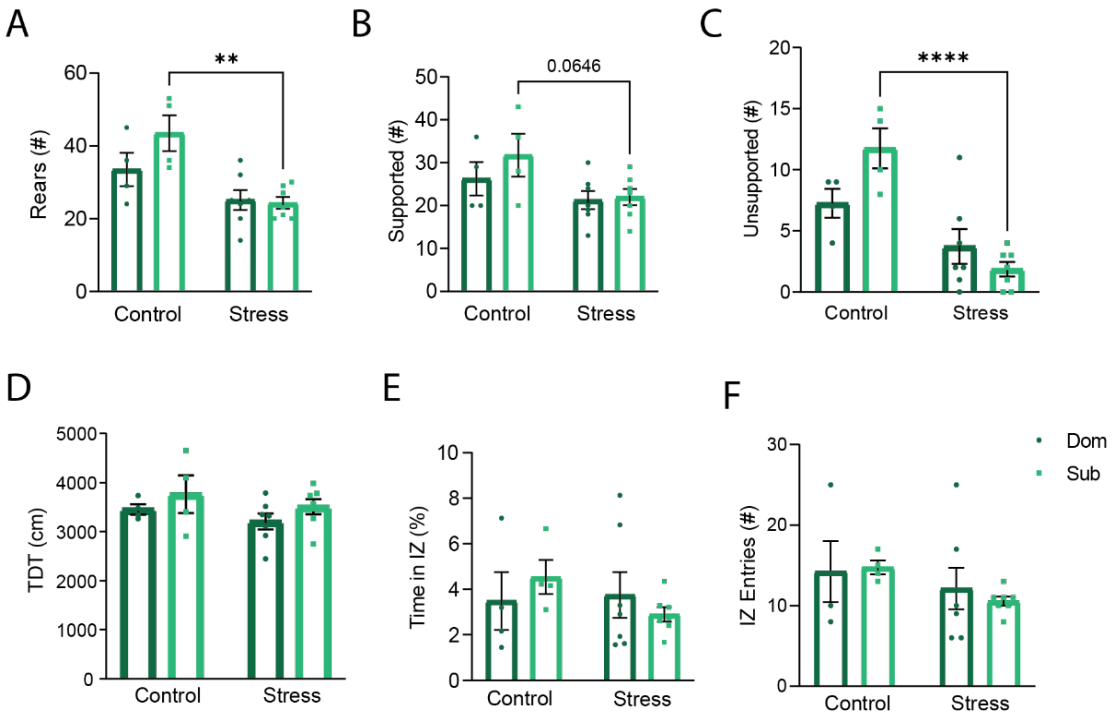

Figure 29. Behavior in the OFT after social isolation

(A) Total rears during post-isolation OFT. Stress N = 14 (7 dom, 7 sub), Ctrl N = 8 (4 dom, 4 sub); no significant interaction between Group x Rank ($F(1, 18) = 2.783$, $p = 0.1126$); significant main effect of Stress ($F(1, 18) = 17.95$, ***$p = 0.0005$, two-way ANOVA; Sidak's multiple comparisons test, Dom $p = 0.1647$, Sub **$p = 0.0011$).

(B) Post-isolation supported rears in the OFT. Stress N = 14 (7 dom, 7 sub), Ctrl N = 8 (4 dom, 4 sub); no significant interaction between Stress x Rank ($F(1, 18) = 0.6438$, $p = 0.4328$); significant main effect of Stress ($F(1, 18) = 6.086$, *$p = 0.0239$, two-way ANOVA; Sidak's multiple comparisons test, Dom $p = 0.4442$, Sub $p = 0.0646$).

(C) Post-isolation unsupported rears in the OFT. Stress N = 14 (7 dom, 7 sub), Ctrl N = 8 (4 dom, 4 sub); significant interaction between Stress x Rank ($F(1, 18) = 6.181$, *$p = 0.0230$); significant main effect of Stress ($F(1, 18) = 27.58$, ****$p < 0.0001$, two-way ANOVA; Sidak's multiple comparisons test, Dom $p = 0.1281$, Sub ****$p < 0.0001$).

(D) Post-isolation TDT in the OFT. Stress N = 14 (7 dom, 7 sub), Ctrl N = 8 (4 dom, 4 sub); no significant interaction between Stress x Rank ($F(1, 18) = 0.00066$, $p = 0.9798$, two-way ANOVA).

(E) Post-isolation time in the inner zone of the OFT. Stress N = 14 (7 dom, 7 sub), Ctrl N = 8 (4 dom, 4 sub); no significant interaction between Stress x Rank ($F(1, 18) = 1.149$, $p = 0.2979$, two-way ANOVA).

(F) Post-isolation entries into the inner zone of the OFT. Stress N = 14 (7 dom, 7 sub), Ctrl N = 8 (4 dom, 4 sub); no significant interaction between Stress x Rank ($F(1, 18) = 0.2073$, $p = 0.6543$, two-way ANOVA).

Data expressed as mean ± SEM. *OFT*, open field test; *TDT*, total distance traveled; *IZ*, inner zone.

Following pair housing and stable rank formation, animals underwent baseline testing in the open field test and were then subjected to 5 weeks of social isolation, followed by a repeat session in the open field test in week 6. Prior to isolation, there were no underlying differences by experimental group in open field behavior (Fig. 28A-D); therefore, groups were combined to look for rank differences. In agreement with the baseline findings in the social instability experiment (Fig. 14), there were no pre-existing rank differences in open field behavior during the light circadian phase prior to social isolation (Fig. 28E-H).

Social isolation disproportionately affected subordinate rearing behavior, notably in reducing the number of unsupported rears (Fig. 29A-C). Supported rearing was diminished in both ranks following social isolation (Fig. 29B). These effects were independent of locomotion and anxiety-like behavior as measured by time and entries into the inner zone (Fig. 29D-F).

6.2.2 Effect of social isolation on FCM, CSS and sucrose preference

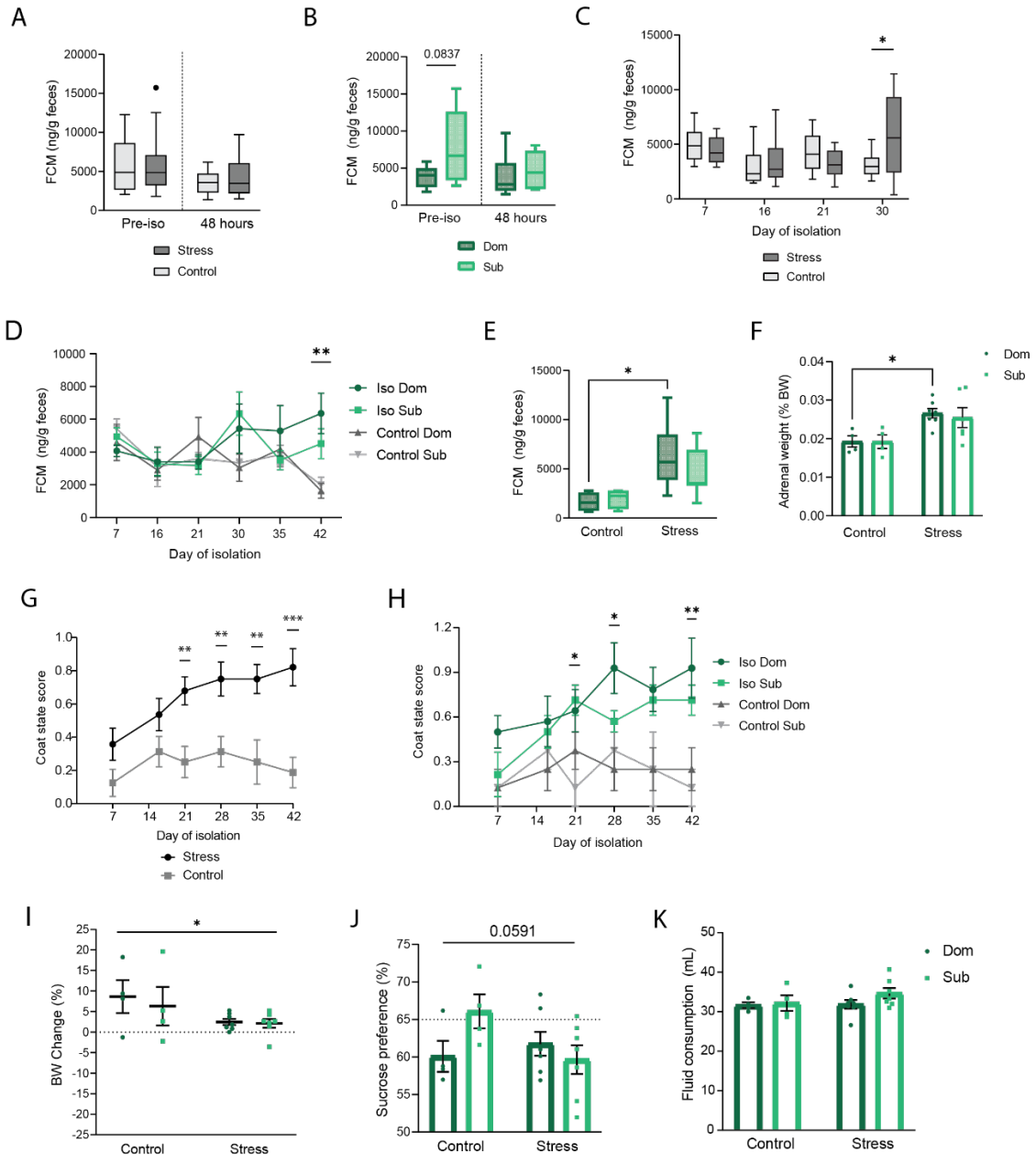

Figure 30. Effect of social isolation on FCM, CSS and sucrose preference

(A) FCM pre-isolation and after 48 hours of isolation. Stress N = 14, Ctrl N = 8; pre-iso p = 0.9734 (Mann-Whitney), 48 hours p = 0.5322 (unpaired t-test, two-tailed).

(B) FCM in Stress group pre-isolation and after 48 hours of isolation, by rank. Stress N = 14 (7 dom, 7 sub); pre-iso p = 0.0837 (Welch's t test, two-tailed), 48 hours p = 0.4557 (Mann-Whitney).

(C) FCM over first 30 days of isolation. Stress N = 14, Ctrl N = 8; Day 30 *p = 0.0213 (Welch's t test, two-tailed).

(D) Ranked FCM taken during the isolation period prior to SPT. Stress N = 14 (7 dom, 7 sub), Ctrl N = 8 (4 dom, 4 sub); significant differences were only identified at day 42; no significant interaction between Stress x Rank ($F (1, 18) = 11.57$, $p = 0.3132$); significant main effect of Stress ($F (1, 18) = 11.57$, $^{**}p = 0.0032$, two-way ANOVA; see Fig. 30E). (E) FCM at the end of isolation (42 days). Stress N = 14 (7 dom, 7 sub), Ctrl N = 8 (4 dom, 4 sub); no significant interaction between Stress x Rank ($F (1, 18) = 11.57$, $p = 0.3132$); significant main effect of Stress ($F (1, 18) = 11.57$, $^{**}p = 0.0032$, two-way ANOVA; Sidak's multiple comparisons test, Dom $^{*}p = 0.0113$, Sub $p = 0.2113$). Final FCM samples were taken prior to SPT, during which control animals were necessarily isolated.

(F) Paired adrenal weight expressed as a percentage of total body weight (BW). Stress N = 13 (7 dom, 6 sub), Ctrl N = 8 (4 dom, 4 sub); no significant interaction between Stress x Rank ($F (1, 17) = 0.0817$, $p = 0.7785$); significant main effect of Stress ($F (1, 17) = 11.84$, $^{**}p = 0.0031$, two-way ANOVA; Sidak's multiple comparisons test, Dom $^{*}p = 0.0317$, Sub $p = 0.0823$). One adrenal was lost during processing and the animals' data was excluded.

(G) Weekly coat state score during isolation. Stress N = 14, Ctrl N = 8; Day 21 $^{**}p = 0.0091$, Day 28 $^{**}p = 0.0089$, Day 35 $^{**}p = 0.0055$, Day 42 $^{***}p = 0.0004$ (Mann-Whitney).

(H) Ranked CSS taken during the isolation period prior to SPT. Stress N = 14 (7 dom, 7 sub), Ctrl N = 8 (4 dom, 4 sub); significant differences were identified at days 21, 28, and 42 of isolation; day 21 ($H (3) = 8.174$, $^{*}p = 0.0426$, Kruskal-Wallis test; Dom $p = 0.4580$, Sub $^{*}p = 0.0199$, Dunn's test); day 28 (($H (3) = 9.669$, $^{*}p = 0.0216$, Kruskal-Wallis test; Dom $^{*}p = 0.0106$, Sub $p = 0.8209$, Dunn's test); day 42 (($H (3) = 11.46$, $^{**}p = 0.0095$, Kruskal-Wallis test; Dom $^{*}p = 0.0411$, Sub $^{*}p = 0.0349$, Dunn's test).

(I) Percent change in body weight from baseline to the end of isolation. Stress N = 14 (7 dom, 7 sub), Ctrl N = 8 (4 dom, 4 sub); no significant interaction between Stress x Rank ($F (1, 18) = 0.1690$, $p = 0.6858$); significant main effect of Stress ($F (1, 18) = 4.650$, $^{*}p = 0.0448$, two-way ANOVA; Dom $p = 0.1649$, Sub $p = 0.4118$, Sidak's multiple comparisons).

(J) Sucrose preference in the final week of isolation, expressed as percentage of total volume consumed over 3 days. Stress N = 14 (7 dom, 7 sub), Ctrl N = 8 (4 dom, 4 sub); no significant interaction between Stress x Rank ($F (1, 18) = 4.058$, $p = 0.0591$, two-way ANOVA).

(K) Total fluid consumption during the SPT. Stress N = 14 (7 dom, 7 sub), Ctrl N = 8 (4 dom, 4 sub); no significant interaction between Stress x Rank ($F (1, 18) = 0.6525$, $p = 0.4298$, two-way ANOVA).

All data except FCM are displayed as mean ± SEM. Box-and-whisker plots are displayed according to the Tukey method; boxes extend from Q1 to Q3, inner fences extend +/- 1.5 IQR, dots convey outliers, and horizontal lines designate the median. FCM values with intra-assay CV > 10% or missing samples were excluded from analysis. No outliers were removed. *Pre-iso*, prior to isolation; *FCM*, fecal corticosterone metabolites; *BW*, body weight; *CSS*, coat state score.

Fecal corticosterone metabolites (FCM) were sampled prior to isolation, 48 hours after initiating isolation protocols, and then weekly throughout the paradigm. Values were compared across experimental groups and rank during the experiment. There were no significant differences in fecal corticosterone metabolite excretion between experimental and control animals after the first two days of isolation, or during the first several weeks of the paradigm (Fig. 30A, C). After one month of isolation, fecal corticosterone metabolites became elevated in the experimental group (Fig. 30C).

In agreement with the dark phase experiment, there was a nonsignificant trend for higher pre-isolation fecal corticosterone metabolites in subordinate animals, which was absent 48 hours after isolation (Fig. 30B). At the end of the isolation period (i.e., taken after 42 days of isolation, prior to performing the sucrose preference test during which control animals would also become temporarily isolated), there was a significant effect of stress on fecal corticosterone metabolites and adrenal weights in dominant mice, but not subordinates (Fig. 30D-F).

As in the social instability experiment, coat state score (CSS) was monitored as a marker of general well-being and to evaluate the effect of the stress paradigm over time. Starting at week 3 of isolation, coat state became significantly worse in isolated animals and remained elevated by group until the sucrose preference test (SPT; Fig. 30G). Although there were some rank differences during the first 30 days of observation (i.e., coat state score was significantly worse in subordinates on day 21 and in dominants on day 28), the difference became independent of rank at the experimental endpoint (Fig. 30H). There was also a stress effect on body weight; socially isolated animals gained less weight during the isolation period, regardless of rank (Fig. 30I).

Following behavioral testing, in week 7 all groups except for subordinate control animals consumed 1% sucrose with a less than 65% preference as determined by total fluid intake (Fig. 30J). There was a nonsignificant trend interaction demonstrating particularly reduced sucrose preference in isolated mice, with subordinates experiencing the greatest reduction (Fig. 30J). This change was independent of total fluid consumption, which did not differ between groups (Fig. 30K)

6.2.3 c-Fos expression following post-isolation social reunion

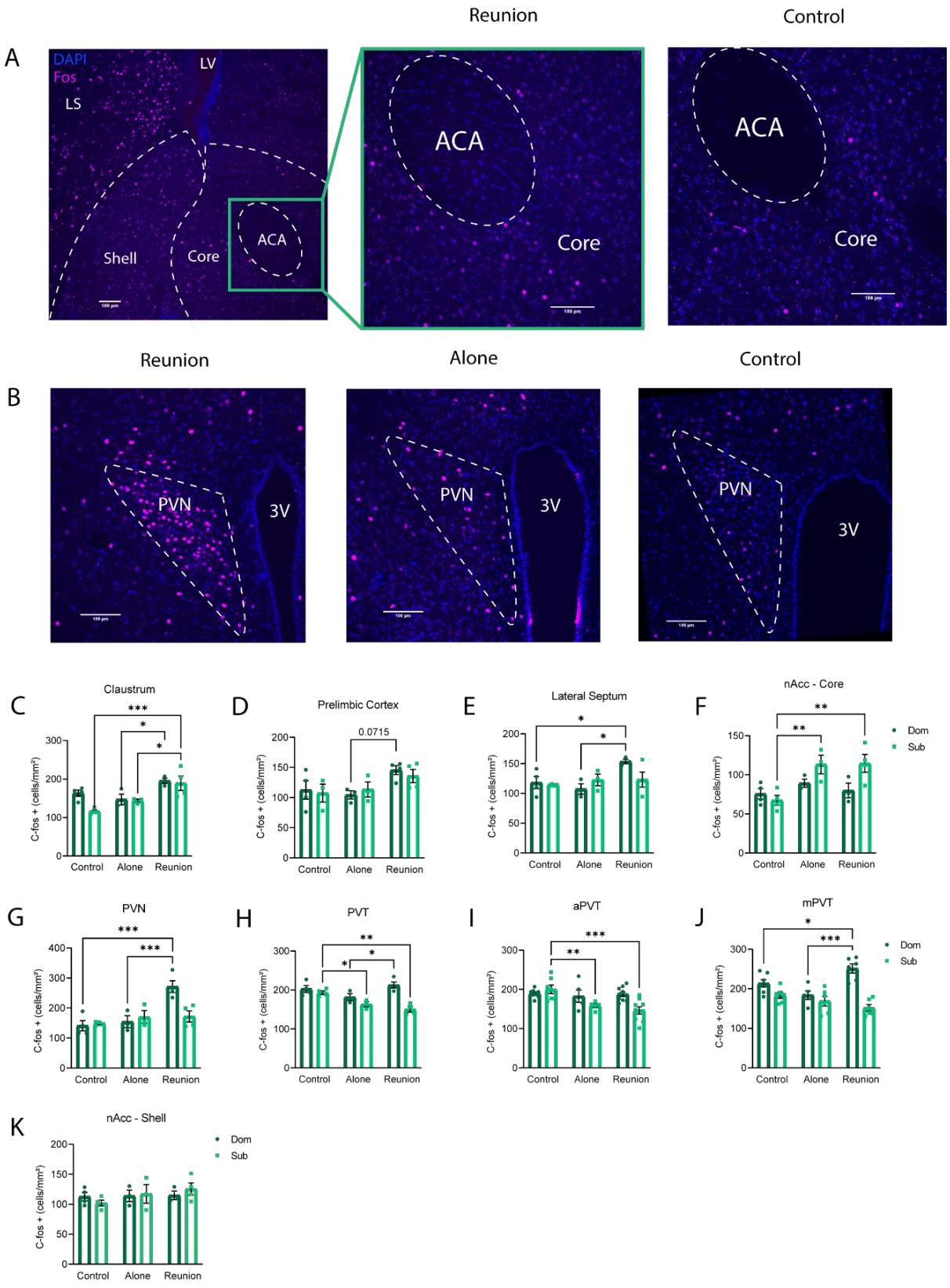

Figure 31. c-Fos expression following post-isolation social reunion or persistent isolation

(A) Representative intensity adjusted images of c-Fos labeling in nAcc. (*Left*) 10x image from a reunited experimental subordinate animal; (*Mid*) 20x image containing the nAcc core of the same animal; (*Right*) 20x image from a control subordinate animal. DAPI counterstain.

(B) Representative intensity adjusted images of c-Fos labeling in PVN. (*Left*) 20x image from a reunited experimental dominant animal; (*Mid*) 20x image from a non-reunited experimental dominant animal; (*Right*) 20x image from a control dominant animal.

(C) c-Fos expression in CLA; R N = 7 (3 dom, 4 sub), A N = 6 (3 dom, 3 sub), C N = 8 (4 dom, 4 sub); no significant interaction between Condition x Rank ($F(2, 15) = 2.455$, $p = 0.1196$); significant main effect of Condition ($F(2, 15) = 13.18$, ***p = 0.0005, two-way ANOVA; Dom R v. A, *p = 0.0332; Sub R v. A, *p = 0.0324; Sub R v. C, ***p = 0.0005, Tukey's multiple comparisons test).

(D) c-Fos expression in PL; R N = 8 (4 dom, 4 sub), A N = 6 (3 dom, 3 sub), C N = 7 (4 dom, 3 sub); no significant interaction between Condition x Rank ($F(2, 15) = 0.3141$, $p = 0.7351$); significant main effect of Condition ($F(2, 15) = 4.798$, *p = 0.0245, two-way ANOVA; Dom R v. A, p = 0.0715, Tukey's test).

(E) c-Fos expression in LS; R N = 7 (3 dom, 4 sub), A N = 6 (3 dom, 3 sub), C N = 8 (4 dom, 4 sub); no significant interaction between Condition x Rank ($F(2, 15) = 2.929$, $p = 0.0843$); significant main effect of Condition ($F(2, 15) = 4.050$, *p = 0.0392, two-way ANOVA; Dom R v. A, *p = 0.0123; Dom R v. C, *p = 0.0395, Tukey's test).

(F) c-Fos expression in nAcc core; R N = 7 (3 dom, 4 sub), A N = 6 (3 dom, 3 sub), C N = 8 (4 dom, 4 sub); no significant interaction between Condition x Rank ($F(2, 15) = 3.409$, $p = 0.0602$); significant main effects of Condition ($F(2, 15) = 6.876$, **p = 0.0076) and Rank ($F(1, 15) = 5.299$, *p = 0.0361, two-way ANOVA); difference by Condition reached significance in subordinate animals post hoc (Sub R v. C, **p = 0.0030; Sub A v. C, **p = 0.0068, Tukey's test).

(G) c-Fos expression in PVN; R N = 8 (4 dom, 4 sub), A N = 6 (3 dom, 3 sub), C N = 8 (4 dom, 4 sub); significant interaction between Condition x Rank ($F(2, 16) = 7.117$, **p = 0.0062); significant main effect of Condition ($F(2, 16) = 11.77$, ***p = 0.0007, two-way ANOVA; Dom R v. A, ***p = 0.0008; Dom R v. C, ***p=0.0001, Tukey's test).

(H) c-Fos expression in PVT; R N = 8 (4 dom, 4 sub), A N = 6 (3 dom, 3 sub), C N = 8 (4 dom, 4 sub); significant interaction between Condition x Rank ($F(2, 16) = 7.542$, **p = 0.0049); significant main effects of Condition ($F(2, 16) = 5.754$, *p = 0.0131) and Rank ($F(1, 16) = 23.88$, ***p = 0.0002, two-way ANOVA; Dom R v. A, *p = 0.0319; Sub R v. C, **p = 0.0018; Sub A v. C, *p = 0.0383, Tukey's test).

(I) c-Fos expression of all aPVT slices; R N = 19 (10 dom, 9 sub), A N = 10 (5 dom, 5 sub), C N = 15 (8 dom, 7 sub); significant interaction between Condition x Rank ($F(2, 38) = 5.370$, **p = 0.0088); significant main effects of Condition ($F(2, 38) = 6.751$, **p = 0.0031) and Rank ($F(1, 38) = 6.493$, *p = 0.0150, two-way ANOVA; Sub R v. C, ***p = 0.0001; Sub A v. C, **p = 0.0099, Tukey's test).

(J) c-Fos expression of all mPVT slices; R N = 12 (6 dom, 6 sub), A N = 11 (5 dom, 6 sub), C N = 13 (7 dom, 6 sub); significant interaction between Condition x Rank (F (2, 30) = 9.880, ***p = 0.0005); significant main effects of Condition (F (2, 30) = 3.530, *p = 0.0420) and Rank (F (1, 30) = 34.10, ****p < 0.0001, two-way ANOVA; Dom R v. C, *p = 0.0264; Dom R v. A, ***p = 0.0003).
(K) c-Fos expression in nAcc shell; R N = 7 (3 dom, 4 sub), A N = 6 (3 dom, 3 sub), C N = 8 (4 dom, 4 sub); no significant interaction between Condition x Rank (F (2, 15) = 0.7718, p = 0.4797, two-way ANOVA).
Data expressed as mean ± SEM. *nAcc*, nucleus accumbens; *LS*, lateral septum; *LV*, lateral ventricle; *ACA*, anterior part of the anterior commissure; *PVN*, paraventricular hypothalamic nucleus; *3V*, third ventricle; *PL*, prelimbic cortex; *CLA*, claustrum; *PVT*, paraventricular thalamic nucleus; *aPVT*, anterior PVT; *mPVT*, middle PVT; *R*, reunion; *A*, alone; *C*, control.

Region	Bregma (range)	Source	SS	F (DFn, DFd)	P value	Post hoc factor	Group	P value
PL	1.54 – 2.22	Inter. Cond. Rank	312.0 4766 23.10	F (2, 15) = 0.3141 F (2, 15) = 4.798 F (1, 15) = 0.0465	0.7351 0.0245 0.8322	Cond.	Dom R v. A R v. C A v. C Sub R v. A R v. C A v. C	 0.0715 0.1274 0.8825 0.4108 0.2497 0.9409
CLA	0.14 – 1.54	Inter. Cond. Rank	2200 11812 1849	F (2, 15) = 2.455 F (2, 15) = 13.18 F (1, 15) = 4.127	0.1196 0.0005 0.0603	Cond.	Dom R v. A R v. C A v. C Sub R v. A R v. C A v. C	 0.0332 0.1441 0.5900 0.0324 0.0005 0.2340
LS	0.14 – 1.18	Inter. Cond. Rank	1699 2349 206.9	F (2, 15) = 2.929 F (2, 15) = 4.050 F (1, 15) = 0.7133	0.0843 0.0392 0.4116	Cond.	Dom R v. A R v. C A v. C Sub R v. A R v. C A v. C	 0.0123 0.0395 0.6958 0.9991 0.7579 0.8096
nAcc - Core	0.74 – 1.70	Inter. Cond. Rank	1863 3758 1448	F (2, 15) = 3.409 F (2, 15) = 6.876 F (1, 15) = 5.299	0.0602 0.0076 0.0361	Cond.	Dom R v. A R v. C A v. C Sub R v. A R v. C A v. C	 0.7733 0.9427 0.5495 0.9923 0.0030 0.0068

nAcc - Shell	0.74 – 1.70	Inter. Cond. Rank	448.3 630.3 4.451	F (2, 15) = 0.7718 F (2, 15) = 1.085 F (1, 15) = 0.0153	0.4797 0.3630 0.9031			
PVN	-0.22 – -1.06	Inter. Cond. Rank	15499 25623 3465	F (2, 16) = 7.117 F (2, 16) = 11.77 F (1, 16) = 3.182	0.0062 0.0007 0.0934	Cond.	Dom R v. A R v. C A v. C Sub R v. A R v. C A v. C	 0.0008 0.0001 0.8577 0.9969 0.5761 0.6672
PVT	-0.34 – -1.46	Inter. Cond. Rank	3097 2363 4903	F (2, 16) = 7.542 F (2, 16) = 5.754 F (1, 16) = 23.88	0.0049 0.0131 0.0002	Cond.	Dom R v. A R v. C A v. C Sub R v. A R v. C A v. C	 0.0319 0.6066 0.1669 0.4762 0.0018 0.0383
aPVT by slice	-0.34 – -0.82	Inter. Cond. Rank	5587 7024 3377	F (2, 38) = 5.370 F (2, 38) = 6.751 F (1, 38) = 6.493	0.0088 0.0031 0.0150	Cond.	Dom R v. A R v. C A v. C Sub R v. A R v. C A v. C	 0.9173 0.9803 0.8528 0.6124 0.0001 0.0099
mPVT by slice	-0.94 – -1.46	Inter. Cond. Rank	12033 4299 20765	F (2, 30) = 9.880 F (2, 30) = 3.530 F (1, 30) = 34.10	0.0005 0.0420 <0.0001	Cond.	Dom R v. A R v. C A v. C Sub R v. A R v. C A v. C	 0.0003 0.0264 0.1155 0.4581 0.0797 0.5590

Table 7. 2-way ANOVA table: c-Fos expression following post-isolation social reunion or persistent isolation

Inter., interaction; *Cond.*, condition; *SS*, sum-of-squares; *PL*, prelimbic cortex; *CLA*, claustrum; *LS*, lateral septum; *nAcc*, nucleus accumbens; *PVN*, paraventricular hypothalamic nucleus; *PVT*, paraventricular thalamic nucleus; *aPVT*, anterior PVT; *mPVT*, middle PVT; *R*, reunion; *A*, alone; *C*, control.

In the original dark phase experiment, stress-naïve mice exhibited rank-associated changes in neural activity following a novel social encounter. In this experiment, using the same hierarchical lens, those findings are expanded upon by examining c-Fos expression in the same regions after a social reunion between chronically isolated mice (Fig. 31, Table 7).

In dominant animals, claustrum (CLA) c-Fos expression trended lower than control after persistent social isolation, resulting in comparatively (and significantly) higher expression than the isolated condition after social reunion, but not the control condition (Fig. 31C, Table 7). This pattern of insignificantly higher claustral expression at baseline in dominant animals was consistent between c-Fos experiments (Fig. 13E). In contrast, in subordinates after social reunion the claustral expression was elevated compared to both the control and persistently isolated condition (Fig. 31C).

In the prelimbic cortex (PL) there was a significant main effect of condition and a corresponding increase in expression in the reunion group (Fig. 31D, Table 7). However, this only reached a nonsignificant trend in dominant animals that were reunited following isolation, and there was no apparent effect of social isolation alone on prelimbic c-Fos expression.

Social reunion also caused a rank-specific increase in c-Fos expression in the lateral septum (LS) that only affected dominant animals (Fig. 31E). In the core of the nucleus accumbens (nAcc), a similar reunion effect was observed in subordinates, although the persistently isolated group also demonstrated increased expression compared to controls (Fig. 31A, F). In the nucleus accumbens shell, there was no significant effect of isolation or reunion in either rank (Fig. 31K).

The paraventricular nucleus of the hypothalamus (PVN) in dominants was responsive to social reunion, but not to persistent social isolation, and there was no effect in subordinate animals (Fig. 31B, G).

In the paraventricular thalamus (PVT), in contrast, there were contrasting changes from control in both ranks (Fig. 31H). In dominants, persistent isolation slightly (and insignificantly) reduced PVT c-Fos expression compared to controls. However, the effect was sufficient to cause a significant difference between the Alone (persistently isolated) and the Reunion groups, between which there was a slight increase in expression upon reunion (Table 7). In subordinates, in contrast, persistent isolation as well as reunion decreased c-Fos expression relative to controls, but there was no significant difference between the Alone and Reunion groups (Table 7).

Accounting for the rostro-caudal distribution of slices revealed differences in the expression in the anterior PVT (aPVT) and the middle PVT (mPVT) which contrasted in both regionality and directionality between ranks. Namely, in the aPVT of subordinate animals there was a progressive decrease in c-Fos expression from control to Alone, and from the Alone to Reunion groups (Fig. 31I, Table 7). The difference was only significant from control, and not between the isolated groups. There was no significant difference in dominant aPVT between groups. In the mPVT, there was an insignificant decrease in expression in the Alone group from control, but a significant increase in the mPVT in the Reunion group; this change was significantly different from both the Alone group and the control group (Fig. 31J, Table 7). In subordinates, there were no differences in mPVT expression between groups.

6.2.4 Comparison of c-Fos expression between two social contexts

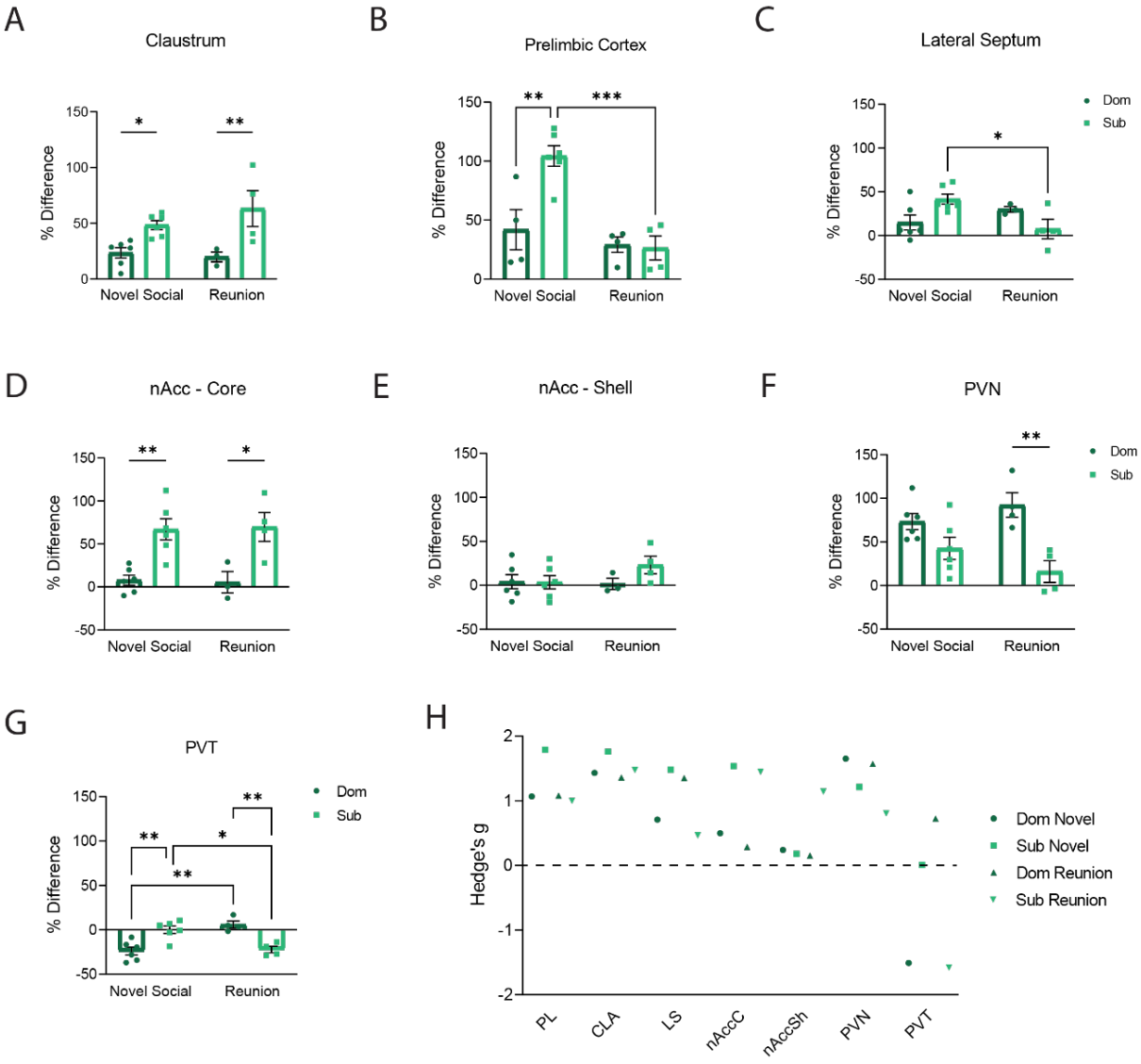

Figure 32. Comparison of c-Fos expression between two social contexts

(A) Difference from control in c-Fos expression in the CLA. Novel Social N = 12 (6 dom, 6 sub), Reunion N = 7 (3 dom, 4 sub); no significant interaction between Stimulus x Rank ($F(1, 15) = 1.275$, $p = 0.2767$); significant main effect of Rank ($F(1, 15) = 17.42$, ***$p = 0.0008$, two-way ANOVA; Sidak's multiple comparisons test, Novel *$p = 0.0461$, Reunion **$p = 0.0092$).

(B) Difference from control in c-Fos expression in the PL. Novel Social N = 10 (4 dom, 6 sub), Reunion N = 8 (4 dom, 4 sub); significant interaction between Stimulus x Rank ($F(1, 14) = 8.652$, *$p = 0.0107$); significant main effects of Stimulus ($F(1, 14) = 16.80$, **$p = 0.0011$) and Rank ($F(1, 14) = 7.294$, *$p = 0.0172$, two-way ANOVA; Sidak's multiple comparisons test, Novel:Dom vs. Novel:Sub **$p = 0.0055$, Novel:Sub vs. Reunion:Sub ***$p = 0.0008$).

(C) Difference from control in c-Fos expression in the lateral septum. Novel Social N = 12 (6 dom, 6 sub), Reunion N = 7 (3 dom, 4 sub); significant interaction between Stimulus x Rank (F (1, 15) = 8.372, *p = 0.0111), two-way ANOVA; Sidak's multiple comparisons test, Dom p = 0.4403, Sub *p = 0.0184).

(D) Difference from control in c-Fos expression in the nAcc core. Novel Social N = 12 (6 dom, 6 sub), Reunion N = 7 (3 dom, 4 sub); no significant interaction between Stimulus x Rank (F (1, 15) = 0.04516, p = 0.8346); significant main effect of Rank (F (1, 15) = 25.23, ***p = 0.0002, two-way ANOVA; Sidak's multiple comparisons test, Novel **p = 0.0024, Reunion *p = 0.0101).

(E) Difference from control in c-Fos expression in the nAcc shell. Novel Social N = 12 (6 dom, 6 sub), Reunion N = 7 (3 dom, 4 sub); no significant interaction between Stimulus x Rank (F (1, 15) = 1.556, p = 0.2313).

(F) Difference from control in c-Fos expression in the PVN. Novel Social N = 12 (6 dom, 6 sub), Reunion N = 8 (4 dom, 4 sub); no significant interaction between Stimulus x Rank (F (1, 16) = 3.464, p = 0.0812); significant main effect of Rank (F (1, 16) = 19.17, ***p = 0.0005, two-way ANOVA; Sidak's multiple comparisons test, Novel p = 0.1238, Reunion **p = 0.0019).

(G) Difference from control in c-Fos expression in the PVT. Novel Social N = 12 (6 dom, 6 sub), Reunion N = 8 (4 dom, 4 sub); significant interaction between Stimulus x Rank (F (1, 16) = 35.18, ****p < 0.0001, two-way ANOVA; Sidak's multiple comparisons test, Novel:Dom vs. Novel:Sub **p = 0.0032, Novel:Dom vs. Reunion:Dom **p = 0.0012, Novel:Sub vs. Reunion:Sub *p = 0.0148, Reunion:Dom vs. Reunion:Sub **p = 0.0047).

(H) Hedge's g statistic for effect size in each brain region. Refer to Table 9 for a complete list of values.

Data expressed as mean ± SEM except for Hedge's g statistics. *PL*, prelimbic cortex; *CLA*, claustrum; *nAccC*, nucleus accumbens core; *nAccSh*, nucleus accumbens shell; *PVN*, paraventricular hypothalamic nucleus; *PVT*, paraventricular thalamic nucleus.

Region	Source	SS	F (DFn, DFd)	P value	Post hoc	Group	P value
PL	Inter.	4637	F (1, 14) = 8.652	0.0107	Both	NS:Dom v. NS:Sub	0.0055
	Con.	9003	F (1, 14) = 16.80	0.0011		NS:Dom v. Re:Dom	0.9713
	Rank	3909	F (1, 14) = 7.294	0.0172		NS:Dom v. Re:Sub	0.9313
						NS:Sub v. Re:Dom	0.0011
						NS:Sub v. Re:Sub	0.0008
						Re:Dom v. Re:Sub	>0.999
CLA	Inter.	371.1	F (1, 15) = 1.275	0.2767	Rank	Novel	0.0461
	Con.	138.8	F (1, 15) = 0.4768	0.5004		Reunion	0.0092
	Rank	5073	F (1, 15) = 17.42	0.0008			
LS	Inter.	2624	F (1, 15) = 8.372	0.0111	Con.	Dom	0.4403
	Con.	402.4	F (1, 15) = 1.284	0.2750		Sub	0.0184
	Rank	19.03	F (1, 15) = 0.0607	0.8087			
nAcc - Core	Inter.	29.70	F (1, 15) = 0.0452	0.8346	Rank	Novel	0.0024
	Con.	0.1763	F (1, 15) = 0.0003	0.9872		Reunion	0.0101
	Rank	16592	F (1, 15) = 25.23	0.0002			
nAcc - Shell	Inter.	523.0	F (1, 15) = 1.556	0.2313			
	Con.	327.3	F (1, 15) = 0.9741	0.3393			
	Rank	474.5	F (1, 15) = 1.412	0.2532			
PVN	Inter.	2486	F (1, 16) = 3.464	0.0812	Rank	Novel	0.1238
	Con.	72.68	F (1, 16) = 0.1013	0.7544		Reunion	0.0019
	Rank	13757	F (1, 16) = 19.17	0.0005			
PVT	Inter.	3251	F (1, 16) = 35.18	<0.0001	Both	NS:Dom v. NS:Sub	0.0032
	Con.	68.55	F (1, 16) = 0.7418	0.4018		NS:Dom v. Re:Dom	0.0012
	Rank	20.24	F (1, 16) = 0.2190	0.6461		NS:Dom v. Re:Sub	0.9999
						NS:Sub v. Re:Dom	0.9321
						NS:Sub v. Re:Sub	0.0148
						Re:Dom v. Re:Sub	0.0047

Table 8. 2-way ANOVA table comparing the percent difference in c-Fos expression from control mean in two social contexts

Inter., interaction; *Con.*, context; *SS*, sum-of-squares; *PL*, prelimbic cortex; *CLA*, claustrum; *LS*, lateral septum; *nAcc*, nucleus accumbens; *PVN*, paraventricular hypothalamic nucleus; *PVT*, paraventricular thalamic nucleus; *NS*, novel social; *Re*, reunion.

Region	Rank	Social novelty	Social reunion
PL	Dom	1.069149	1.081811
	Sub	1.791699	1.000898
CLA	Dom	1.431556	1.359753
	Sub	1.761188	1.477597
LS	Dom	0.71025	1.352007
	Sub	1.483243	0.466802
nAcc - core	Dom	0.497797	0.28478
	Sub	1.537996	1.449346
nAcc - shell	Dom	0.240544	0.152498
	Sub	0.179938	1.145957
PVN	Dom	1.652356	1.570533
	Sub	1.214748	0.807276
PVT	Dom	-1.50830593	0.484049004
	Sub	0.00936	-1.579373093

Table 9. Hedge's g effect sizes for groups by region

PL, prelimbic cortex; *CLA*, claustrum; *LS*, lateral septum; *nAcc*, nucleus accumbens; *PVN*, paraventricular hypothalamic nucleus; *PVT*, paraventricular thalamic nucleus

It was possible to compare the magnitude and directionality of c-Fos expression between the two social contexts by calculating the percent difference of every individual from their corresponding within-rank control mean (Fig. 32, Table 8). Effect sizes of the magnitude of the differences were compared using Hedge's g statistic (Table 9).

In the claustrum both social contexts produced an increase in c-Fos expression, but the largest difference from control was in subordinate animals (Fig. 32A). The effect size was large and in the positive direction (i.e., $g > 1.0$) for all groups (Fig. 32H, Table 9).

Social novelty produced the largest difference in expression in the prelimbic cortex from control and this was especially pronounced in subordinate animals (Fig. 32B). As in the claustrum, the effect size of the difference in the prelimbic region was large for all groups Fig. 32H, Table 9).

As in the prelimbic cortex, in the lateral septum the largest difference was in subordinate animals exposed to social novelty (Fig. 32C). There was a difference in the

effect sizes, however, with the largest effect in subordinates exposed to social novelty and dominants exposed to social reunion; the other groups had moderate effect sizes (Fig. 32H, Table 9).

In the nucleus accumbens core, as in the claustrum, the largest differences from control in both contexts were seen in subordinate animals (Fig. 32D), who had corresponding large effect sizes (Fig. 32H, Table 9). In the shell, there were no significant differences in change from the control mean (Fig. 32E) and effect sizes were generally small, except for reunited subordinate animals which experienced a directionally consistent positive change (Fig. 32H, Table 9).

Both social novelty and social reunion produced an increase in PVN c-Fos expression in dominant animals, but the rank effect was only significantly different in the context of social reunion (Fig. 32F). The effect sizes of the changes in the PVN were large for all groups (Fig.32 H, Table 9).

In the paraventricular thalamus (PVT), the social contexts produced negative changes in the directional consistency of the difference from the control mean, as well as opposing effects by rank. These significant opposing rank effects in directionality were unique to the PVT. Social novelty produced a significant decrease in expression in dominant animals, whereas social reunion produced the same effect in subordinate animals (Fig. 32G). These conditions also produced the largest effect sizes, while in reunited dominants there was a moderate effect size in the positive direction (Fig.32 H, Table 9).

6.3 Discussion

6.3.1 Rank behavior in the OFT before and after isolation

Different forms of stress have been shown to elicit distinct behavioral and neurobiological responses (Blanchard et al 2001, Patel et al 2019). To explore how social rank moderates the response to different psychosocial stressors, I next evaluated the effects of chronic social isolation.

In contrast to social instability, which produced a universal hyperlocomotive phenotype, social isolation produced overt stress effects observable as behavioral changes in the open field test. Both ranks experienced a reduction in supported rearing, indicating social isolation inhibited the expression of exploratory behaviors (Fig. 29B). Unsupported rearing is considered a stress-sensitive behavior in that acute stress and aversive environmental changes have been shown to reduce its occurrence in the open field (Sturman et al 2018). Isolation produced a decrease in unsupported rearing that was most pronounced in subordinate animals (Fig. 29C), suggesting social isolation produced a disproportionate stress effect on subordinate behavior. Isolation stress did not impact locomotion as measured by total distance traveled (Fig. 29D), nor did it affect anxiety-like behavior (Fig. 29E, F), further substantiating the findings of the previous experiments which found an ethological distinction between rearing, general activity and anxiety.

6.3.2 Effect of social isolation on FCM, CSS and sucrose preference

Social isolation did not affect fecal corticosterone metabolite (FCM) excretion in the first 48 hours (Fig. 30A, B). Interestingly, at baseline subordinates had a nonsignificant trend of higher fecal CORT metabolites (Fig. 30B), which was consistent with the rank pattern of baseline fecal CORT metabolite excretion in the social instability stress

experiment (Fig. 15). Since both of these experiments were performed in the light phase, this supports the existence of circadian influence on rank-specific FCM excretion patterns. Fecal corticosterone metabolites became significantly elevated in isolated animals only after 30 days of isolation, suggesting a period of chronicity was necessary to produce changes in endocrine status (Fig. 30C). Interestingly, the post-isolation effect on fecal CORT metabolites and adrenal weights only reached significance in dominant animals (Fig. 30D-F), indicating their stress status was disproportionately affected by chronic social isolation. This contrasted with social instability, which disproportionately affected the FCM status of subordinate animals (Fig. 25F). This also was in opposition to the open field test behavioral effects of social isolation, which manifested primarily in subordinate animals (Fig. 29). One potential explanation for these differences is that social instability was reinforcing for dominants, whereas it was de-stabilizing for subordinates, and that social isolation exposed a dominant endocrinologic vulnerability to the loss of social reinforcement. In contrast, subordinates experience socially-responsive endocrine changes which engage adaptive behaviors, and therefore exhibit stress effects behaviorally following social isolation.

Compared to fecal CORT metabolites, changes in coat state were evident earlier in the paradigm, first reaching significance at 21 days (Fig. 30G). As with social instability, the changes in coat state were independent of rank (Fig. 30F). This correlated with weight changes at the end of isolation, which caused stressed animals to gain less weight over the isolation period compared to control animals (Fig. 30H). It appears that while coat state is a useful and early indicator of isolation-induced stress effects, it does not appear to be helpful in identifying rank-based stress vulnerabilities. However, it is possible that, as was

observed in the social instability experiment, the degree of individual dominance can influence self-maintenance habits (Fig. 25G, H). Since we did not expose animals to multiple social partners in this experiment and therefore did not calculate David's score, a future social isolation experiment of established triad hierarchies could explore this further. Also, since coat state scores are known to exhibit pronounced strain differences (Nollet et al 2013), it would be interesting to explore whether it is sensitive to rank differences in mice of a non-C57 background.

Overall, the only group to consume sucrose with more than 65% preference were control subordinate animals (Fig. 30I), and this was in the absence of polydipsia in any group (Fig. 30K). Interestingly, in male C57BL6/J mice, vulnerability to stress-induced anhedonia has previously been associated with submissive behavioral attributes (Strekalova et al 2004). One interpretation is that persistent paired housing may be stressful for dominant females; dominant controls demonstrated both a trend of lower unsupported rears compared to subordinate controls (Fig. 29C) and had a sucrose preference under 65% in post-testing, which was sufficient to reduce the effect of isolation on sucrose preference to non-significance (Fig. 30K). Contradictorily, control dominants did not have higher FCM at the end of testing (Fig. 30F). Therefore, an alternative interpretation is that despite 2-bottle acclimation, dominant controls may have been expressing neophobia to the sucrose solution. Neophobia was not a generalized trait according to results from the three-chamber social approach task or the novel object recognition test (Fig. 11, Fig. 24). Alternatively, it could be that subordinate animals were more sensitive to the hedonic effects of even a mildly concentrated sweet solution (1% sucrose was used in this experiment). Another parallel experiment investigating rank-based preference for varying

concentrations of sucrose, and prior exposure to sucrose during the acclimation period, would lend more insight into these findings.

In summary, social isolation produced a stressed behavioral phenotype in subordinate animals in the open field test but affected sucrose preference, coat state score and body weight independent of rank. In contrast to behavioral changes, fecal CORT metabolite excretion was disproportionately elevated in isolated dominant animals. This suggests that the subordinate females may be resilient to the endocrinological effects of social isolation but susceptible to behavioral changes, with the reverse being true for dominant animals. Collectively this indicates differences by rank in the behavioral and endocrine coping strategies to social isolation.

6.3.3 c-Fos expression following post-isolation social reunion

After social isolation, c-Fos expression in reunited subordinate animals was disproportionately elevated from control, whereas dominant animals only experienced a significant difference between the isolated and reunion groups (Fig. 31C). This was due to a slight (insignificant) decrease in c-Fos expression in persistently isolated dominants compared to control. Control dominants, compared to subordinates, exhibited an insignificant increase in claustral c-Fos expression from the baseline condition (i.e., continued pair housing). Social isolation eliminated this rank trend as seen in the Alone (persistently isolated) group. What is particularly interesting is the difference between ranks in response to social isolation; although insignificant, persistently isolated dominants exhibited decreased claustral c-Fos expression whereas persistent isolation had the opposite effect in subordinates (Fig. 31C, Table 7). Overall, given the potential role of the claustrum in salience detection (Smith et al 2019) and the disproportionate stress effects of

social isolation on dominant animals, this difference in c-Fos expression could reflect a dampening of dominant claustral activity in the absence of social stimuli, whereas subordinates experience reduced claustral expression only in the absence of novel (or stimulating) social stimuli, such as that experienced from reunion after prolonged social isolation. Indeed, social reunion and isolation produced similar expression patterns in subordinates (Fig, 31F, H, I), with the exception that only reunion increased expression in the claustrum, supporting a role for the claustrum in mediating social investigation in subordinates.

In the prelimbic cortex, social reunion produced a nonspecific increase in c-Fos expression (Fig. 31D) that is consistent with its known role in differentiating novel and familiar social encounters (Zhao et al 2022). Elevated prelimbic and infralimbic FosB transcription has been documented in female C57BL/6J mice isolated in adolescence (Noback et al 2021); however, in this experiment adult social isolation alone was insufficient to produce elevated c-Fos expression in the absence of social reunion (Fig. 31D, Table 7). Further experiments could explore the salience of the social encounter in eliciting differential Fos expression, such as by exposing one cohort to a novel social partner after isolation, or by exposing isolated females to a male conspecific. Adult social isolation is a particularly critical area of research as it has relevant implications for neurobiological resilience to adult-onset psychiatric disorders, such those experienced as a result of quarantine-related lockdowns during the COVID19 pandemic (Wu et al 2020).

In the lateral septum, a rank-specific increase in c-Fos expression was documented in reunited dominant animals (Fig. 31E). The increase was contingent upon social exposure, as there was no difference between the isolated and control groups (Fig. 31E,

Table 7). Given the well-described role of both the lateral septum (Menon et al 2021) and social isolation (Mumtaz et al 2018) in mediating aggression, this disproportionate signal increase may also represent the social assertion of dominance in isolated female mice presented with a social challenge.

Both persistent isolation and social reunion increased c-Fos expression in the nucleus accumbens core, and not the shell, of subordinate animals compared to control (Fig. 31F, K). Since this trend was not significantly different between the isolated groups (Table 7), it was interpreted as a rank-specific effect of prolonged isolation. Early life stress models of social isolation have demonstrated an important role for dopaminergic and glutamatergic signaling in the nucleus accumbens in gating behavioral responses in rodents (Mumtaz et al 2018, Yorgason et al 2013, Deutschmann et al 2022). Socially isolated rearing is also used to study addiction in rodents, as it has been shown to increase drug seeking via alterations in glutamatergic signaling in the accumbens core in both male and female mice (Deutschmann et al 2022). This effect on the nucleus accumbens is not isolated to psychosocial stress, since following food restriction stress behavioral sensitization to cocaine in rats has been linked to selective dopamine sensitization in the accumbens core (Cadoni et al 2003). On the other hand, in male mice, ΔFosB expression in the nucleus accumbens following voluntary wheel running has been shown to promote resilience to chronic social defeat stress (Mul et al 2018). Since these studies did not investigate social status specifically, one can only speculate upon the relevance of the animals' subjective rank in mediating the accumbens response. However, in addition to exhibiting stress-responsive signaling changes, the nucleus accumbens is heavily implicated in mediating social reward and approach (Dolen et al 2013, Rogers-Carter et al

2019, Saddoris et al 2013). It is possible that elevated accumbens core c-Fos expression in socially isolated subordinate female mice represents a sex-specific neurologic mechanism underlying their apparent resilience observed endocrinologically, and which informs the observed rank-differences in motivated approach behavior. The long-term effects of elevated nucleus accumbens core activity requires further study, and additional investigation into whether there exists a fundamental sex-based rank difference in accumbens dopaminergic signaling is warranted.

Although chronic social isolation increased dominant fecal corticosterone metabolite excretion and adrenal weight (Fig. 30D-F), persistently isolated dominants did not exhibit increased PVN c-Fos expression in the absence of social exposure (Fig. 31G). Exposure to brief (<24 hr) social isolation in preadolescence has been shown to selectively reduce PVN CRH neuron excitability in female mice (Senst et al 2016). In female but not male prairie voles, chronic social isolation elevated oxytocin (OXT) in both plasma and the PVN without affecting CRH immunoreactivity (Grippo et al 2007). These findings support the notion that OXT-mediated social investigation rather than CRH-mediated social stress may be the instigator of the increased PVN expression pattern in dominant female animals, although further functional and cell type experiments are necessary to confirm this hypothesis. Indeed, in the absence of stress dominant females do not display avoidance behaviors in the three-chamber social approach task and instead exhibit behavioral patterns consistent with sociability (Fig. 11).

Social reunion and persistent isolation both suppressed c-Fos expression in the paraventricular thalamus (PVT) in subordinate animals, whereas social reunion increased expression in the thalamus in dominants relative to the persistent isolation group (Fig.

31H). This suppressing effect was found to be significant only in the anterior PVT of subordinates, and not the middle PVT (Fig. 31I, J). As discussed in Chapter 3, the aPVT is responsible for conveyance of arousal and state-specific information to the cortex (Gao et al 2020, Zhu et al 2022). In rats subjected to chronic social isolation, PVT Fos expression was negatively correlated with the expression of social interactions with a novel social partner (Ahern et al 2016). Social isolation may induce a pro-homeostatic state in the aPVT of subordinate animals by suppressing neuronal subpopulations associated with arousal when alone and during social reunion (Fig. 31I). This could represent another biological coping mechanism employed because of the intrinsic state of subordinates under the conditions of social isolation. Whether this could be recreated in a familiar social encounter without prolonged social isolation requires further experiments.

Interestingly, social reunion selectively increased c-Fos expression in the mPVT of dominants compared to the persistently isolated group (Fig. 31J). Enhanced mPVT c-Fos expression in dominants is consistent with the increased expression in the lateral septum (Fig. 31E) and may reflect increased aversive signaling associated with social agonism and assertion of dominance (Menon et al 2021, Zhu et al 2022). Future studies extending the examination of c-Fos expression to the more posterior regions of the paraventricular thalamus will lend further insight into the role of the pPVT in mediating dominant responses to social challenges.

6.3.4 Comparison of c-Fos expression between two social contexts

In addition to obtaining absolute values, I characterized the magnitude and directionality of c-Fos expression arising from stress-naïve animals exposed to social novelty and socially isolated animals reunited with their familiar social partner. To

accomplish this, rank effects were compared between paradigms by calculating the percent difference of every animal from the control mean of their corresponding rank in each experiment.

In either context, control dominant animals in the social isolation experiment exhibited greater claustral c-Fos expression than subordinates (Fig. 13E, Fig. 31C), and experimental subordinates experienced the greatest increase in expression from control (Fig. 32A). Overall, it appears that the claustrum may exhibit stronger baseline activity in dominant animals, so that introduction of a social stimulus causes a disproportionate increase in activity in subordinate animals. Indeed, since it appears that control subordinates have lower claustral c-Fos expression than dominants at 'social baseline' conditions such as during continuous pair housing or while alone (Fig 13E, Fig. 31C), it is possible that the claustrum of subordinate female mice is more sensitive and responsive to high-arousal social interactions. These nuanced rank differences could be further explored with fiber photometry studies to see if moment-to-moment claustral GCaMP dynamics are elevated in dominants at baseline, and to determine whether social isolation dampens this effect.

Social novelty, but not social reunion, increased c-Fos expression disproportionately in the prelimbic cortex of subordinate mice (Fig. 32B, Table 8). While social reunion following isolation increased prelimbic c-Fos expression in dominant mice, the trend did not reach significance (Fig. 31D). Given the role of the prelimbic cortex in differentiating social novelty, it is possible that the novel social environment elicited a differential response in subordinates that was reflected in their preference in the three-chamber social approach task (Fig. 11), whereas the recognition of the previous social

partner was responsible for the lack of rank-specific increase in the social isolation context. This is also consistent with the pattern of elevated/unchanged expression in the lateral septum of novel/reunited subordinates, respectively (Fig. 13G and Fig. 31E), as that region has been similarly associated with novelty discrimination (Gabor et al 2012). An analysis of the response to social reunion in the absence of prolonged social isolation would provide needed information. For example, since 48 hours of isolation was shown not to elicit a stress response in fecal corticosterone metabolite excretion (Fig. 30A, B), this could be a benchmark for examining rank differences in response to social recognition in the absence of stress. Collectively these findings suggest a role for the prelimbic cortex in regulating social experiences differentially in subordinate females that is absent after exposure to chronic social isolation.

Increased c-Fos expression was documented in the lateral septum in subordinate animals following social novelty (Fig. 13G) and in dominant animals following social reunion after chronic social isolation (Fig. 31E), with the greatest change from control existing in the subordinate population (Fig. 32C, Table 8). In the case of subordinate mice exposed to social novelty, we saw in the three-chamber social approach task that subordinates exhibit a novelty preference (Fig. 11) and stress-naïve subordinates did not fail to discriminate a novel object in the novel object recognition test (Fig. 24C). Therefore, the lack of a change in subordinate lateral septum expression following a familiar social reunion supports the role of the lateral septum in discriminating social novelty in subordinate females.

Elevated AVP signaling in the lateral septum is thought to be important for mediating social recognition in male rodents, but not females (Bluthe et al 1990, Aspesi &

Choleris 2021), suggesting the rank difference observed in dominants following social reunion (Fig. 31E) is not likely to be related to a difference in AVP-moderated recognition of the familiar social partner. Additionally, this increase in expression was not observed in stress-naïve dominants in the context of social novelty (Fig. 13G and Fig. 32C). While further studies investigating the cell types activated in response to social reunion will be necessary to explore the specific activation pattern in the lateral septum, it is possible that the Fos expression is attributable in the case of social novelty to preference in subordinate females whereas following reunion it involves the reassertion of dominance in dominant females. This is further supported by lower prelimbic engagement during social reunion (Fig. 13), suggesting a role in regulating novel social experiences differentially in subordinate females.

In the nucleus accumbens core, social reunion, isolation and novelty produced the same effect of increased c-Fos expression in subordinate animals (Fig. 31F and Fig. 32D). In fact, social isolation on its own only produced significant changes in the accumbens core and anterior PVT of subordinate females, as demonstrated by a significant difference in persistently isolated subordinates compared to control (Fig. 31F, I). Since significant changes in nucleus accumbens core expression were specific to subordinate mice regardless of novelty (Fig. 32D, H, Table 8 and Table 9), it is possible that social investigation dictates a behavioral response of greater magnitude compared to dominants, characterized by either approach or avoidance (Saddoris et al 2013). This supports a generalized pro-exploratory motivation, and elevated expression during persistent isolation could represent a form of biological coping (Fig. 31F). Further experiments investigating the types of neurons activated during novel or reunion social exposure, and their

involvement in motor output, are necessary to explore the salience of social encounters by rank. Collectively, these data suggest that social reunion and social novelty produce opposing rank effects on c-Fos expression in the lateral septum, but similar effects in the prelimbic cortex and nucleus accumbens core.

In the PVN, the percent change from control animals was greatest in dominant animals in either context, but the difference between ranks was significant only in the context of social reunion (Fig. 32F, Table 8 and Table 9). This is attributable to the fact that social novelty did produce a nonsignificant increase in PVN c-Fos expression in subordinate animals (Fig. 13I), a finding that is consistent with the social novelty preference identified in subordinates in the three-chamber social approach task (Fig. 11).

Increased PVN c-Fos expression in dominants likely reflects its known role in regulating social encounters and prosocial behavior (Wu et al 2022). Interestingly, while social novelty produced a nonsignificant increase in expression in the PVN of subordinates, reunion had no effect (Fig. 31G). One interpretation is that PVN activity is associated with social investigation or challenge in dominants and is more relevant for novelty recognition in subordinates. This is supported by the fact that disproportionately increased c-Fos expression was observed in novelty-exposed subordinates in both the lateral septum and prelimbic cortex (Fig. 32B, C), regions which are linked to novelty discrimination and social memory (Menon et al 2018, Rodriguez et al 2021, Xing et al 2021). Elevated baseline FCM status could represent biological coping or priming to lower social status in novel social encounters, which, in agreement with changes in PVN c-Fos expression, becomes attenuated in the context of social or hierarchical familiarity. Further studies are necessary to determine the relative contribution of PVN cell types in signaling social context by rank.

Further, both the lateral septum and the PVN have a potential role in the valence modulation of social stimuli (Menon et al 2021, Froemke et al 2021). Since social reunion, but not social novelty, increased expression in both regions in dominant females (Fig. 32D, F), this suggests that dominants may experience enhanced recruitment of social discrimination pathways after social isolation. Enhanced septal activation could represent prosocial behavior, or it could belong to a larger pro-stress, pro-dominance behavioral circuit, especially given the well-described role of the lateral septum in mediating aggression (Menon et al 2021). This latter interpretation is supported by the isolation-induced elevation in middle PVT expression (Fig. 31J), possibly engaging aversive state signaling while the PVN and lateral septum facilitate negatively-valenced social investigation. Given the divergent nature of the lateral septum in salience and behavioral output regulation, future studies should determine which cell types are involved and whether there are identifiable traits which could be used to designate dominance assertion in female mice, since in our study we did not observe aggressive agonistic behaviors in the home cage.

In dominants, social novelty reduced c-Fos expression specifically in the middle PVT (Fig. 13J, L), whereas social isolation and reunion suppressed expression in the anterior PVT in subordinates and increased expression in the middle PVT in dominants (Fig. 31I, J). The rank difference in thalamic expression was reproduced when difference from control means was analyzed in both contexts, with the largest effect sizes in social novelty for dominant animals and reunion for subordinate animals (Fig. 32G, H, Table 8 and Table 9). Collectively, this suggests that novelty-induced suppression of mPVT signaling in dominant animals may serve to engage prosocial behavior – speculatively

directed through OXT-mediated signaling in the PVN – serving a rank-based homeostatic mechanism that becomes disrupted by chronic social isolation. Further studies are also indicated to determine what effect a novel social encounter after prolonged isolation would have on PVN and mPVT c-Fos expression in dominant females, and to determine whether isolation alters social reward salience.

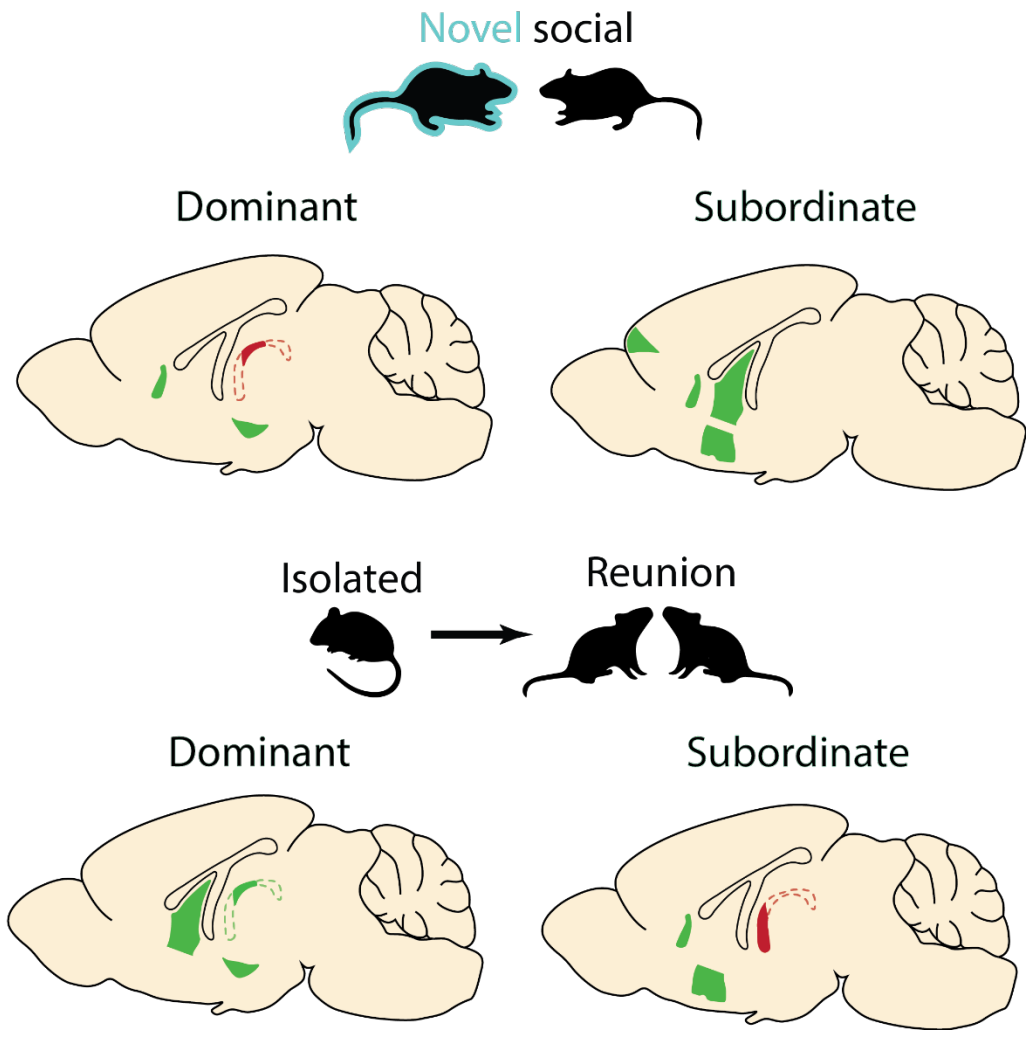

Figure 33. Summary of the context-specific changes in c-Fos expression

Schematic summarizing the rank-specific changes in c-Fos expression in response to different social and stress contexts. Green indicates regions with increased expression, and red indicates regions with decreased expression.

These experiments explored the formation and maintenance of dyadic female social hierarchies. Females rapidly formed stable rank pairings and subordinates exhibited context-dependent behavioral and endocrine attributes traditionally associated with rank in

male mice, including higher CORT status and diminished access to a food reward. Subordinate characteristics underlying a pro-exploratory motivation were over-represented in arousing contexts, such as during hierarchical nascency, anxiogenic testing protocols, and dark phase exploration of novel environments. Future studies should explore the circadian influences on tube test behavior and hierarchy formation in female triads, wherein a third social partner would add the variable of social buffering as well as possibly reducing hierarchical stability through social challenge of the alpha. It would be interesting to see whether increasing group size thereby prolongs the period of elevated FCM excretion by subordinate females.

In response to psychosocial stress, female mice displayed rank-characteristic endocrine and behavioral changes which did not always occur in parallel; I theorize that this may be due to inherent differences in how animals of either rank experience stressors and engage appropriate behavioral responses. Supporting this argument is the fact that in these experiments subordinate animals exhibit rank characteristic behaviors only in the context of belonging to a stable social group (i.e., at baseline, when they belonged to the social group with which they arrived at the vivarium, and in the three-chamber social approach task, after belonging to a new stable social pair) and during the active phase of their circadian cycle. This lends credence to the theory that individual rank serves a role-based social purpose that is adaptive for social living. Future experiments should explore rank characteristic behaviors in a variety of other tasks involving approach-avoidance conflict and social motivation in established pairs and social groups of different sizes. Pharmacologic experiments are also warranted to determine the responsiveness of animals

of different social ranks to therapeutic interventions after being subjected to ethologically relevant forms of chronic psychosocial stress.

Stress-naïve and stress-exposed animals also exhibited rank characteristics in the neural response to different social scenarios (Fig. 33). A particularly interesting phenomenon exists in the paraventricular thalamus, wherein novel and familiar social encounters induced opposing rank-based stress-sensitive changes with nuanced regional specificity. From these results, I propose a neuro-modulatory framework wherein the middle PVT of dominant animals exposed to social novelty suppresses aversive signaling pathways and facilitates prosocial behavior through PVN and claustral activation. Social isolation in turn reverses the dominant mPVT suppression, engaging aversive state signaling while the PVN and lateral septum facilitate social recognition and potentially assertion of dominance. In contrast, social isolation induces a pro-homeostatic state in the anterior PVT of subordinate animals by suppressing neuronal subpopulations associated with arousal. This could represent another biological coping mechanism employed as a result of maintaining subordinate status. Whether this reduced-arousal pattern would be recreated in a familiar social encounter without prolonged social isolation requires further study. Further experiments involving genetic identification of mPVT neurons are also necessary to confirm the relative contribution of neuronal subpopulations in mediating rank-dependent phenotypes and to determine whether social reward salience is altered in dominant females following chronic social isolation.

The results of these studies also further highlight the need for experiments investigating neurobiological responses of adult and post-adolescents to psychosocial stressors, as the literature has a distinct predilection for evaluating psychosocial factors in

the context of early life stress. Here I discovered that isolation stress exposure in post-adolescence also has significant effects on the social biology of female rodents, and that there are relevant factors beyond early life experience which influence stress vulnerability. These factors may include individual social status and the variable constitution of social lives in adulthood.

Collectively, these findings suggest a motivation difference by rank that is stress-sensitive and engages various behavioral, endocrinological, and neurobiological responses to maintain homeostasis. I propose a scenario wherein subordinate status is associated with baseline endocrinological priming, a pro-exploratory motivation that is sensitive to psychosocial stress, and a neuro-modulatory strategy that responds with pro-exploratory and approach signaling to social encounters, and which engages homeostatic coping pathways to reduce arousal following chronic social isolation. In contrast, dominant status is associated with a pro-social motivation reinforced by a lower endocrine stress status in baseline social situations. However, dominants do not engage the endocrinological coping mechanisms of subordinates and are therefore susceptible to social isolation, which is associated with an increase in aversive state processing upon familiar social encounters. This makes subordinates more susceptible to the consequences of social uncertainty, and dominants to those of social isolation.

REFERENCES

Tolkien, J. R. R. 1. (1973). The Hobbit: or, There and back again. Rev. ed. New York, Ballantine Books.

Kogler, L., Müller, V. I., Chang, A., Eickhoff, S. B., Fox, P. T., Gur, R. C., & Derntl, B. (2015). Psychosocial versus physiological stress—Meta-analyses on deactivations and activations of the neural correlates of stress reactions. Neuroimage, 119, 235-251.

Hüther, G. (1996). The central adaptation syndrome: psychosocial stress as a trigger for adaptive modifications of brain structure and brain function. Progress in neurobiology, 48(6), 569-612.

Moosa, M. M., & Ud-Dean, S. M. (2011). The role of dominance hierarchy in the evolution of social species. Journal for the Theory of Social Behaviour, 41(2), 203-208.

Schweda, A., Faber, N. S., Crockett, M. J., & Kalenscher, T. (2019). The effects of psychosocial stress on intergroup resource allocation. Scientific reports, 9(1), 1-12.

Heaney, C. A., & Israel, B. A. (2008). Social networks and social support. Health behavior and health education: Theory, research, and practice, 4, 189-210.

Kupriyanov, R., & Zhdanov, R. (2014). The eustress concept: problems and outlooks. World Journal of Medical Sciences, 11(2), 179-185.

Rutter, M., & Sandberg, S. (1992). Psychosocial stressors: Concepts, causes and effects. European child & adolescent psychiatry, 1(1), 3-13.

Crane, M. F., Searle, B. J., Kangas, M., & Nwiran, Y. (2019). How resilience is strengthened by exposure to stressors: The systematic self-reflection model of resilience strengthening. Anxiety, Stress, & Coping, 32(1), 1-17.

Siegrist, J. (2008). Chronic psychosocial stress at work and risk of depression: evidence from prospective studies. European archives of psychiatry and clinical neuroscience, 258(5), 115-119.

Backé, E. M., Seidler, A., Latza, U., Rossnagel, K., & Schumann, B. (2012). The role of psychosocial stress at work for the development of cardiovascular diseases: a systematic review. International archives of occupational and environmental health, 85(1), 67-79.

Kang, D., Zhao, D., Ryu, S., Guallar, E., Cho, J., Lazo, M., ... & Sung, E. (2020). Perceived stress and non-alcoholic fatty liver disease in apparently healthy men and women. Scientific reports, 10(1), 1-8.

Greenwood, D. C., Muir, K. R., Packham, C. J., & Madeley, R. J. (1996). Coronary heart disease: a review of the role of psychosocial stress and social support. Journal of Public Health, 18(2), 221-231.

Friedler, B., Crapser, J., & McCullough, L. (2015). One is the deadliest number: the detrimental effects of social isolation on cerebrovascular diseases and cognition. Acta neuropathologica, 129(4), 493-509.

Farrer, L. M., Gulliver, A., Bennett, K., Fassnacht, D. B., & Griffiths, K. M. (2016). Demographic and psychosocial predictors of major depression and generalised anxiety disorder in Australian university students. BMC psychiatry, 16(1), 1-9.

Muntaner, C., Anthony, J. C., Crum, R. M., & Eaton, W. W. (1995). Psychosocial dimensions of work and the risk of drug dependence among adults. American Journal of Epidemiology, 142(2), 183-190.

Ahmed, A. S. (2007). Post-traumatic stress disorder, resilience and vulnerability. Advances in Psychiatric treatment, 13(5), 369-375.

Jacka, F. N., Pasco, J. A., Mykletun, A., Williams, L. J., Hodge, A. M., O'Reilly, S. L., ... & Berk, M. (2010). Association of Western and traditional diets with depression and anxiety in women. American journal of psychiatry, 167(3), 305-311.

Wang, J., Zhou, Y., Chen, K., Jing, Y., He, J., Sun, H., & Hu, X. (2019). Dietary inflammatory index and depression: A meta-analysis. Public Health Nutrition, 22(4), 654-660.

Blume, C., Garbazza, C., & Spitschan, M. (2019). Effects of light on human circadian rhythms, sleep and mood. Somnologie, 23(3), 147-156.

Osibona, O., Solomon, B. D., & Fecht, D. (2021). Lighting in the Home and Health: A systematic Review. International journal of environmental research and public health, 18(2), 609.

Patel, V., Burns, J. K., Dhingra, M., Tarver, L., Kohrt, B. A., & Lund, C. (2018). Income inequality and depression: a systematic review and meta-analysis of the association and a scoping review of mechanisms. World Psychiatry, 17(1), 76-89.

McQuaid, R. J., Cox, S. M., Ogunlana, A., & Jaworska, N. (2021). The burden of loneliness: Implications of the social determinants of health during COVID-19. Psychiatry Research, 296, 113648.

Santini, Z. I., Jose, P. E., Cornwell, E. Y., Koyanagi, A., Nielsen, L., Hinrichsen, C., ... & Koushede, V. (2020). Social disconnectedness, perceived isolation, and symptoms of depression and anxiety among older Americans (NSHAP): a longitudinal mediation analysis. The Lancet Public Health, 5(1), e62-e70.

Viseu, J., Leal, R., de Jesus, S. N., Pinto, P., Pechorro, P., & Greenglass, E. (2018). Relationship between economic stress factors and stress, anxiety, and depression: Moderating role of social support. Psychiatry research, 268, 102-107.

Roohafza, H. R., Afshar, H., Keshteli, A. H., Mohammadi, N., Feizi, A., Taslimi, M., & Adibi, P. (2014). What's the role of perceived social support and coping styles in depression and anxiety?. Journal of research in medical sciences : the official journal of Isfahan University of Medical Sciences, 19(10), 944–949.

Hidaka, B. H. (2012). Depression as a disease of modernity: explanations for increasing prevalence. Journal of affective disorders, 140(3), 205-214.

Bracken, P. J. (2001). Post-modernity and post-traumatic stress disorder. Social science & medicine, 53(6), 733-743.

Layte, R., McCrory, C., Cheallaigh, C. N., Bourke, N., Kivimaki, M., Ribeiro, A. I., ... & Vineis, P. (2019). A comparative analysis of the status anxiety hypothesis of socio-economic inequalities in health based on 18,349 individuals in four countries and five cohort studies. Scientific reports, 9(1), 1-12.

Liu, M. Y., Li, N., Li, W. A., & Khan, H. (2017). Association between psychosocial stress and hypertension: a systematic review and meta-analysis. Neurological research, 39(6), 573-580.

Williams, D. R., & Neighbors, H. (2001). Racism, discrimination and hypertension: evidence and needed research. Ethn Dis, 11(4), 800-816.

Noh, S., & Kaspar, V. (2003). Perceived discrimination and depression: Moderating effects of coping, acculturation, and ethnic support. American journal of public health, 93(2), 232-238.

Lindström, M. (2022). Psychosocial stress and social capital pathways and health: Perspectives from Lund University, Malmö. Scandinavian Journal of Public Health, 14034948221075015.

U.S. Department of Health and Human Services, Substance Abuse and Mental Health Services Administration, Center for Behavioral Health Statistics and Quality. (2022). National Survey on Drug Use and Health 2020 (NSDUH-2020-DS0001). https://datafiles.samhsa.gov/

Terlizzi, E. P., & Villarroel, M. A. (2020). Symptoms of generalized anxiety disorder among adults: United States, 2019. US Department of Health and Human Services, Centers for Disease Control and Prevention, National Center for Health Statistics. p. 8.

Vahratian A., Blumberg S.J., Terlizzi E.P., Schiller J.S. (2021). Symptoms of Anxiety or Depressive Disorder and Use of Mental Health Care Among Adults During the COVID-19 Pandemic — United States, August 2020–February 2021. MMWR Morb Mortal Wkly Rep 2021; 70:490–494.

Powell, N. D., Tarr, A. J., & Sheridan, J. F. (2013). Psychosocial stress and inflammation in cancer. Brain, behavior, and immunity, 30, S41-S47.

Osborne, M. T., Shin, L. M., Mehta, N. N., Pitman, R. K., Fayad, Z. A., & Tawakol, A. (2020). Disentangling the links between psychosocial stress and cardiovascular disease. Circulation: Cardiovascular Imaging, 13(8), e010931.

Murphy, S. L., Kochanek, K. D., Xu, J., & Arias, E. Mortality in the United States, 2020. NCHS Data Brief, (427).

Gururajan, A., Reif, A., Cryan, J. F., & Slattery, D. A. (2019). The future of rodent models in depression research. Nature Reviews Neuroscience, 20(11), 686-701.

Campos, A. C., Fogaça, M. V., Aguiar, D. C., & Guimaraes, F. S. (2013). Animal models of anxiety disorders and stress. Brazilian Journal of Psychiatry, 35, S101-S111.

Weiss, S. M., Wadsworth, G., Fletcher, A., & Dourish, C. T. (1998). Utility of ethological analysis to overcome locomotor confounds in elevated maze models of anxiety. Neuroscience & Biobehavioral Reviews, 23(2), 265-271.

Sturman, O., Germain, P. L., & Bohacek, J. (2018). Exploratory rearing: a context- and stress-sensitive behavior recorded in the open-field test. Stress, 21(5), 443-452.

Pollak, D. D., Rey, C. E., & Monje, F. J. (2010). Rodent models in depression research: classical strategies and new directions. Annals of medicine, 42(4), 252-264.

Gaskill, B. N., Karas, A. Z., Garner, J. P., & Pritchett-Corning, K. R. (2013). Nest building as an indicator of health and welfare in laboratory mice. JoVE (Journal of Visualized Experiments), (82), e51012.

Smolinsky, A. N., Bergner, C. L., LaPorte, J. L., & Kalueff, A. V. (2009). Analysis of grooming behavior and its utility in studying animal stress, anxiety, and depression. In Mood and anxiety related phenotypes in mice (pp. 21-36). Humana Press, Totowa, NJ.

Nollet, M., Guisquet, A. M. L., & Belzung, C. (2013). Models of depression: unpredictable chronic mild stress in mice. Current Protocols in Pharmacology, 61(1), 5-65.

Kokras, N., & Dalla, C. (2014). Sex differences in animal models of psychiatric disorders. British journal of pharmacology, 171(20), 4595–4619.

LeClair, K. B., & Russo, S. J. (2021). Using social rank as the lens to focus on the neural circuitry driving stress coping styles. Current Opinion in Neurobiology, 68, 167-180.

Wang, F., Kessels, H. W., & Hu, H. (2014). The mouse that roared: neural mechanisms of social hierarchy. Trends in neurosciences, 37(11), 674-682.

Rusu, A. S., & Krackow, S. (2004). Kin-preferential cooperation, dominance-dependent reproductive skew, and competition for mates in communally nesting female house mice. Behavioral Ecology and Sociobiology, 56(3), 298-305.

Chase, I. D., & Seitz, K. (2011). Self-structuring properties of dominance hierarchies: a new perspective. Advances in genetics, 75, 51-81.

Cornwallis, C. K., Botero, C. A., Rubenstein, D. R., Downing, P. A., West, S. A., & Griffin, A. S. (2017). Cooperation facilitates the colonization of harsh environments. Nature Ecology & Evolution, 1(3), 1-10.

Ebensperger, L. A. (2001). A review of the evolutionary causes of rodent group-living. Acta Theriologica, 46(2), 115-144.

Ulrich, Y., Saragosti, J., Tokita, C. K., Tarnita, C. E., & Kronauer, D. J. (2018). Fitness benefits and emergent division of labour at the onset of group living. Nature, 560(7720), 635-638.

Kleiman, E. M., & Liu, R. T. (2013). Social support as a protective factor in suicide: Findings from two nationally representative samples. Journal of affective disorders, 150(2), 540-545.

Birtel, M. D., Wood, L., & Kempa, N. J. (2017). Stigma and social support in substance abuse: Implications for mental health and well-being. Psychiatry research, 252, 1-8.

Beery, A. K., & Kaufer, D. (2015). Stress, social behavior, and resilience: insights from rodents. Neurobiology of stress, 1, 116-127.

D'Amato, F. R. (1988). Effects of male social status on reproductive success and on behavior in mice (Mus musculus). Journal of Comparative Psychology, 102(2), 146.

Wesson, D. W. (2013). Sniffing behavior communicates social hierarchy. Current Biology, 23(7), 575-580.

Huang, B., Wey, T. W., & Blumstein, D. T. (2011). Correlates and consequences of dominance in a social rodent. Ethology, 117(7), 573-585.

Fulenwider, H. D., Caruso, M. A., & Ryabinin, A. E. (2022). Manifestations of domination: Assessments of social dominance in rodents. Genes, Brain and Behavior, 21(3), e12731.

Kunkel, T., & Wang, H. (2018). Socially dominant mice in C57BL6 background show increased social motivation. Behavioural brain research, 336, 173-176.

Varholick, J. A., Bailoo, J. D., Palme, R., & Würbel, H. (2018). Phenotypic variability between Social Dominance Ranks in laboratory mice. Scientific Reports, 8(1), 6593.

Fan, Z., Zhu, H., Zhou, T., Wang, S., Wu, Y., & Hu, H. (2019). Using the tube test to measure social hierarchy in mice. Nature Protocols, 14(3), 819-831.

Schrage, B., Lund, L. H., Benson, L., Stolfo, D., Ohlsson, A., Westerling, R., ... & Savarese, G. (2021). Lower socioeconomic status predicts higher mortality and morbidity in patients with heart failure. Heart, 107(3), 229-236.

Varholick, J. A., Pontiggia, A., Murphy, E., Daniele, V., Palme, R., Voelkl, B., ... & Bailoo, J. D. (2019). Social dominance hierarchy type and rank contribute to phenotypic variation within cages of laboratory mice. Scientific reports, 9(1), 1-11.

Williamson, C. M., Lee, W., DeCasien, A. R., Lanham, A., Romeo, R. D., & Curley, J. P. (2019). Social hierarchy position in female mice is associated with plasma corticosterone levels and hypothalamic gene expression. Scientific reports, 9(1), 1-14.

Van Den Berg, W. E., Lamballais, S., & Kushner, S. A. (2015). Sex-specific mechanism of social hierarchy in mice. Neuropsychopharmacology, 40(6), 1364-1372.

Blanchard, D. C., Spencer, R. L., Weiss, S. M., Blanchard, R. J., McEwen, B., & Sakai, R. R. (1995). Visible burrow system as a model of chronic social stress: behavioral and neuroendocrine correlates. Psychoneuroendocrinology, 20(2), 117-134.

Creel, S. (2001). Social dominance and stress hormones. Trends in ecology & evolution, 16(9), 491-497.

Bartolomucci, A., Palanza, P., Gaspani, L., Limiroli, E., Panerai, A. E., Ceresini, G., ... & Parmigiani, S. (2001). Social status in mice: behavioral, endocrine and immune changes are context dependent. Physiology & behavior, 73(3), 401-410.

Williamson, C. M., Lee, W., Romeo, R. D., & Curley, J. P. (2017). Social context-dependent relationships between mouse dominance rank and plasma hormone levels. Physiology & behavior, 171, 110-119.

Šabanović, M., Liu, H., Mlambo, V., Aqel, H., & Chaudhury, D. (2020). What it takes to be at the top: The interrelationship between chronic social stress and social dominance. Brain and Behavior, 10(12), e01896.

Varholick, J. A., Bailoo, J. D., Jenkins, A., Voelkl, B., & Würbel, H. (2021). A systematic review and meta-analysis of the relationship between social dominance status and common behavioral phenotypes in male laboratory mice. Frontiers in Behavioral Neuroscience, 14, 624036.

Kopp, C. (2001). Locomotor activity rhythm in inbred strains of mice: implications for behavioural studies. Behavioural brain research, 125(1-2), 93-96.

Hossain, S. M., Wong, B. K. Y., & Simpson, E. M. (2004). The dark phase improves genetic discrimination for some high throughput mouse behavioral phenotyping. Genes, Brain and Behavior, 3(3), 167-177.

Yang, M., Weber, M. D., & Crawley, J. N. (2008). Light phase testing of social behaviors: not a problem. Frontiers in Neuroscience, 2, 186–191.

Beeler, J. A., Prendergast, B., & Zhuang, X. (2006). Low amplitude entrainment of mice and the impact of circadian phase on behavior tests. Physiology & behavior, 87(5), 870-880.

Bains, R. S., Wells, S., Sillito, R. R., Armstrong, J. D., Cater, H. L., Banks, G., & Nolan, P. M. (2018). Assessing mouse behaviour throughout the light/dark cycle using automated in-cage analysis tools. Journal of neuroscience methods, 300, 37-47.

Bourin, M., & Hascoët, M. (2003). The mouse light/dark box test. European journal of pharmacology, 463(1-3), 55-65.

Zhang, Z., Wang, H. J., Wang, D. R., Qu, W. M., & Huang, Z. L. (2017). Red light at intensities above 10 lx alters sleep–wake behavior in mice. Light: Science & Applications, 6(5), e16231.

DeVries, A. C., Glasper, E. R., & Detillion, C. E. (2003). Social modulation of stress responses. Physiology & behavior, 79(3), 399-407.

Zhou, T., Sandi, C., & Hu, H. (2018). Advances in understanding neural mechanisms of social dominance. Current Opinion in Neurobiology, 49, 99-107.

Sheng, J. A., Bales, N. J., Myers, S. A., Bautista, A. I., Roueinfar, M., Hale, T. M., & Handa, R. J. (2021). The hypothalamic-pituitary-adrenal axis: development, programming actions of hormones, and maternal-fetal interactions. Frontiers in Behavioral Neuroscience, 14, 601939.

Touma, C., Sachser, N., Möstl, E., & Palme, R. (2003). Effects of sex and time of day on metabolism and excretion of corticosterone in urine and feces of mice. General and Comparative Endocrinology, 130(3), 267-278.

Munck, A., Guyre, P. M., & Holbrook, N. J. (1984). Physiological functions of glucocorticoids in stress and their relation to pharmacological actions. Endocrine reviews, 5(1), 25-44.

Sapolsky, R. M., Romero, L. M., & Munck, A. U. (2000). How do glucocorticoids influence stress responses? Integrating permissive, suppressive, stimulatory, and preparative actions. Endocrine reviews, 21(1), 55-89.

Heck, A. L., & Handa, R. J. (2019). Sex differences in the hypothalamic–pituitary–adrenal axis' response to stress: an important role for gonadal hormones. Neuropsychopharmacology, 44(1), 45-58.

Dominique, J. F., Aerni, A., Schelling, G., & Roozendaal, B. (2009). Glucocorticoids and the regulation of memory in health and disease. Frontiers in neuroendocrinology, 30(3), 358-370.

Haemisch, A., Voss, T., & Gärtner, K. (1994). Effects of environmental enrichment on aggressive behavior, dominance hierarchies, and endocrine states in male DBA/2J mice. Physiology & behavior, 56(5), 1041-1048.

Blanchard, D. C., Sakai, R. R., McEwen, B., Weiss, S. M., & Blanchard, R. J. (1993). Subordination stress: behavioral, brain, and neuroendocrine correlates. Behavioural brain research, 58(1-2), 113-121.

Kozorovitskiy, Y., & Gould, E. (2004). Dominance hierarchy influences adult neurogenesis in the dentate gyrus. Journal of Neuroscience, 24(30), 6755-6759.

Hunt, C., & Hambly, C. (2006). Faecal corticosterone concentrations indicate that separately housed male mice are not more stressed than group housed males. Physiology & behavior, 87(3), 519-526.

Pallé, A., Zorzo, C., Luskey, V. E., McGreevy, K. R., Fernández, S., & Trejo, J. L. (2019). Social dominance differentially alters gene expression in the medial prefrontal cortex without affecting adult hippocampal neurogenesis or stress and anxiety-like behavior. The FASEB Journal, 33(6), 6995-7008.

Zhao, Y., Xie, W., Dai, J., Wang, Z., & Huang, Y. (2009). The varying effects of short-term and long-term corticosterone injections on depression-like behavior in mice. Brain research, 1261, 82-90.

Murray, F., Smith, D. W., & Hutson, P. H. (2008). Chronic low dose corticosterone exposure decreased hippocampal cell proliferation, volume and induced anxiety and depression like behaviours in mice. European journal of pharmacology, 583(1), 115-127.

Ali, S. H., Madhana, R. M., Athira, K. V., Kasala, E. R., Bodduluru, L. N., Pitta, S., ... & Lahkar, M. (2015). Resveratrol ameliorates depressive-like behavior in repeated corticosterone-induced depression in mice. Steroids, 101, 37-42.

Mekiri, M., Gardier, A. M., David, D. J., & Guilloux, J. P. (2017). Chronic corticosterone administration effects on behavioral emotionality in female c57bl6 mice. Experimental and clinical psychopharmacology, 25(2), 94.

Audet, M. C., Mangano, E. N., & Anisman, H. (2010). Behavior and pro-inflammatory cytokine variations among submissive and dominant mice engaged in aggressive encounters: moderation by corticosterone reactivity. Frontiers in behavioral neuroscience, 4, 156.

Timmer, M., & Sandi, C. (2010). A role for glucocorticoids in the long-term establishment of a social hierarchy. Psychoneuroendocrinology, 35(10), 1543-1552.

Weger, M., Sevelinges, Y., Grosse, J., de Suduiraut, I. G., Zanoletti, O., & Sandi, C. (2018). Increased brain glucocorticoid actions following social defeat in rats facilitates the long-term establishment of social subordination. Physiology & behavior, 186, 31-36.

Solomon, M. B., Loftspring, M., De Kloet, A. D., Ghosal, S., Jankord, R., Flak, J. N., ... & Herman, J. P. (2015). Neuroendocrine function after hypothalamic depletion of glucocorticoid receptors in male and female mice. Endocrinology, 156(8), 2843-2853.

Choleris, E., Cazzin, L., Lymer, J. M., Amor, T. R., Lu, R., Kavaliers, M., & Valsecchi, P. (2013). Acute corticosterone sexually dimorphically facilitates social learning and inhibits feeding in mice. Neuropharmacology, 75, 191-200.

Holson, R. R. (1986). Mesial prefrontal cortical lesions and timidity in rats. III. Behavior in a semi-natural environment. Physiology & behavior, 37(2), 239-247.

Wang, F., Zhu, J., Zhu, H., Zhang, Q., Lin, Z., & Hu, H. (2011). Bidirectional control of social hierarchy by synaptic efficacy in medial prefrontal cortex. Science, 334(6056), 693-697.

Zhou, T., Zhu, H., Fan, Z., Wang, F., Chen, Y., Liang, H., ... & Hu, H. (2017). History of winning remodels thalamo-PFC circuit to reinforce social dominance. Science, 357(6347), 162-168.

Hoover, W. B., & Vertes, R. P. (2007). Anatomical analysis of afferent projections to the medial prefrontal cortex in the rat. Brain Structure and Function, 212(2), 149-179.

Bluthe, R. M., & Dantzer, R. (1990). Social recognition does not involve vasopressinergic neurotransmission in female rats. Brain research, 535(2), 301-304.

Choleris, E., & Kavaliers, M. (1999). Social learning in animals: sex differences and neurobiological analysis. Pharmacology Biochemistry and Behavior, 64(4), 767-776.

Dalla, C., & Shors, T. J. (2009). Sex differences in learning processes of classical and operant conditioning. Physiology & behavior, 97(2), 229-238.

Maren, S., De Oca, B., & Fanselow, M. S. (1994). Sex differences in hippocampal long-term potentiation (LTP) and Pavlovian fear conditioning in rats: positive correlation between LTP and contextual learning. Brain research, 661(1-2), 25-34.

Gupta, R. R., Sen, S., Diepenhorst, L. L., Rudick, C. N., & Maren, S. (2001). Estrogen modulates sexually dimorphic contextual fear conditioning and hippocampal long-term potentiation (LTP) in rats. Brain research, 888(2), 356-365.

Chang, Y. J., Yang, C. H., Liang, Y. C., Yeh, C. M., Huang, C. C., & Hsu, K. S. (2009). Estrogen modulates sexually dimorphic contextual fear extinction in rats through estrogen receptor β. Hippocampus, 19(11), 1142-1150.

Van Haaren, F., Van Hest, A., & Heinsbroek, R. P. (1990). Behavioral differences between male and female rats: effects of gonadal hormones on learning and memory. Neuroscience & Biobehavioral Reviews, 14(1), 23-33.

Dalla, C., Edgecomb, C., Whetstone, A. S., & Shors, T. J. (2008). Females do not express learned helplessness like males do. Neuropsychopharmacology, 33(7), 1559-1569.

Touma, C., Palme, R., & Sachser, N. (2004). Analyzing corticosterone metabolites in fecal samples of mice: a noninvasive technique to monitor stress hormones. Hormones and behavior, 45(1), 10-22.

Schuhr, B. (1987). Social structure and plasma corticosterone level in female albino mice. Physiology & behavior, 40(6), 689-693.

Lindzey, G., Winston, H., & Manosevitz, M. (1961). Social dominance in inbred mouse strains. Nature, 191(4787), 474-476.

Benton, D., & Brain, P. F. (1979). Behavioural comparisons of isolated, dominant and subordinate mice. Behavioural Processes, 4(3), 211-219.

Williamson, C. M., Lee, W., & Curley, J. P. (2016). Temporal dynamics of social hierarchy formation and maintenance in male mice. Animal behaviour, 115, 259-272.

Stevens, J. M., Vervaecke, H., De Vries, H., & van Elsacker, L. (2007). Sex differences in the steepness of dominance hierarchies in captive bonobo groups. International Journal of Primatology, 28(6), 1417-1430.

Gammell, M. P., Vries, H. D., Jennings, D. J., Carlin, C. M., & Hayden, T. J. (2003). David's score: a more appropriate dominance ranking method than Clutton-Brock et al.'s index. Animal behaviour, 66(3), 601-605.

Petersen, C. L., Davis, S. E., Patel, B., & Hurley, L. M. (2021). Social experience interacts with serotonin to affect functional connectivity in the social behavior network following playback of social vocalizations in mice. Eneuro, 8(2).

Franklin. K. B. J., & Paxinos, G. (2008). The Mouse Brain in Stereotaxic Coordinates. Compact Third Edition (Third). Academic Press. Elsevier.

Gao, C., Leng, Y., Ma, J., Rooke, V., Rodriguez-Gonzalez, S., Ramakrishnan, C., Deisseroth, K., & Penzo, M. A. (2020). Two genetically, anatomically and functionally distinct cell types segregate across anteroposterior axis of paraventricular thalamus. Nature neuroscience, 23(2), 217-228.

Zhu, Y. B., Wang, Y., Hua, X. X., Xu, L., Liu, M. Z., Zhang, R., ... & Mu, D. (2022). PBN-PVT projections modulate negative affective states in mice. Elife, 11, e68372.

Choleris, E., Thomas, A. W., Kavaliers, M., & Prato, F. S. (2001). A detailed ethological analysis of the mouse open field test: effects of diazepam, chlordiazepoxide and an extremely low frequency pulsed magnetic field. Neuroscience & Biobehavioral Reviews, 25(3), 235-260.

Simon, P., Dupuis, R., & Costentin, J. (1994). Thigmotaxis as an index of anxiety in mice. Influence of dopaminergic transmissions. Behavioural Brain Research, 61(1), 59-64.

Cryan, J. F., & Holmes, A. (2005). The ascent of mouse: advances in modelling human depression and anxiety. Nature reviews Drug discovery, 4(9), 775-790.

Scott, J. (1966). Agonistic behavior of mice and rats: a review. American Zoologist, 6(4), 683-701.

Nordman, J. C., Ma, X., Gu, Q., Potegal, M., Li, H., Kravitz, A. V., & Li, Z. (2020). Potentiation of divergent medial amygdala pathways drives experience-dependent aggression escalation. Journal of Neuroscience, 40(25), 4858-4880.

Mogil, J. S. (2012). The surprising empathic abilities of rodents. Trends in cognitive sciences, 16(3), 143-144.

Zhao, Z., Zeng, F., Wang, H., Wu, R., Chen, L., Wu, Y., Li, S., Shao, J., Wang, Y., Wu, J., Feng, Z., Gao, W et al. (2022). Encoding of social novelty by sparse GABAergic neural ensembles in the prelimbic cortex. Science Advances, 8(35), eabo4884.

Goll, Y., Atlan, G., & Citri, A. (2015). Attention: the claustrum. Trends in Neurosciences, 38(8), 486-495.

Jackson, J., Smith, J. B., & Lee, A. K. (2020). The anatomy and physiology of claustrum-cortex interactions. Annu. Rev. Neurosci, 43, 231-247.

Gabor, C. S., Phan, A., Clipperton-Allen, A. E., Kavaliers, M., & Choleris, E. (2012). Interplay of oxytocin, vasopressin, and sex hormones in the regulation of social recognition. Behavioral neuroscience, 126(1), 97.

Zoicas, I., Slattery, D. A., & Neumann, I. D. (2014). Brain oxytocin in social fear conditioning and its extinction: involvement of the lateral septum. Neuropsychopharmacology, 39(13), 3027-3035.

Menon, R., Grund, T., Zoicas, I., Althammer, F., Fiedler, D., Biermeier, V., Bosch, O. J., Hiraoka, Y., Nishimori, K., Eliava, M., Grinevich, V., & Neumann, I. D. (2018). Oxytocin signaling in the lateral septum prevents social fear during lactation. Current Biology, 28(7), 1066-1078.

Menon, R., Süß, T., de Moura Oliveira, V. E., Neumann, I. D., & Bludau, A. (2021). Neurobiology of the lateral septum: regulation of social behavior. Trends in Neurosciences.

Salgado, S., & Kaplitt, M. G. (2015). The nucleus accumbens: a comprehensive review. Stereotactic and functional neurosurgery, 93(2), 75-93.

Dölen, G., Darvishzadeh, A., Huang, K. W., & Malenka, R. C. (2013). Social reward requires coordinated activity of nucleus accumbens oxytocin and serotonin. Nature, 501(7466), 179-184.

Rogers-Carter, M. M., Djerdjaj, A., Gribbons, K. B., Varela, J. A., & Christianson, J. P. (2019). Insular cortex projections to nucleus accumbens core mediate social approach to stressed juvenile rats. Journal of Neuroscience, 39(44), 8717-8729.

Saddoris, M. P., Sugam, J. A., Cacciapaglia, F., & Carelli, R. M. (2013). Rapid dopamine dynamics in the accumbens core and shell: learning and action. Frontiers in bioscience (Elite edition), 5, 273.

Froemke, R. C., & Young, L. J. (2021). Oxytocin, neural plasticity, and social behavior. Annu Rev Neurosci, 44, 359-381.

Wu, Y. E., & Hong, W. (2022). Neural basis of prosocial behavior. Trends in Neurosciences.

Sterley, T. L., Baimoukhametova, D., Füzesi, T., Zurek, A. A., Daviu, N., Rasiah, N. P., ... & Bains, J. S. (2018). Social transmission and buffering of synaptic changes after stress. Nature neuroscience, 21(3), 393-403.

Matthews, G. A., & Tye, K. M. (2019). Neural mechanisms of social homeostasis. Annals of the New York Academy of Sciences, 1457(1), 5-25.

Buwalda, B., Scholte, J., de Boer, S. F., Coppens, C. M., & Koolhaas, J. M. (2012). The acute glucocorticoid stress response does not differentiate between rewarding and aversive social stimuli in rats. Hormones and behavior, 61(2), 218-226.

Penzo, M. A., & Gao, C. (2021). The paraventricular nucleus of the thalamus: an integrative node underlying homeostatic behavior. Trends in Neurosciences, 44(7), 538-549.

Yamamuro, K., Bicks, L. K., Leventhal, M. B., Kato, D., Im, S., Flanigan, M. E., ... & Morishita, H. (2020). A prefrontal–paraventricular thalamus circuit requires juvenile social experience to regulate adult sociability in mice. Nature Neuroscience, 23(10), 1240-1252.

Choi, E. A., & McNally, G. P. (2017). Paraventricular thalamus balances danger and reward. Journal of Neuroscience, 37(11), 3018-3029.

Choi, E. A., Jean-Richard-dit-Bressel, P., Clifford, C. W., & McNally, G. P. (2019). Paraventricular thalamus controls behavior during motivational conflict. Journal of Neuroscience, 39(25), 4945-4958.

Figueiredo, H. F., Bruestle, A., Bodie, B., Dolgas, C. M., & Herman, J. P. (2003). The medial prefrontal cortex differentially regulates stress-induced c-fos expression in the forebrain depending on type of stressor. European Journal of Neuroscience, 18(8), 2357-2364.

Pobbe, R. L., Pearson, B. L., Defensor, E. B., Bolivar, V. J., Blanchard, D. C., & Blanchard, R. J. (2010). Expression of social behaviors of C57BL/6J versus BTBR inbred mouse strains in the visible burrow system. Behavioural Brain Research, 214(2), 443-449.

Bartolomucci, A., Pederzani, T., Sacerdote, P., Panerai, A. E., Parmigiani, S., & Palanza, P. (2004). Behavioral and physiological characterization of male mice under chronic psychosocial stress. Psychoneuroendocrinology, 29(7), 899-910.

Richetto, J., Polesel, M., & Weber-Stadlbauer, U. (2019). Effects of light and dark phase testing on the investigation of behavioural paradigms in mice: relevance for behavioural neuroscience. Pharmacology Biochemistry and Behavior, 178, 19-29.

Hostetter, R. C. (1966). Time of day effects on learning and open field activity. Psychonomic Science, 5(7), 257-258.

Valentinuzzi, V. S., Buxton, O. M., Chang, A. M., Scarbrough, K., Ferrari, E. A., Takahashi, J. S., & Turek, F. W. (2000). Locomotor response to an open field during C57BL/6J active and inactive phases: differences dependent on conditions of illumination. Physiology & behavior, 69(3), 269-275.

Tsao, C. H., Flint, J., & Huang, G. J. (2022). Influence of diurnal phase on behavioral tests of sensorimotor performance, anxiety, learning and memory in mice. Scientific reports, 12(1), 1-10.

M.V. Schmidt, V. Sterlemann, K. Ganea, C. Liebl, S. Alam, D. Harbich, M. Greetfeld, M. Uhr, F. Holsboer, M.B. Muller. (2007). Persistent neuroendocrine and behavioral effects of a novel, etiologically relevant mouse paradigm for chronic social stress during adolescence. Psychoneuroendocrinology, 32, pp. 417-429.

V. Sterlemann, K. Ganea, C. Liebl, D. Harbich, S. Alam, F. Holsboer, M.B. Muller, M.V. Schmidt. (2008). Long-term behavioral and neuroendocrine alterations following chronic social stress in mice: implications for stress-related disorders. Horm. Behav., 53, pp. 386-394.

M.V. Schmidt, S.H. Scharf, C. Liebl, D. Harbich, B. Mayer, F. Holsboer, M.B. Muller. (2010). A novel chronic social stress paradigm in female mice. Horm. Behav., 57, pp. 415-420.

Yohn, C. N., Ashamalla, S. A., Bokka, L., Gergues, M. M., Garino, A., & Samuels, B. A. (2019). Social instability is an effective chronic stress paradigm for both male and female mice. Neuropharmacology, 160, 107780.

Hess, S. E., Rohr, S., Dufour, B. D., Gaskill, B. N., Pajor, E. A., & Garner, J. P. (2008). Home improvement: C57BL/6J mice given more naturalistic nesting materials build better nests. Journal of the American Association for Laboratory Animal Science, 47(6), 25-31.

Gaskill, B. N., Karas, A. Z., Garner, J. P., & Pritchett-Corning, K. R. (2013). Nest building as an indicator of health and welfare in laboratory mice. JoVE (Journal of Visualized Experiments), (82), e51012.

Walf, A. A., & Frye, C. A. (2007). The use of the elevated plus maze as an assay of anxiety-related behavior in rodents. Nature protocols, 2(2), 322-328.

Bourin, M., & Hascoët, M. (2003). The mouse light/dark box test. European journal of pharmacology, 463(1-3), 55-65.

Kulkarni, S. K., Singh, K., & Bishnoi, M. (2007). Elevated zero maze: a paradigm to evaluate antianxiety effects of drugs. Methods and findings in experimental and clinical pharmacology, 29(5), 343-348.

Spruijt, B. M., Van Hooff, J. A., & Gispen, W. H. (1992). Ethology and neurobiology of grooming behavior. Physiological reviews, 72(3), 825-852.

Blanchard, R. J., McKittrick, C. R., & Blanchard, D. C. (2001). Animal models of social stress: effects on behavior and brain neurochemical systems. Physiology & behavior, 73(3), 261-271.

Patel, D., Kas, M. J., Chattarji, S., & Buwalda, B. (2019). Rodent models of social stress and neuronal plasticity: Relevance to depressive-like disorders. Behavioural brain research, 369, 111900.

Liu, M. Y., Yin, C. Y., Zhu, L. J., Zhu, X. H., Xu, C., Luo, C. X., ... & Zhou, Q. G. (2018). Sucrose preference test for measurement of stress-induced anhedonia in mice. Nature protocols, 13(7), 1686-1698.

Strekalova, T., Spanagel, R., Bartsch, D., Henn, F. A., & Gass, P. (2004). Stress-induced anhedonia in mice is associated with deficits in forced swimming and exploration. Neuropsychopharmacology, 29(11), 2007-2017.

Strekalova, T., Gorenkova, N., Schunk, E., Dolgov, O., & Bartsch, D. (2006). Selective effects of citalopram in a mouse model of stress-induced anhedonia with a control for chronic stress. Behavioural pharmacology, 17(3), 271-287.

Strekalova, T., & Steinbusch, H. W. (2010). Measuring behavior in mice with chronic stress depression paradigm. Progress in Neuro-Psychopharmacology and Biological Psychiatry, 34(2), 348-361.

Becker, L. A. (2000). Effect size (ES). Online. URL: https://www.uv.es/~friasnav/EffectSizeBecker.pdf

Hentschke, H., & Stüttgen, M. C. (2011). Computation of measures of effect size for neuroscience data sets. European Journal of Neuroscience, 34(12), 1887-1894.

Heckert, A. (2018). *Hedge's g Statistic*. National Institute of Standards and Technology. Online. URL: https://www.itl.nist.gov

Smith, J. B., Watson, G. D., Liang, Z., Liu, Y., Zhang, N., & Alloway, K. D. (2019). A role for the claustrum in salience processing?. Frontiers in neuroanatomy, 13, 64.

Noback, M., Zhang, G., White, N., Barrow, J. C., & Carr, G. V. (2021). Post-weaning social isolation increases ΔFosB/FosB protein expression in sex-specific patterns in the prelimbic/infralimbic cortex and hippocampus in mice. Neuroscience Letters, 740, 135423.

Wu, B. (2020). Social isolation and loneliness among older adults in the context of COVID-19: a global challenge. Global health research and policy, 5(1), 1-3.

Mumtaz, F., Khan, M. I., Zubair, M., & Dehpour, A. R. (2018). Neurobiology and consequences of social isolation stress in animal model—A comprehensive review. Biomedicine & Pharmacotherapy, 105, 1205-1222.

Yorgason, J. T., España, R. A., Konstantopoulos, J. K., Weiner, J. L., & Jones, S. R. (2013). Enduring increases in anxiety-like behavior and rapid nucleus accumbens dopamine signaling in socially isolated rats. European journal of neuroscience, 37(6), 1022-1031.

Deutschmann, A. U., Kirkland, J. M., & Briand, L. A. (2022). Adolescent social isolation induced alterations in nucleus accumbens glutamate signalling. Addiction Biology, 27(1), e13077.

Cadoni, C., Solinas, M., Valentini, V., & Di Chiara, G. (2003). Selective psychostimulant sensitization by food restriction: differential changes in accumbens shell and core dopamine. European journal of neuroscience, 18(8), 2326-2334.

Mul, J. D., Soto, M., Cahill, M. E., Ryan, R. E., Takahashi, H., So, K., ... & Goodyear, L. J. (2018). Voluntary wheel running promotes resilience to chronic social defeat stress in mice: a role for nucleus accumbens ΔFosB. Neuropsychopharmacology, 43(9), 1934-1942.

Senst, L., Baimoukhametova, D., Sterley, T. L., & Bains, J. S. (2016). Sexually dimorphic neuronal responses to social isolation. Elife, 5, e18726.

Grippo, A. J., Gerena, D., Huang, J., Kumar, N., Shah, M., Ughreja, R., & Carter, C. S. (2007). Social isolation induces behavioral and neuroendocrine disturbances relevant to depression in female and male prairie voles. Psychoneuroendocrinology, 32(8-10), 966-980.

Ahern, M., Goodell, D. J., Adams, J., & Bland, S. T. (2016). Brain regional differences in social encounter-induced Fos expression in male and female rats after post-weaning social isolation. Brain research, 1630, 120-133.

Aspesi, D., & Choleris, E. (2022). Neuroendocrine underpinning of social recognition in males and females. Journal of Neuroendocrinology, 34(2), e13070.

Rodriguez, L. A., Kim, S. H., Page, S. C., Nguyen, C. V., Pattie, E. A., Hallock, H. L.,et. al (2021). Expression of brain-derived neurotrophic factor in basolateral amygdala inputs to lateral septum is necessary for mice to identify socially novel individuals.

Xing, B., Mack, N. R., Guo, K. M., Zhang, Y. X., Ramirez, B., Yang, S. S., et. al (2021). A subpopulation of prefrontal cortical neurons is required for social memory. Biological psychiatry, 89(5), 521-531.